

AGGREGATION OF PARTICLES IN HORIZONTALLY  
CONVERGING AIR MOTION

BY

Ramesh Patel . July, 1976

A Thesis submitted for the degree of  
Master of Philosophy of the  
University of London .

Department of Mathematics,  
Imperial College of Science and Technology,  
LONDON SW7.

### Acknowledgement

The author wishes to express his gratitude to Professor R.S. Scorer for all his invaluable assistance and guidance, making this thesis possible and to Science Research Council for financial support. He is also indebted to a number of people working with Professor Scorer for their useful suggestions at the beginning of this work, to Paul Newton who contributed towards computing work, and to Mrs. Susan Miller for tackling the task of typing this thesis.

## Contents

	Page
Abstract	1
Symbols	2
<u>Chapter I</u> : The Desert Locust and Convergence Zone.	
Section I : Introduction	4
Section II(i) : Locust Flight Behaviour	6
II(ii) : Convergence	11
II(iii) : Cocheme's contribution	14
Section III : Philosophy of Method	15
Section IV : Analysis of $\nu = \text{constant}$	17
<u>Chapter II</u> : Particle Motion in Potential Flows	
Section I : Steady concentration and Flow in a Corner	24
Section II : Unsteady concentration in a Flow in a Corner	34
Section III : Steady Concentration in a Convergence - Divergence zone	45
<u>Chapter III</u> : Consideration of Non-potential Flows:	
Preamble	53
Section I : A Flow with max. horizontal velocity on the x-axis	56
Calculation I(i): Steady concentration	60
Calculation I(ii): Unsteady concentration	66
Section II : A flow with max. horizontal velocity away from x-axis	70
Calculation II(i): Steady concentration	75
Calculation II(ii): Unsteady concentration	81
<u>Chapter IV</u> : More Potential Flows.	
Section I : Particle Concentration in a Flow with a tilted Interface	85
Section II : Particle Concentration in a Flow Past an Obstacle	92
<u>Chapter V</u> : Summary and Conclusion	
Recommendation	101
Appendix I : .	103
Appendix II : .	105
Bibliography : .	106

Abstract

In the last few decades field studies have shown that the Desert Locust swarms tend to accumulate in the lower levels of convergence because the temperature reduction of air masses above a certain height causes locusts to sink.

Accordingly, the aim of this exercise is to study by way of mathematical modelling the effects of falling speed upon particles (analogue of insects) travelling towards, into and out of the convergence zone. In chapters II and IV we use the method of potential flows into which a particle distribution is introduced. Using the equation of continuity, effects of downstream motion have been constructed. In chapter III we extend our model to include non-potential flows; however, the overall treatment, as far as the behaviour of particles is concerned, remains the same.



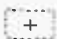
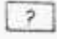
From this work, we confirm the validity of our hypothesis that falling speed leads to higher downstream concentration. We have demonstrated from non-potential flows in chapter III that convergence acts as a concentrator, and that divergence acts as a disperser, of particles. From the steady distributions, we are able to conclude that a falling speed greater than or equal to a 'critical' value will tend to concentrate particles in the lower levels of convergence zone.

Symbols

$c$	-	velocity of sound	
$\underline{f}$	-	coriolis acc <sup>n</sup> . vector	
$\underline{g} = (0, 0, -g)$	-	gravity vector	
$p$	-	pressure	
$q$	-	scalar value of $\underline{U}$	
$\rho$	-	density of air	
$\sigma$	-	concentration of particles	} - non-dimensionalised
$t$	-	time	
$\underline{U} = (u, , w)$	-	flow velocity	
$\underline{U}_p$	-	particle velocity	
$v$	-	falling speed	
$x, y, z$	-	cartesian co-ordinates	

Chapter 3 defines its own symbols.



-  Limit of recorded distribution of swarms
-  Areas where breeding has been recorded in seven or more years during 1939 - 58
-  Areas where locusts have been reported at sea
-  Areas from which reports are largely or wholly lacking

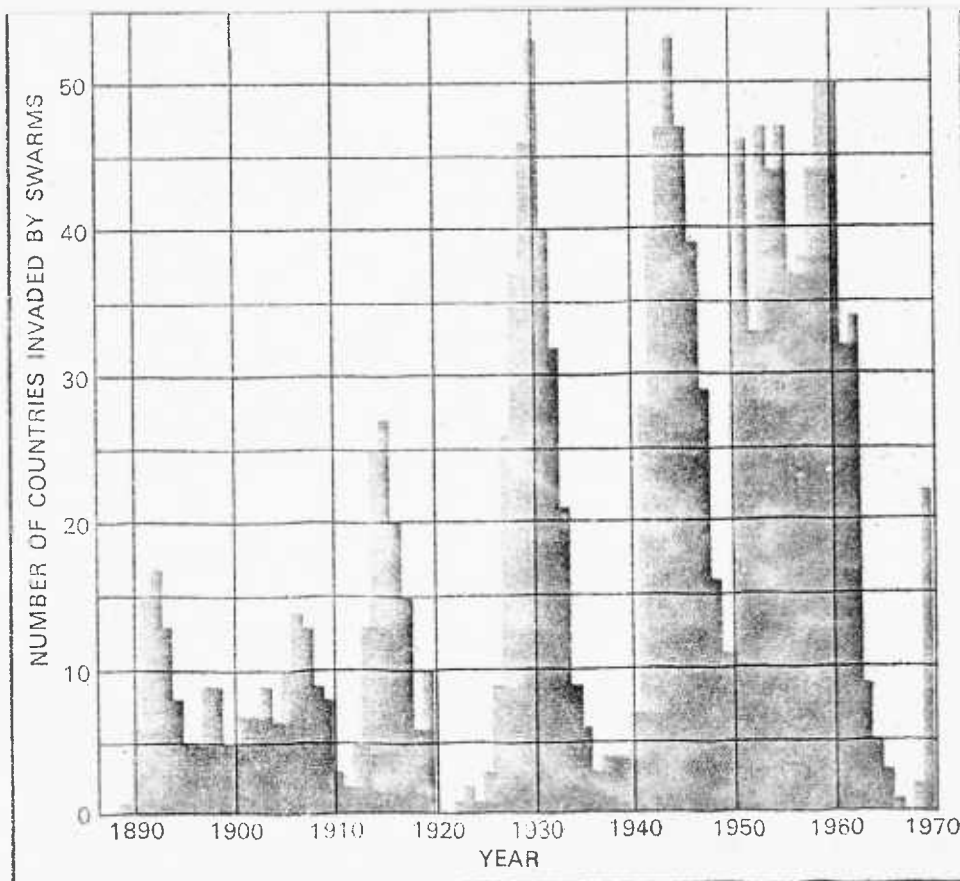
Kilometres  
0 500 1000 1500 2000

Chapter I

The Desert Locust and Convergence Zone

Section 1 : Introduction

During the last one hundred years, we have accumulated and studied vast quantities of data on the feeding, breeding and migratory activities of many insects and other pests. Much attention has been focused upon, in particular the 'desert locust' (one of the dozen or so species of Orthoptera, the so-called 'swarming locust'), because the damage that they inflict upon agriculture is so enormous and paralysing, economically speaking. The extent of the area of their periodical invasion may actually amount to one-sixth or more of the land on earth and it comprises much of the Middle East, and North and Central Africa and South West Asia. (See the map on previous page). There are similarly behaving species in Australia and central South America.



One of the reasons why they are a gargantuan menace is that they are capable of forming vast populations - a typical and dangerous manifestation of their behaviour and migrating over vast distances. In a typical swarm there may be 35-70 million locusts in a square kilometre. Each adult weighs between two and three grams and can eat its own weight of food a day. So, a large swarm covering 400 square kilometres - amounting to more than 15,000 million locusts - could very comfortably devour in a day a quantity of green material, which, if it were all to be human food, could provide for a day's supply for the entire population of England. Apart from causing the direct crop losses, locusts can do severe damage to rangeland, thereby adversely affecting production of meat from stock.

Vast resources have been utilised to record field observations for the forecasting of day-to-day and seasonal movement of swarms to make the control of the pest possible. Also, there have been conducted laboratory experiments at the Centre for Overseas Pest Research (COPR), which have thrown light upon the necessity of maintaining the body temperature (which is generally the same as the surroundings) above a certain value in order to ensure that the efficiency of flight muscle performance does not wane. The experiments have also established that the average airspeed of the locust is found to be between 13 and 15 kilometres per hour.

The extensive biographical analysis of the distribution of the desert locust has vividly revealed that migrations were not haphazard, but indicated definite seasonal patterns. In summer, for example, the locusts are found in a straddling belt across Africa from Senegal to Ethiopia, across South Arabian Peninsula



and on to India and Pakistan. As season changes, swarms from this area move along well-defined routes to the spring breeding areas and after breeding there, the resultant populations move back to the summer breeding areas to complete the cycle.<sup>1</sup> These migratory routes do evidently coincide with the seasonal variations of positions of convergent wind systems, but more about that will be mentioned later.

Before we proceed with the general discussion of the characteristic flight behaviour of the desert locust, one thing worthy of mention is the association of concentration of locusts with types of swarms. Depending upon the weather conditions and topography of the area, there are found to be two structures of swarms. One is known as a stratified swarm and the other as the cumuliform swarm (See Plates 1(a) and 1(b)). The former could range from a few metres to several tens of metres in vertical extent with volume concentration of the order of one to ten locusts per cubic metre, while the latter, with the volume concentration of 0.1 to .001 (or less) locusts per cubic metre, could range in vertical extent from above 100 metres to over a thousand metres. Maximum height could be attained with the topmost locusts flying within 150 metres of the upper limit of the dry convection from the ground.

## Section 2(i)

### Locust Flight Behaviour

(a) Each airborne swarm is constituted of a number of groups of locusts with a common orientation clearly recognizable within each group and with the widest possible diversity of tracks between the

Plate 1



(a). A stratiform swarm of desert locusts, flying in air in which there was very little convection. (Photo by H. J. Sayer).



(b). A column of locusts carried temporarily by a thermal to heights to which they would not fly on their own. (Photo by H. J. Sayer).

groups, giving an impression of a network of interlacing streams. It is possible that the diversity of tracks could be due to the influence of varying direction (and the strength) of the wind with height and the associated turbulence, which may be partly responsible for the spacing of the locusts also. Moreover, the photographic evidence supports that the direction of displacement of the whole swarm remains, more often than not, constant and roughly in the direction of the wind. A study of records for 49 cases under observation between 1951 and 1955 indicates beyond doubt that in 24 of the cases the direction of displacement was less than  $10^\circ$  of that of the wind. (Meteorology and the Migration of Desert Locust. WMO report- Technical Note No.54).

b) Much is known about an important mechanism called an 'edge effect', which may be partly responsible for maintenance of the cohesion of swarms. This effect, in which locusts on the edges direct their flight into the swarm, may also contribute to gregarization, producing high concentrations in front of a swarm following a wind whose value increases with height. The effects of gregarization would generally cause a downdraught effect making locusts sink. For example, a concentration of 2 locusts  $/m^3$  of air at, say  $300^\circ K$  would increase the weight of air  $/m^3$  by that produced by cooling the air more than  $1^\circ C$ . So, locusts in front land below and spend some time there until the conditions are favourable enough to join the hind part of the swarm.

c) One other notable but controversial feature of the desert locust flight is the occurrence of regular spacings between the locusts. According to some, this is maintained by interaction caused by emission

of sound by a flying locust, inducing an electrical response in the tympanal organ of the neighbouring locusts. The range of spacing of flying locusts in swarms and the continual cohesion of many travelling swarms (observed in the past) would thus be consistent with possible behaviour reactions operating to keep each locust within visual range of its neighbours, while perhaps avoiding the wakes and collision.

d) What has just been mentioned in (c) however has not been conclusively proved. And there is another school of thought which advocates that such biological interaction is not always necessary and may not always work as far as the maintenance of the cohesion of a swarm is concerned. According to this philosophy, the atmospheric conditions will also play a very significant role in the determination of the structure forms, direction of movement, shape and, therefore, the size of a swarm, obviously affecting the spacings between locusts and the concentration distribution within the swarm.

A three-fold explanation can be given to elucidate how this is possible. First, airborne swarms will fly about at random until their flight becomes 'organised' when meteorological conditions exert influence upon them. Second, it is evidently clear that an inanimate particle cloud (of smoke etc.) will generally be dispersed or broken up when under the influence of convection currents or any other turbulence. Many insect pests such as aphids are affected in a similar way. An airborne swarm will, however, continually strive to ensure bodily cohesion in spite of potentially disruptive weather conditions. Nevertheless, there are recorded situations where swarms have been led to be broken up or dispersed. At any rate, in almost all cases where cohesion is maintained, it is expected that shapes

and sizes of swarms and concentrations within the composite groups must continually vary. Let's go a little further.

As Professor Scorer says, a small swarm would generally be bodily moved rather than be broken up or be dispersed when influenced by a large eddy. This does not necessarily imply that parts of an eddy will not affect the structure of the swarm. Also, a small eddy will not affect a large swarm in a significant way. It could cause certain amount of diffusion but this is counteracted by the edge effect, and when affecting a particular group of locusts (within the swarm) for some time, it could alter its direction of displacement and the spacing between locusts within it, perhaps, to an extent.

Third, the effect upon swarms become much more pronounced when the size of a swarm is comparable to that of an eddy. In such cases, according to Professor Scorer, the shape and the size may alter, reducing or raising concentration distributions within the swarm.

Moreover, to say that the swarms accumulate in the convergence zones is primarily due to their gregarious behaviour alone is to be unimaginative and decidedly irrational. Locusts sink because reduction of temperature of air masses leads to the loss of efficiency of their flight muscles.

e) Dr. Rainey's Postulate

Although the rainfall in much of the area connected with desert locust is scanty and extremely erratic, the locust swarms, time and again, have been observed to find these areas unerringly, so much so that their arrival with rainfall has been recognised as remarkable for a long time.

Explanation of this was given by Dr. Rainey in 1951, then working

in close cooperation with W.M.O.; he put forward a hypothesis that major displacement of swarms occur downwind, into zones of convergence, and that swarms in general may be expected to collect in the vicinity of such areas.

This theory obviously and lucidly demonstrates a purposeful relationship between the distribution and movement of swarms and the rainfall which is essential for successful breeding; for convergence is an intrinsic factor for the production of widespread, perhaps, heavy rainfall and, as the amount of water present in the eggs at the time of laying is less than half the amount required for the successful completion of embryonic cycle, water and moisture are absorbed from the sand or soil in which they are laid. Moreover, there is another extra-ordinary factor which nature takes into account: absent in the desert is the vegetation required by the 'nymphs' (young locusts) which they feed on voraciously. This need is automatically provided for by rainfall which almost literally causes the whole area to blossom in a matter of a few days.

This idea has provided a tremendous impetus in revolutionizing the method of application of pesticide for locust control. The older methods, namely, spraying over crops, was like spraying on people in order to kill malarial mosquitoes. Grossly inefficient, it could easily introduce unwanted chemicals in large concentrations into soil, thereby hindering biological activities conducive to crop production in various ways.

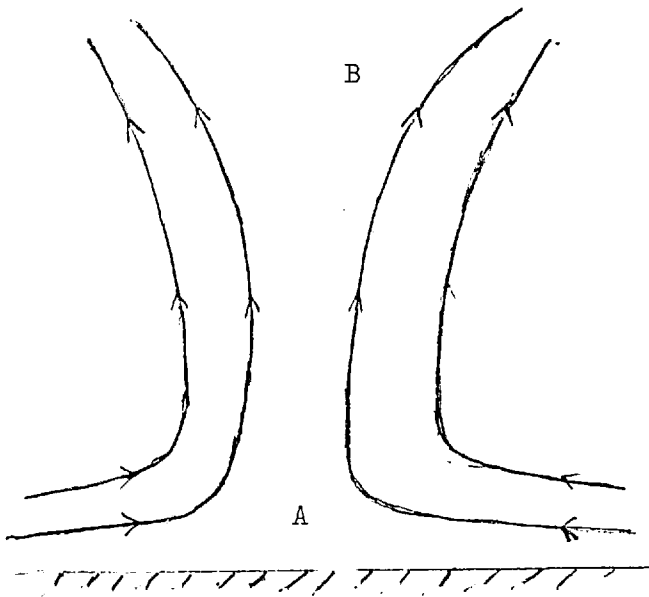
The modern method, on the contrary, cannot only reduce to nearly zero the quantities of these hideous agents entering into soil, but also eliminate chances of polluting the crops as it could be utilised just as effectively in the barren or desert areas. This new much improved method, namely, spraying of airborne swarms, can be

made over a million times more efficient in terms of insecticide used than the old one. Furthermore, better timely manipulation of it during the occurrence of certain atmospheric phenomena (convergence etc.) which would aggregate insects may enable the use of insecticides to be minimised.

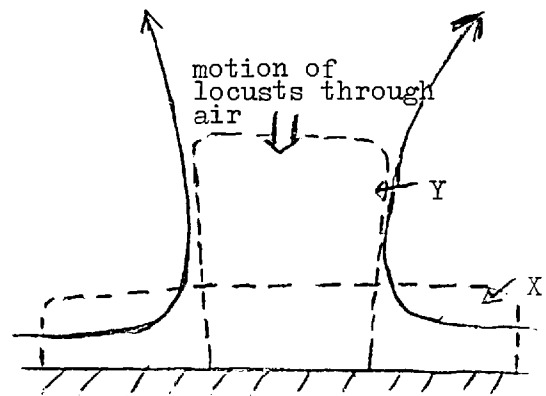
Section II (ii)

Convergence

The point is, should the direction of displacement of insects remain in the direction of the wind, they cannot fail to be driven towards the zones of convergence, in the lower levels of which they accumulate.



Diag. 1a showing convergence in the region A and divergence in B.



Diag. 1b Motion of locusts  
x= initial position  
y= final position  
(high concentration)

One reason why the atmosphere may be an effective concentrator is that it is essentially flat; that is to say that its vertical motions are comparatively smaller in magnitude and more ephemeral in nature than horizontal motions. What happens, in particular, when insects reach the convergence zone is that they 'follow' the air lift and ride up to a height where they sense the temperature of the air is too cool to continue any further, so they start gliding down.

According to Dr. Rainey, in the case of a small-scale thunderstorm with an inflow of air during the early stages from a distance of the order of 10 km, convergence of the order of  $10^{-3} \text{ sec}^{-1}$  is found. This corresponds in straight flow to a  $1 \text{ m s}^{-1}$  decrease in wind velocity over a distance of 1 km and would double the number per unit area of airborne particles under consideration in 17 minutes. Some radar observations confirm that convergence is very much a responsible factor for the formation of high concentrations in swarms. There are, in addition to that, strong indications that convergent winds can, and do, bring insects together from solitary-living populations to form new swarms. All this provides a good case for more intensive study of wind fields in order to gain deeper insight into any quantifiable behaviour of locusts.

A converging motion associated with an upward motion takes place when there is a net excess of inflow of air over outflow. On a broad synoptic scale, it occurs as a result of wind-making circulation of atmosphere, depending upon the pressure belts and other factors from two or more directions. In the case of a sea breeze the air masses from an area of high pressure are driven into areas of depressions or low pressure to produce an upward motion which terminates in divergence. The effects of friction at ground



level could determine how the winds move towards the convergence zone, thereby possibly altering the angle that the line of discontinuity makes with the ground. In low latitudes the earth moves faster than the air, and, therefore, the easterly winds are present in the trade wind belts. These regions are commonly called Inter-tropical Convergence Zone (ITCZ), in which trades converge towards the equator.

On a small scale, convergence can take place when the air on the shore and inland becomes warmer, while the temperature variation of air over the sea remains small. This kind of heating creates pressure differences, setting up the motion. More technically, differential heating along coastlines causing temperature differences (between air on land and air on sea) creates a landward flow, setting up density gradients as the sea air moving into the warmer regions of the land is warmed. These horizontal density gradients combined with operation of gravity on the rising masses of warmed air (travelling from the sea) create vorticity and, hence, there is a converging motion. For instance, sea breeze fronts can develop if the large scale pressure systems produce only a weak wind-flow near the coast and a well-defined boundary is formed between the air flow from the sea and the air already existing over land. Hence, there is a strong convergence of the leading edge of the sea air as it advances.

Examples of areas of convergence affecting regions invaded by the desert locust are the ITCZ between the trade winds and monsoons originating on the opposite sides of the equator, associated with 'short' and 'long' monsoon rains of most of Africa and India; the westerly depressions which give the winter and spring rains in the Persian Gulf; and semi-permanent points between north-westerly

and south-easterly winds associated with winter rains of central and southern Red Sea.

Section II(iii)      Cochame's Contribution

Before writing down and setting out from our assumptions, it is worthwhile mentioning a few things regarding Cochame's contribution (1963 - Tehran); it was one of the very few mathematically deduced explanations of the air motion and its effects on the behaviour of locusts in quantified terms.

His main assumption consisted taking convergence as negative divergence - a terminology common in physics and mathematics - which he defined in terms of the Cartesian and natural co-ordinates (non-dimensionalized). This helped him to visualize the process in the following two ways.

The first entails the rate at which the air is leaving an area (fixed relative to the ground) in excess of that entering it, and yields an outflow out of a fixed area when integration (of divergence) with respect to time is carried out. The second deals with the rate of increase in area of a surface bounded by air particles moving with the stream. However, the integrations were not easy to carry out. So, Cochame' resorted to, insofar as the first approach was concerned, the use of average divergence for periods of time or the assumption that instantaneous values are representative of conditions during this period. Once the inflow or contraction was estimated, he then went on to relate it quantitatively to the changes in concentration of airborne particles at a constant level. According to his calculations an

average convergence of one per day of effective 10 hours (about three units of  $10^{-5} \text{ sec}^{-1}$ ) would bring about a concentration of about a thousand times the original concentration within a week.

His analysis led him to conclude that the relationship between the downstream concentration and the original concentration can be expressed by an equation of continuity for particles at a constant level. Moreover, he makes two points which cannot escape our attention. (a) Since the fraction, locust transport/air displacement decreases as the wind increases the effects of convergence on locust concentration must increase with the increased ageostrophy and constantly decreasing latitude. (b) A certain amount of convergence and corresponding ageostrophic displacement of air will be more effective at lower latitudes than at higher latitudes where such ageostrophy will correspond to a movement of air along isobars and consequently higher wind speeds.

At any rate, his derivation of equation of continuity to relate the final concentration to upstream original concentration is a decisively important step that may lead us to further realise that it may, though one of the basic equations in physics, hold good in describing the locust motion.

Section III Philosophy of method

With the exception<sup>of</sup> the mathematical approach that Cochme' adopted, there is yet a general lack of sufficient quantitative information regarding locust behaviour in a converging airstream. The problem has been that very little or no consideration have been given to the methods of particle dynamics, based on the integration of the primitive

equation of motion. Our primary interest, therefore, is to model the effects of convergence, various patterns of which have been deduced to carry out our exercise. Most patterns are due to some powerful mathematical techniques that enable us to attain potential flows, but the flows discussed in Chapter 3 possess some essential features resembling atmospheric motions and, in that sense, they are realistic. We have to be satisfied with these rather simple flows owing to the common difficulty in attaining accurate mathematical description of atmospheric motions (such as convergence).

We then proceed to work out idealised distributions of concentrations as particles progress downstream towards zones of convergence from a given area when the initial condition is specified. The assumptions we have made have been deliberately kept simple in order to bring out all their feasible effects on moving particles. This has meant excluding from consideration all features that the locusts may possess but are not mathematically quantifiable. Assumptions such as biological interaction, which some affirm to be the principle cause for regular spacings between insects occurring so commonly, have obviously been avoided for the same reason.

The following assumptions have been made, upon which our models have been fundamentally based. First and foremost, we recognise, as did Cocheme, that the equation of continuity is the major requisite equation of motion that will enable us adequately to gain insight into the particle motion tending to create a higher downstream concentration; this equation can be verified by elementary considerations. The second most important factor is the sink speed of particles travelling relative to the flow. Various forms of sinking speed will be used to find out their effects: first, a

constant value will be used and then a value directly proportional to the vertical component of the flow velocity. We have departed from this convention in Chapter III, Section I, where the sinking speed has been specified rather differently.

The locusts can normally fly with a horizontal velocity different from the flow. This is particularly true when the air stream is much too fast for them to follow. So, they fly upstream. The edge effect taking place at the leading edge is also an example of the locusts opposing the air streams; so the occurring horizontal speeds are different. However, the particles will be constrained to have the same horizontal velocity as the flow.

These assumptions, together with the initial condition for concentration, specified in analytical terms, have been the main ingredients used to formulate this model. Retention of a certain degree of control over computer calculation was made possible especially, for all solutions in Chapter 2 which have been analytically expressible. But, owing to the complexity of the differential equations obtained in Chapters 3 and 4, the solutions could not be simply expressed and had to be evaluated using special computing methods for the solutions of differential equations. Two different computing methods were employed to ensure that the obtained results were correct, although overall direct control over computer calculation of results was not possible.

#### Section IV Analysis of $\nu = \text{constant}$

We carry out a brief analysis for the falling speed  $\nu = \text{constant}$ . Given below is the statement and the proof of a theorem in three

dimensions followed by a simple illustrative example for a two dimensional case.

Theorem : Provided the falling speeds of particles travelling in a converging motion of air are all kept the same, the magnitude of concentration along a particle path remains constant.

Proof : Consider the  $(x,y,z)$  frame of reference with  $z$  vertical, directed upwards. Let  $\underline{U} = (u,v,w)$  be the velocity field vector pertaining to the flow and let  $\underline{U}_p = \underline{U} + \underline{V}$  represent the particle velocity, where  $u, v$  and  $w$ , functions of  $x, y$  and  $z$ , are the velocity components in the  $x$ -,  $y$ -, and  $z$ - directions respectively and  $\underline{V} = (0,0,-V)$  is a constant falling velocity of the particles relative to the flow.

The equation of continuity for steady particle concentration is given by

$$\text{div} (\sigma(x,y,z) \underline{U}_p) = 0 \quad \dots\dots (1.4.1)$$

where  $\sigma(x,y,z)$  denotes the particle concentration.

Expanding (1.4.1) we get

$$\frac{D\sigma}{Dt} = u \frac{\partial \sigma}{\partial x} + v \frac{\partial \sigma}{\partial y} + (w - V) \frac{\partial \sigma}{\partial z} = -(\text{div} \underline{U} - \frac{\partial V}{\partial z}) \sigma \dots (1.4.2)$$

where  $\frac{D}{Dt}$  is the rate of change following a parcel of fluid.

As  $V = \text{constant}$

$$\frac{\partial \nu}{\partial z} = 0, \quad \dots \quad (1.4.3a)$$

and

$$\text{div } \underline{U} \simeq 0 \quad \dots \quad (1.4.3b)$$

in the light of the relationship

$$\text{div } \underline{U} = \frac{gw}{c^2}, \quad \dots \quad (1.4.4)$$

because the right hand side expression  $gw/c^2$  can be regarded as being negligibly small for our purposes, where  $g$  and  $c$  are the acceleration due to gravity and the velocity of sound in air respectively. [For the proof of (1.4.4) see Appendix I].

Therefore the equation (1.4.2) reduces to

$$\frac{D\sigma}{Dt} = u \frac{\partial \sigma}{\partial x} + v \frac{\partial \sigma}{\partial y} + (w - \nu) \frac{\partial \sigma}{\partial z} = 0$$

from which, given  $u(x,y,z)$  etc, we may obtain  $\sigma$  in the form

$$\sigma(x,y,z) = \text{constant } (c_0), \quad \dots \quad (1.4.5)$$

and

$$\text{and } \left. \begin{aligned} f_1(x,y) &= c_1 \\ f_2(x,z) &= c_2 \end{aligned} \right\} \dots \quad (1.4.6)$$

using the differential equation relationship

$$\frac{dx}{u(x,y,z)} = \frac{dy}{v(x,y,z)} = \frac{dz}{(w(x,y,z)-U)} \quad ,$$

where  $c_0$ ,  $c_1$  and  $c_2$  are arbitrary constants due to integration and  $f_1(x,y)$  and  $f_2(x,z)$  together define particle paths.

On eliminating  $c_0$ ,  $c_1$  and  $c_2$  from (1.4.5) and (1.4.6), we find

$$\sigma(x,z) = F(f_1(x,y), f_2(x,z)),$$

and since  $f_1$  and  $f_2$  are constants for all  $x$ ,  $y$  and  $z$ ,  $F(f_1, f_2)$  is also constant.

#### Example

Let us take the two-dimensional flow used in section I of the next chapter to demonstrate this theorem. The velocity fields as given in (2.1.3) is

$$\underline{U} = (-2AUx, 0, 2AUz)$$

where  $A$  and  $U$  are constant.

As the condition (1.4.3a) naturally holds when we write

$$AUU = \text{constant}$$

and as (1.4.3b) modifies to



$$\text{div } \underline{U} = 0$$

for a two-dimensional flow, (1.4.2) becomes

$$\frac{D\sigma}{Dt} = -2x \frac{\partial \sigma}{\partial x} + (2z - \nu) \frac{\partial \sigma}{\partial z} = 0 \quad \dots \quad (1.4.7)$$

Integration yields the solution

$$\sigma(x, z) = F(x(2z - \nu))$$

where the variable

$$x(2z - \nu) = \text{constant} \quad \dots \quad (1.4.8)$$

describes the particle paths and is obtained by integrating

$$\frac{dx}{-2x} = \frac{dz}{(2z - \nu)}$$

If we define the initial distribution of concentration at  $x = 1$

by way of example as

$$\sigma(1, z) = z^2 \exp(-z^2)$$

the solution satisfying (1.4.7) is

$$\sigma(x, z) = \frac{1}{4} \left\{ \nu + (2z - \nu)x \right\}^2 \exp \left\{ -(\nu + (2z - \nu)x)^2 / 4 \right\} \dots (1.4.9)$$

for all  $x$  and  $z$  and  $\nu < 2z$ .

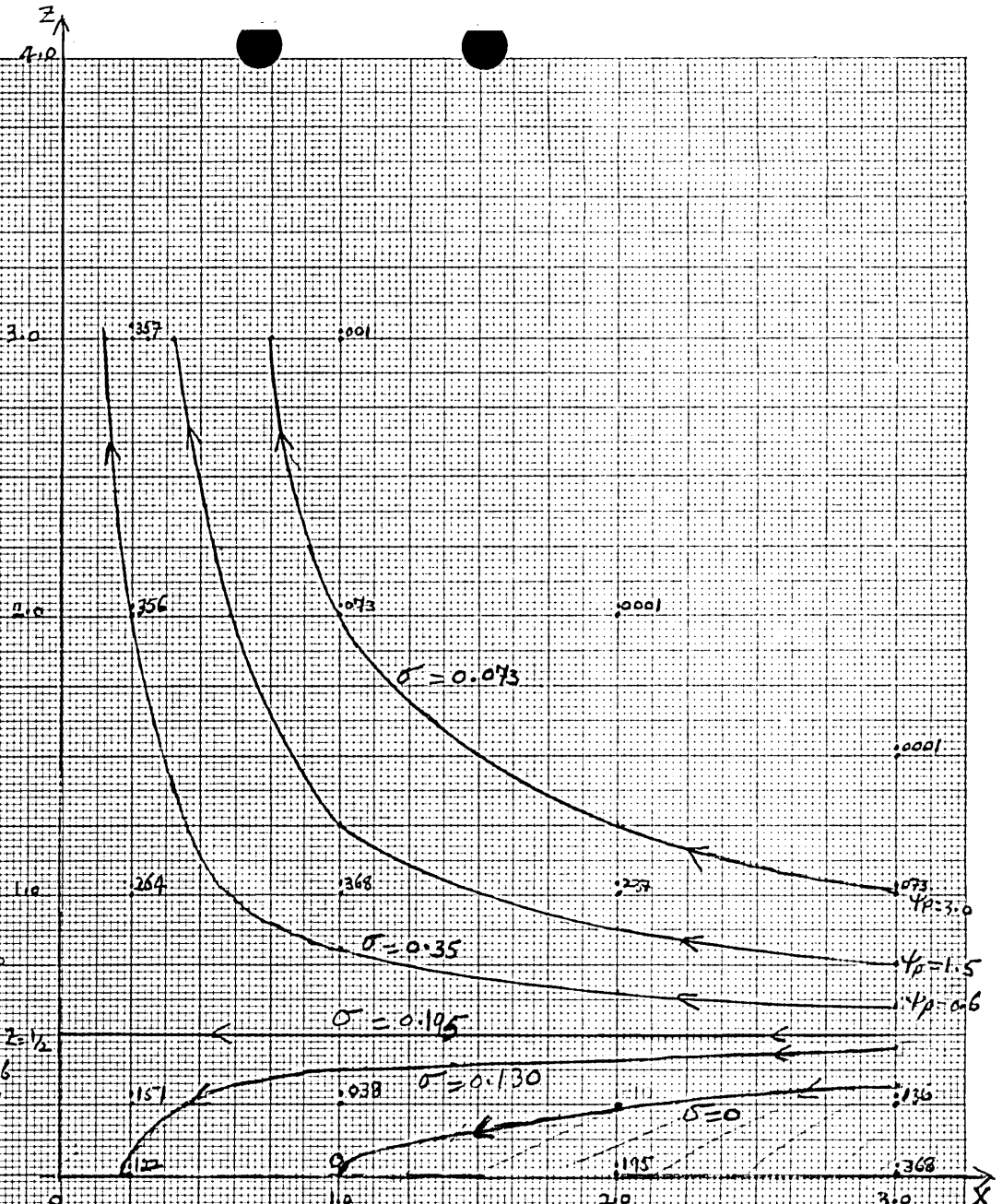
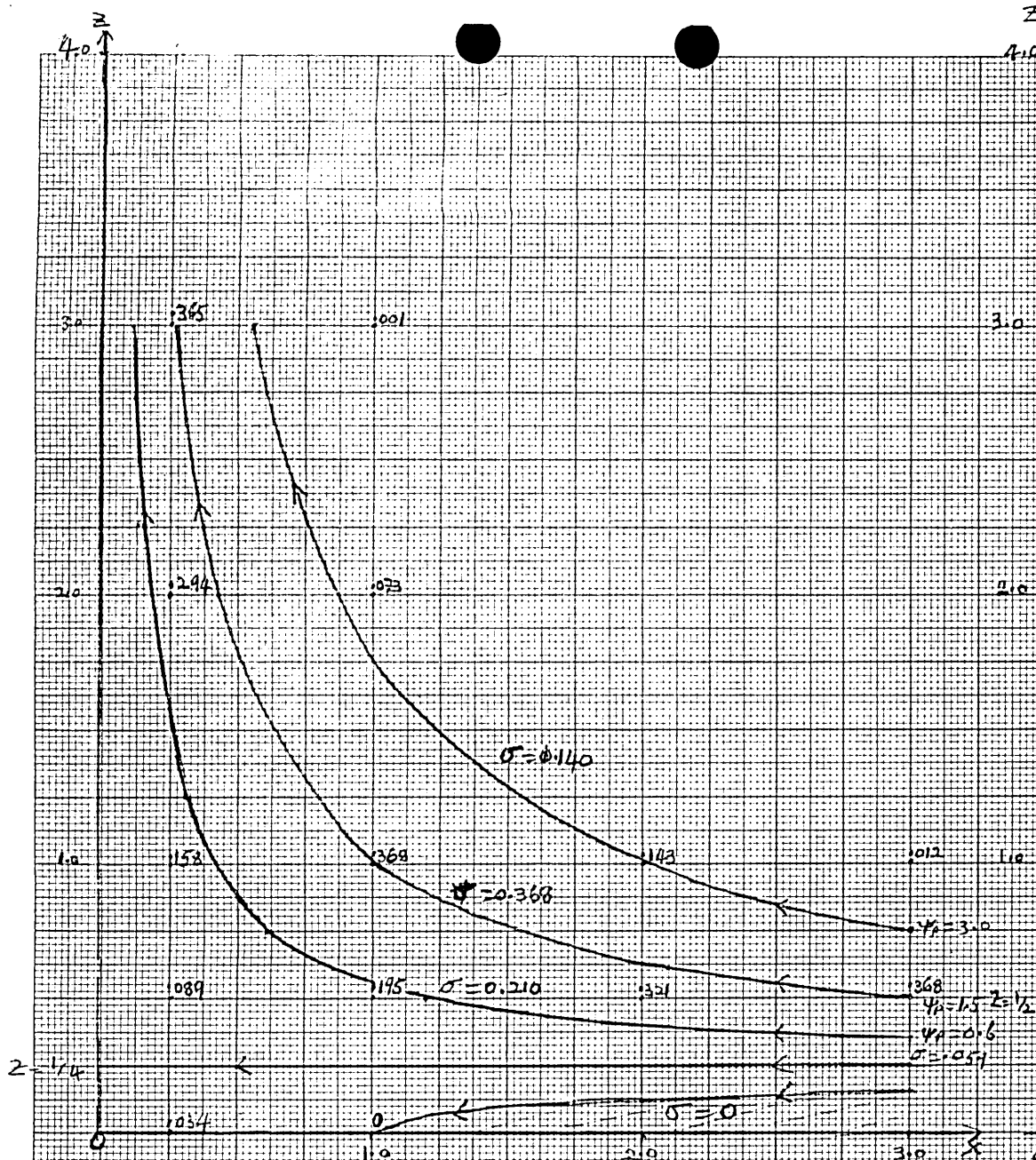


Fig. 1

Fig. 2

An example of a distribution with constant concentration along particle paths, obtained for  $\nu = \frac{1}{2}$  in (1.4.9). The constant values  $\psi_F$  in (1.4.8) define positions of particle paths for all  $\nu$ .

Another distribution, illustrating the theorem, is obtained for  $\nu = 1$ .

The concentration distributions for the values of the falling speed  $\nu = \frac{1}{2}$  and  $\nu = 1$  are shown in Fig. 1 and 2 on the page 22. Besides fulfilling our objective - substantiating that concentration along particle paths is constant - they bring out one main feature. The horizontal line,  $z = \nu/2$ , divides the particle motion into two regions : the upper, in which the particles move upwards ; and the lower, in which they are constrained to a downward motion. The lower region is divided into two sub-regions; and only the particle motion in the sub-region bounded by the axes and the contour  $\sigma = 0$  and the line  $z = \nu/2$  is observed to be directed towards the 'corner' formed by the axes of reference. A few people have commented that some contribution to accumulation of particles in the convergence zone is made by those travelling below a certain height. The lower region (and especially the upper sub-region in the lower region) we believe would match vaguely with this.

One implication of this theorem is that downstream accumulation of particles is not possible. We must, therefore, of necessity choose not to take the falling speed  $\nu$  as a constant but rather as a function of height or of some other form. The falling speed as a function of height is crudely in accordance with the locust behaviour in that the higher the locusts ascend (above a certain height) the greater the falling speed with which they have to respond in order to avoid being carried higher up and dispersed by divergence.

Chapter II

Particle Motion in Potential Flows

We concentrate on simple potential flows in this chapter, as in the Chapter 4. In such flows the velocity distribution is entirely determined by a linear equation signifying the absence of vorticity (i.e. the flows are irrotational) and the equation of conservation of mass. This linearity is a special characteristic of irrotational flows which allow the employment of several powerful mathematical techniques.

Section I Flow in a corner and steady concentration

Using one of the well-known techniques, namely, complex transformation, a stream function  $\psi(x, z)$  of flow is evaluated. The complex analytic function,  $W = f(Z)$ , satisfying the Cauchy-Riemann condition determines a mapping of  $Z$ -plane in the  $W$ -plane, i.e. the streamlines of the fluid motion in the  $Z$ -planes maps into the straight lines

$$\psi = \text{constant parallel to the real axis in the } W\text{-plane.}$$

For a flow in a corner, the complex potential is

$$\Omega = UW(Z) = AUZ^2 .$$

Therefore, the velocity potential denoted by  $\phi(x, z)$  and the corresponding stream function  $\psi(x, z)$  are given respectively by

$$\phi(x, z) = AU(x^2 - z^2) \dots \dots \dots (2.1.1a)$$

and

$$\psi(x, z) = 2AU xz \dots \dots \dots (2.1.1b)$$

where  $A$  is a constant describing the transformation,  $U$  is a constant velocity of the flow in the  $W$ -plane with a direction parallel to the real axis and

$$Z = x + iz$$

Assuming that the flow velocity  $\underline{U}$  is defined in the conventional sense  $\underline{U} = \underline{\text{grad}} \phi$  we have

$$\underline{U} = (-2AUx, 0, 2AUz) \quad \dots \quad (2.1.2)$$

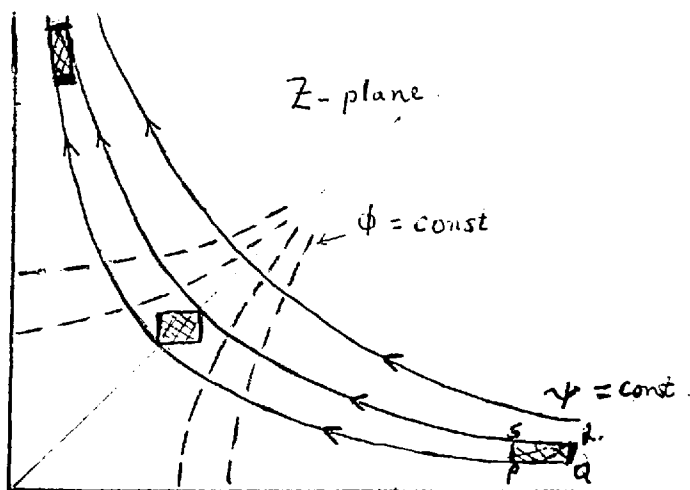


Diagram 3a Sketches of streamlines  $\psi = \text{const}$  and equipotential lines of the flow

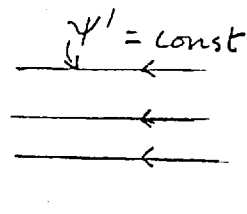


Diagram 3b. Flat flow in  $W$ -plane.

The mechanism operating on this motion can be better understood by considering an element of fluid PQRS (as shown in the diagram) whose sides are parallel to the axes. We notice from the velocity vector (2.1.2) that the horizontal velocity, which is the same for all points on QR, depends on  $x$  only, while the vertical velocity which remains constant for all points on PQ depends on  $z$  alone. This means that the horizontal velocity decreases,

producing horizontal contraction in the element PQRS as it progresses towards the z-axis and, as a result, producing vertical expansion, bringing about an ascending motion.

We now choose the particle falling speed as proportional to the vertical component of the flow velocity,

$$\text{i.e. } \nu = \frac{nW}{2} = AU_n z \quad .$$

This is conveniently dependent upon height. Hence, the particle velocity becomes

$$\underline{U}_p = (-2AU_x, 0, (2-n) AU_z) \quad . \quad . \quad . \quad (2.1.3)$$

Substituting this into the continuity equation (1.4.1) we get

$$\frac{\partial}{\partial x} [-2AU_x \sigma(x, z)] + \frac{\partial}{\partial z} [(2-n) AU_z \sigma(x, z)] = 0$$

which reduces to

$$-2x \frac{\partial \sigma}{\partial x} + (2-n) \frac{z \partial \sigma}{\partial z} = n\sigma \quad \dots \quad (2.1.4)$$

By the method of characteristics (see Appendix II) the equation (2.1.4) is equivalently represented by the relationship

$$\frac{dx}{-2x} = \frac{dz}{(2-n)z} = \frac{d\sigma}{n\sigma} \quad .$$

Integration yields

$$\sigma(x, z) = A_0 x^{-n/2}$$

and

$$x^{\frac{1}{2}} z^{\frac{1}{2-n}} = B_0^*$$

where  $A_0$  and  $B_0$  are arbitrary constants of integration. These two equations can be linked by means of putting  $A_0$  as a function of  $B_0$ ,

$$\text{i.e. } A_0 = f\left(x^{\frac{1}{2}} z^{\frac{1}{2-n}}\right).$$

Thus, the general solution for concentration is given by

$$\sigma(x, z) = x^{-n/2} f\left(x^{\frac{1}{2}} z^{\frac{1}{2-n}}\right) \dots \quad (2.1.5)$$

Let a hypothetical distribution of particle concentration be given by a function

$$\sigma(a, z) = \lambda \exp(-z)$$

defined at some distance  $a$  away from the  $z$ -axis. When we substitute  $x = a$  in (2.1.5) and compare it with the initial concentration given above we obtain

$$f\left(a^{\frac{1}{2}} z^{\frac{1}{2-n}}\right) = [\lambda/a^{-n/2}] \exp(-z)$$

where  $\lambda$  is constant.

\* It is values of  $B_0$  which determine the position of particle trajectories - - - incorporated with distributions of concentration (see Fig. 4, 5 and 6).

$$\text{If } R = a^{\frac{1}{2}} \frac{1}{z^{2-n}}$$

$$\text{so that } z = \left( R/a^{\frac{1}{2}} \right)^{\frac{1}{2-n}},$$

then

$$f(R) = \left( \lambda/a^{-n/2} \right) \exp \left[ -\left( R/a^{\frac{1}{2}} \right)^{\frac{2-n}{2}} \right]$$

when  $R$  is substituted in terms of  $x$  and  $z$ .

$$f(x, z) = \left( \lambda/a^{-n/2} \right) \exp \left[ -z(x/a)^{\frac{2-n}{2}} \right], \dots \quad (2.1.5a)$$

Therefore (2.1.5) renders the solution

$$\sigma(x, z) = \lambda(x/a)^{-n/2} \exp \left[ -z(x/a)^{\frac{2-n}{2}} \right] \dots \quad (2.1.6)$$

When  $n = 0$  in the last equation

$$\sigma(x, z) = \lambda \exp \left[ -z(x/a) \right],$$

and so, we have an example of a situation where constant concentration along a particle path occurs, with a constant value  $\lambda$  of concentration forming on the axes. But when  $n > 0$ , there is a downstream increase with an infinite concentration resulting on the  $z$ -axis owing to the factor  $(x/a)^{-n/2}$  in (2.1.6). On the  $x$ -axis, the distribution would be

$$\sigma(x, 0) = \lambda(x/a)^{-n/2}.$$

Since it is evident that the number of cases we can consider



from (2.1.6) is limited we define another initial distribution

$$\sigma(a, z) = z^2 \exp(-3z) \quad \dots \quad (2.1.7)$$

at  $x = a$ , which has a minimum at  $z = 0$  and a maximum at  $z = 2/3$ .

One main reason for selecting an exponentially decreasing factor has been to maintain the low-level concentration comparatively higher, at least, at the outset to match the conditions of a flying swarm.

Using (2.1.5) and (2.1.7) we determine  $f(x, z)$  in the same way as the function (2.1.5a) and hence,

$$\sigma(x, z) = z^2 (x/a)^{\frac{4-3n}{2}} \exp \left\{ -3z (x/a)^{\frac{2-n}{2}} \right\} \dots \quad (2.1.8a)$$

For convenience we choose  $a = 3$ .

$$\text{Therefore, } \sigma(x, z) = z^2 (x/3)^{\frac{4-3n}{2}} \exp \left\{ -3z (x/3)^{\frac{2-n}{2}} \right\} \dots \quad (2.1.8)$$

The restriction

$$\left. \begin{array}{l} \sigma(x, z) = 0 \\ \text{when } z(x/3)^{\frac{2-n}{2}} \geq 2 \end{array} \right\} \dots \quad (2.1.9)$$

has been applied to the solution (2.1.8).

By varying  $n$ , it is now possible to discuss three distinct cases:

We shall introduce them separately, before making any comparison

and discussing any common features.

Case I

(a) First of all, taking  $n = 0$  amounts to arriving at a situation where the particles would be travelling with the flow and, therefore, no downstream growth in concentration is expected. This is another example where concentration along particle paths remains constant (see Fig. 3 page 31 ).

(b) Second, choosing  $n = 1$  for study in the range  $0 < n < 4/3$ , the distribution (see Fig. 4 page 31 )

$$\sigma(x, z) = z^2 (x/3)^{\frac{1}{2}} \exp (-3z(x/3)^{\frac{1}{2}}) \dots \quad (2.1.10)$$

is obtained from (2.1.8). According to this distribution, the progressive growth in concentration gets closer and closer to z-axis (though without touching it) as the particles ascend higher and higher. The particles obviously get carried up to infinity and there would be no tangible accumulation in the convergence zone, in spite of the downstream increase.

Case II

$n = 4/3$ . This is a critical case in that the factor  $(x/3)^{\frac{4-3n}{2}}$  vanishes from the equation (2.1.8) which consequently reduces to

$$\sigma(x, z) = z^2 \exp [-3z(x/3)^{\frac{1}{3}}] , \dots \quad (2.1.11)$$

the concentration contours for which are given in the Fig. 5 (Page 32 ).

Fig. 3 This is yet another example where constant concentration along particle paths occur. As  $n=0$  in (2.1.8), particles are travelling with the flow.

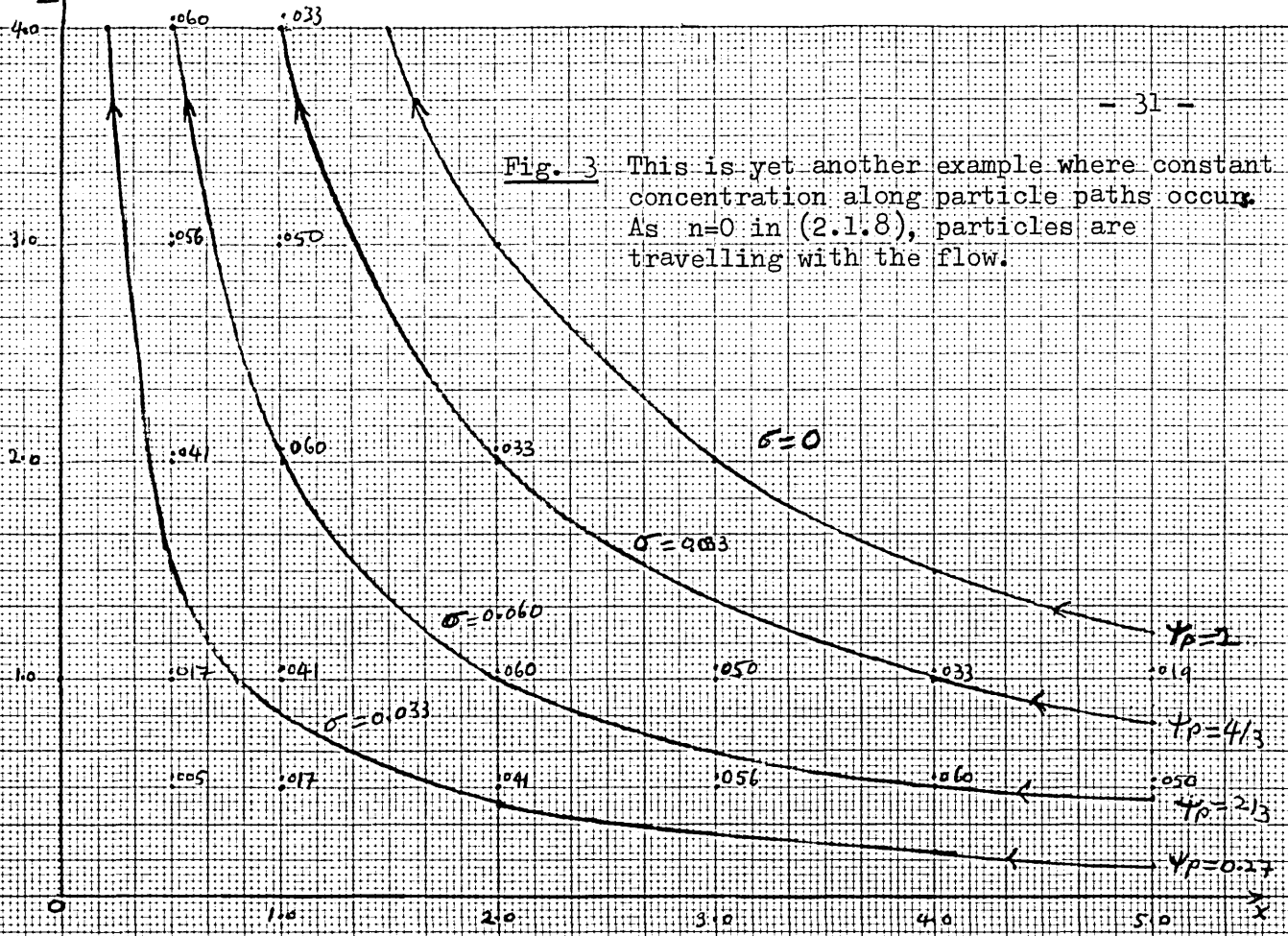
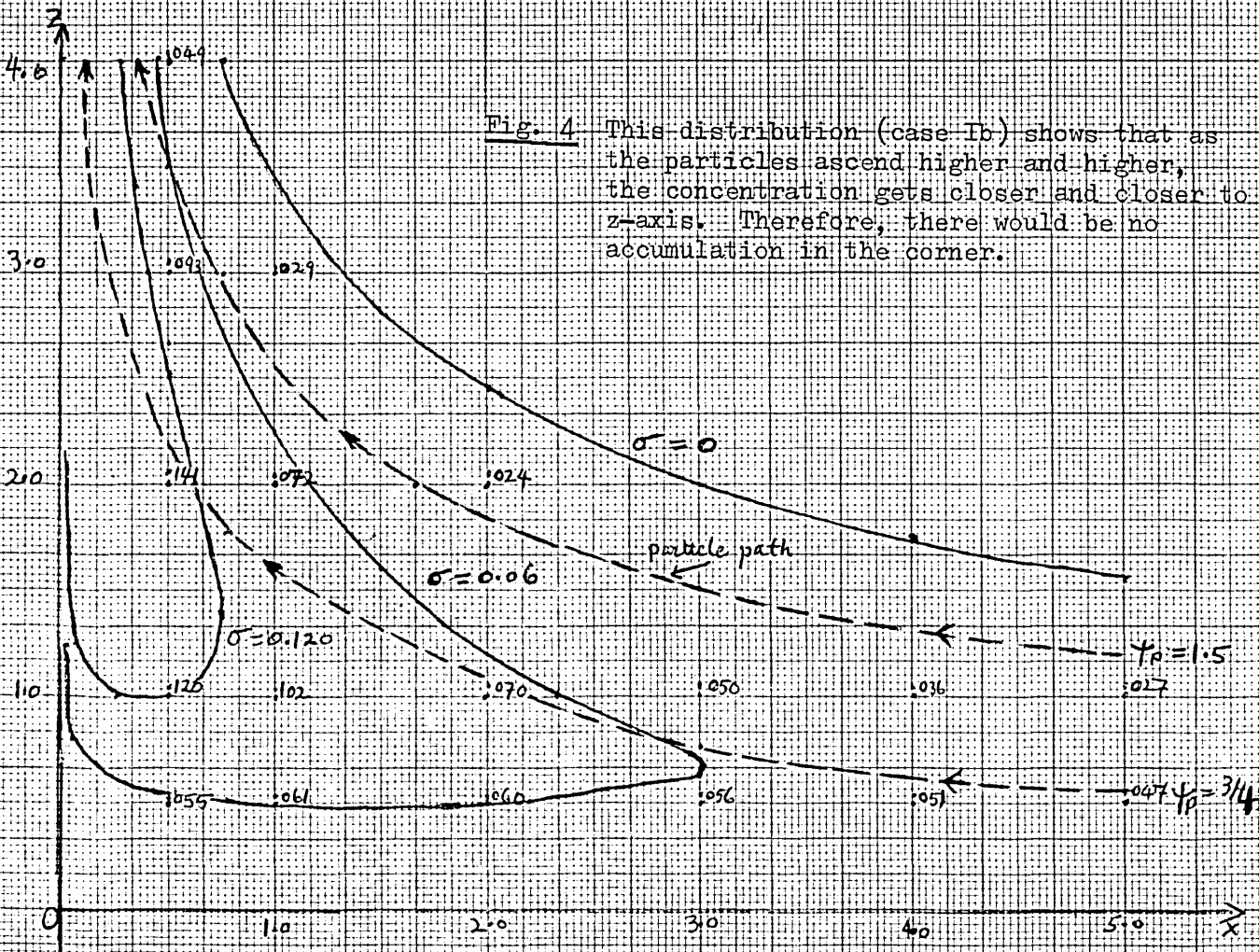


Fig. 4 This distribution (case Ib) shows that as the particles ascend higher and higher, the concentration gets closer and closer to z-axis. Therefore, there would be no accumulation in the corner.





In this case we obtain maximum concentration on the z-axis, which has a value equal to the square of height. Again, though there is a certain downstream increase, there is comparatively low accumulation in the convergence zone.

### Case III

For any value of n between 4/3 and 2.0, the function  $\sigma(x, z)$  becomes infinite for  $x = 0$ . For the purpose of our analysis we have chosen  $n = 1\frac{1}{2}$ , which renders the following equation from (2.1.8):

$$\sigma(x, z) = z^2(x/3)^{\frac{1}{4}} \exp [-3z(x/3)^{\frac{1}{4}}] \dots \dots \dots (2.1.12)$$

the contours for which can be seen in the Fig. 6 (page 32). This is the only case which can be said to have downstream accumulation in the convergence zone, although infinitely large.

If we, nevertheless, consider first a particle moving along a trajectory (dotted lines in the Figs. 4, 5 and 6)  $\psi_p = 0.75$  whose rate of ascent decreases (with increasing n) between its intersection of contours  $\sigma = 0.06$  and  $\sigma = 0.12$ , we can at least understand quantifiably the effects of successively increasing falling speed. (Between the points of intersection, the horizontal distance traversed in all cases would be the same.) For example, in case I(b) (Fig 4), the particle, in order to double the concentration, rises a vertical distance of unity above the point of intersection between the trajectory in question and the contour  $\sigma = 0.06$ , while in the cases II and III there are corresponding decreases in the height to which the particle rises before the concentration is doubled (see Figs 5 and 6).

Also, when  $n = 2$ , we have a case with particles travelling horizontally, the effect of which is to bring about infinite value of concentration on the  $z$ -axis, and (2.1.8) becomes

$$\sigma(x, z) = z^2(x/3)^{-1} .$$

And, when  $n = 2\frac{1}{2}$  (2.1.8) would be written as

$$\sigma(x, z) = z^2(x/3)^{-7/4} \exp [- 3z(x/3)^{-3/4}]$$

according to which for any value of  $n > 2$ , we would have zero concentration on the axes, which is only due to the manner of specification of  $\sigma$ .

We have, therefore, by considering this flow and steady distributions achieved what we set out to do, although the region in question is unbounded which is why large concentrations are carried up to infinity. In addition to this, dealing with a steady distribution does not provide a picture of how concentrations develop in time. We therefore examine the movement of a given distribution at some initial time  $t_0$ , using the same flow.

## Section II Unsteady concentration in a Flow in a Corner

Using the same flow velocity field and falling speed as in the last section, we derive a similar equation of motion given by

$$\frac{\partial \sigma}{\partial t} + \text{div} \quad (\underline{U}_p \sigma(x, z)) = 0 \quad \dots \quad (2.2.1)$$

which now becomes

$$\bullet \quad \frac{\partial \sigma}{\partial t} - \frac{2x}{\partial x} \frac{\partial \sigma}{\partial x} + (2-n)z \frac{\partial \sigma}{\partial z} = n\sigma \quad \dots \quad (2.2.2)$$

AU in (2.1.3), being used here, is taken as unity.

This equation is reduced by the method of characteristics to

$$\frac{dt}{1} = \frac{dx}{-2x} = \frac{dz}{(2-n)z} = \frac{d\sigma}{n\sigma} ,$$

from which a set of equations

$$\sigma(x, z, t) = A_0 e^{nt}$$

$$x^{\frac{1}{2}} z^{\frac{1}{2-n}} = B_0$$

and  $x^{\frac{1}{2}} e^t = C_0$

is obtained by integration, where  $A_0$ ,  $B_0$  and  $C_0$  are arbitrary constants. By writing  $A_0$  as a function of  $B_0$  and  $C_0$  we get the general solution

$$\sigma(x, z, t) = e^{nt} f\left(x^{\frac{1}{2}} z^{\frac{1}{2-n}}, x^{\frac{1}{2}} e^t\right) \dots \quad (2.2.3)$$

Let the initial distribution whose development in time we want to examine be defined by

$$\sigma(x, z, 0) = \frac{1+z}{1+x} \exp [1-z] \dots \quad (2.2.3a)$$

at the time  $t = 0$ .

One noticeable feature of this distribution, unlike the one specified in the last or the next section, is that it is specified

over the whole region and, therefore, is more realistic.

Comparing it with (2.2.3), we have

$$f(x^{\frac{1}{2}}, z^{\frac{1}{2-n}}, x^{\frac{1}{2}}) = \frac{1+z}{1+x} \exp(1-z), \dots \quad (2.2.4)$$

Assuming  $P = x^{\frac{1}{2}} z^{\frac{1}{2-n}}$

and  $Q = x^{\frac{1}{2}}$

so that  $z = (P/Q)^{2-n}$

(2.2.4) can be written in terms of P and Q,

i.e.

$$f(P, Q) = \frac{1 + (P/Q)^{2-n}}{1 + Q^2} \exp(1 - (P/Q)^{2-n}),$$

which becomes

$$f(x, z, t) = \frac{1 + z e^{(n-2)t}}{1 + x e^{2t}} \exp[1 - z e^{(n-2)t}]$$

when P and Q are substituted back, with Q this time put in terms of x and t.

Therefore (2.2.3) is now rendered as

$$\sigma(x, z, t) = \frac{e^{nt} + z e^{2(n-1)t}}{1 + x e^{2t}} \exp[1 - z e^{(n-2)t}] \dots \quad (2.2.5)$$

for all x, z, and t.

Of the three cases possible for n less than 2, we shall only study two cases which should provide us with adequate evidence of the effects of the increasing falling speed of particles on its concentration.





Fig. 7a For  $t = -3$ , concentration bound very close to x-axis is almost uniformly distributed in layers. All of the following distributions up to Fig. 11 have been evaluated from (2.2.6) for  $v = w/4$ .

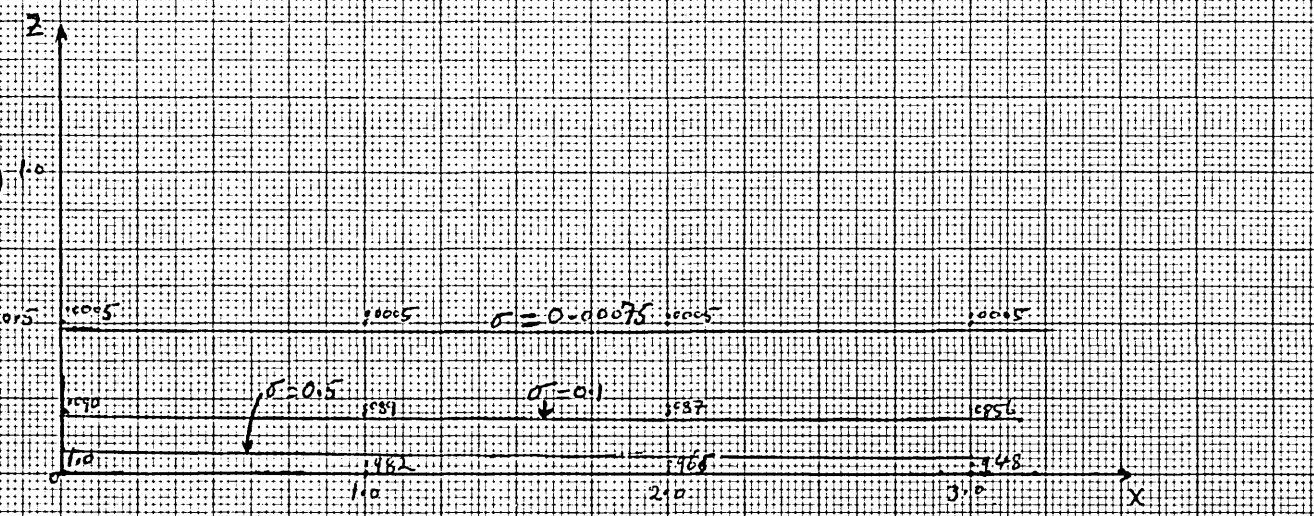


Fig. 7b Gradual upward displacement of particles, and increase of concentration in the corner, are observed when  $t = -2$ .

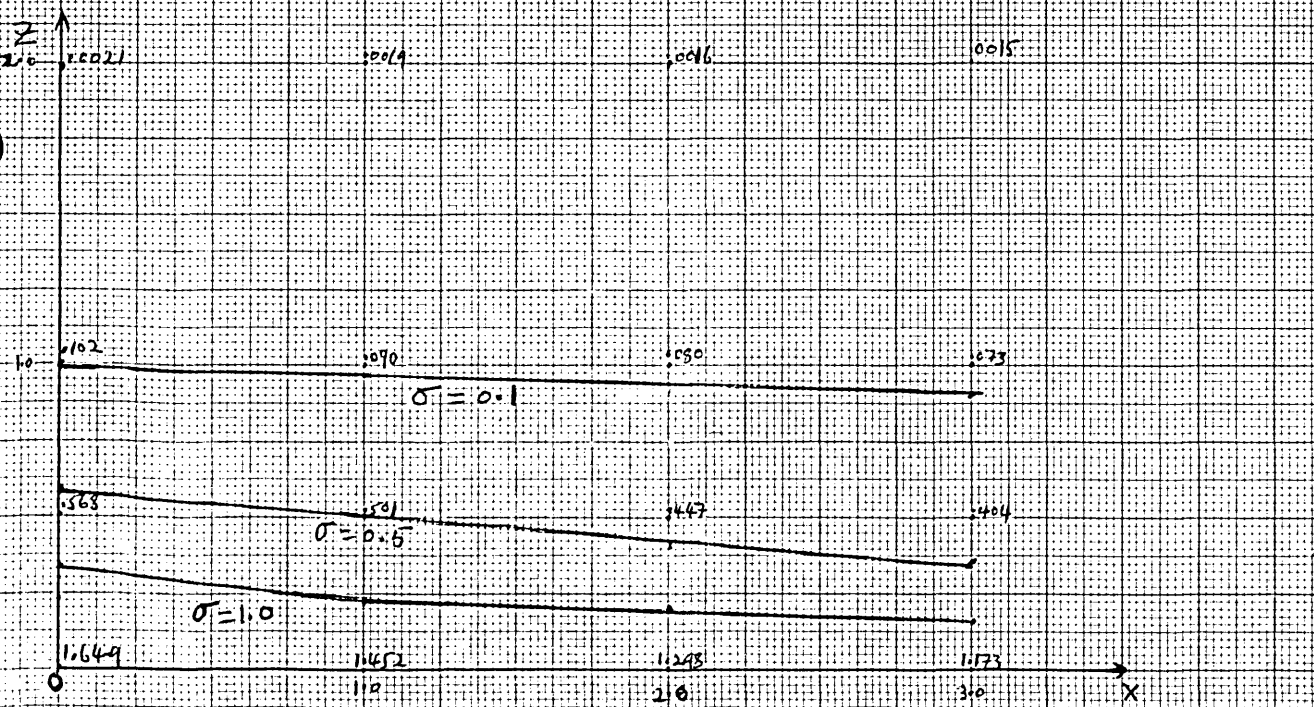


Fig. 7c At time  $t = -1$ , convergence effects become apparent; gradually the contours begin to tilt as particles in the corner are displaced upwards relatively faster.

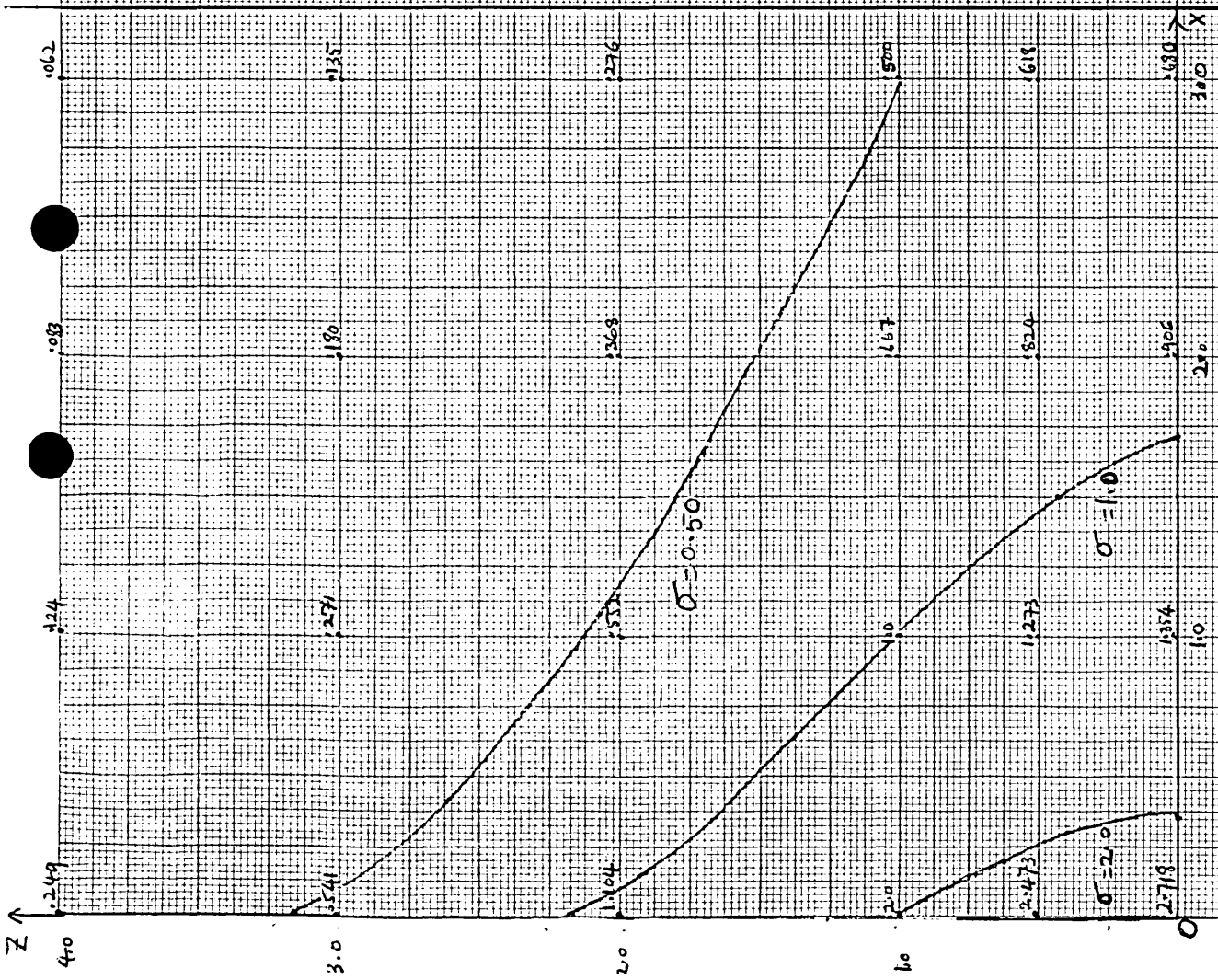


FIG. 8 When  $t=0$ , we have (2.2.3a) from which this distribution is obtained. Concentration in the former continues to grow and  $4\frac{1}{2}$  times the max amount in Fig. 7a occurs.

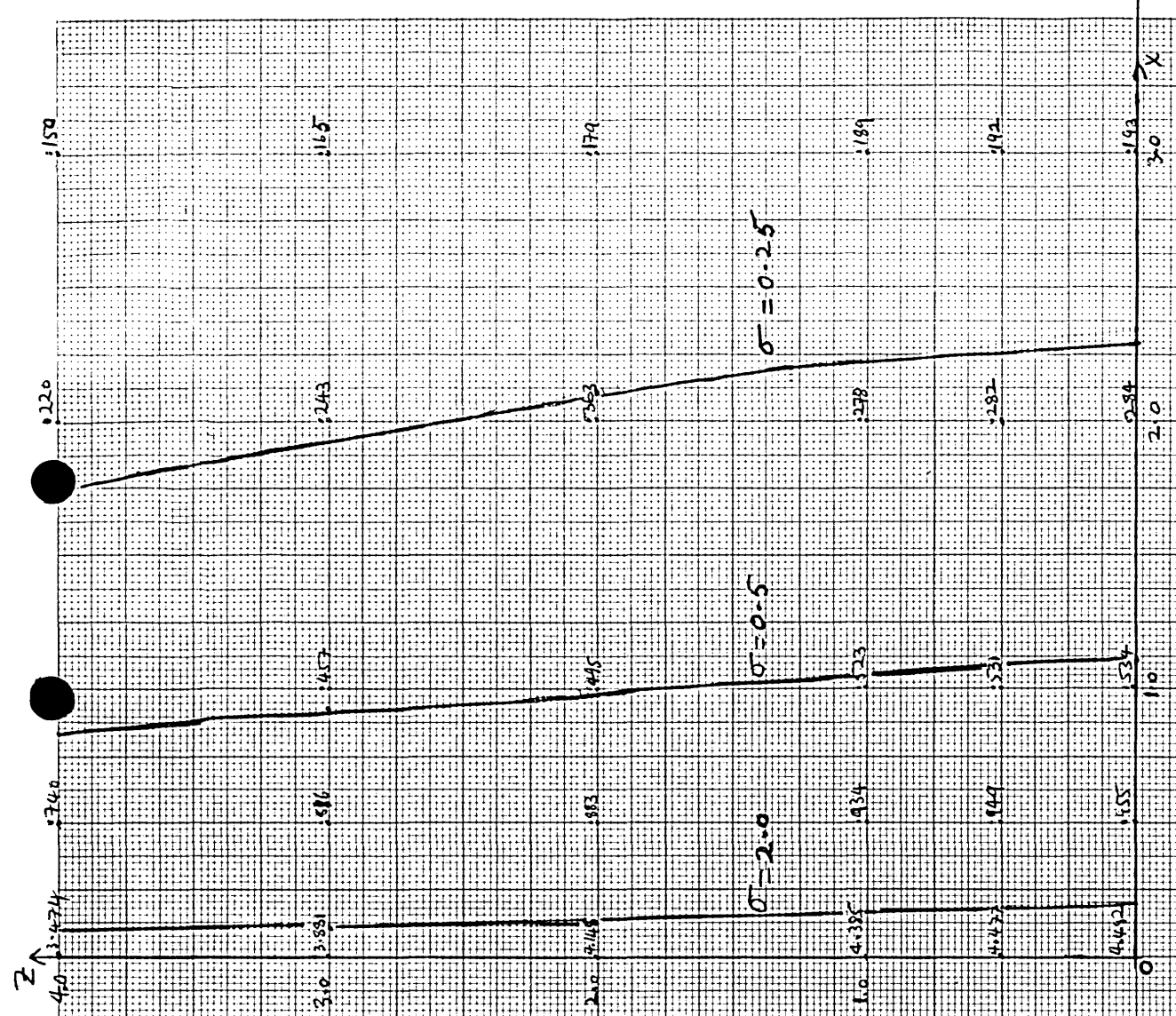


FIG. 9 When  $t=1$ , we notice the concentration begins to grow rapidly on the  $z$ -axis and in its vicinity.

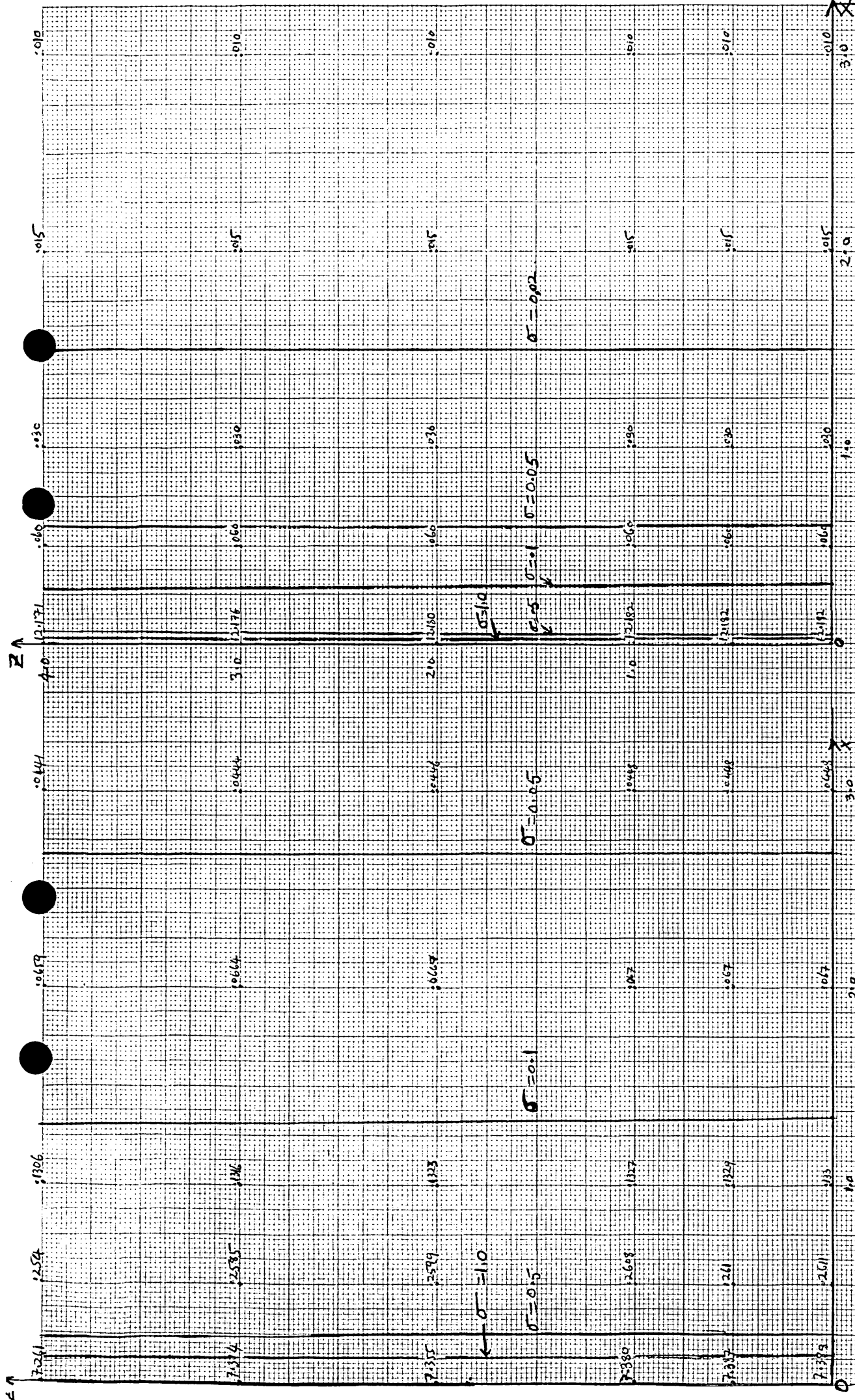


Fig. 10 Growth of vertical columns of concentration, similar to those found in cumuliiform swarms, is observed in this distribution for  $t=2$ .

Fig. 11 At  $t=3$ , in 6 units of time, we have a situation where most of the upstream concentration has been transported to  $Z$ -axis and into its vicinity.

Case 1  $0 < n < 1$ .

One obvious advantage of having an explicit solution like (2.2.5) is that we can easily examine its behaviour by going backward or forward in time as much as we like. We have taken a step back to see how the distribution we specified in (2.2.3a) has developed in the first place. We have taken the falling speed to be  $\mathcal{V} = w/4$  (i.e.  $n = \frac{1}{2}$ ), when the concentration  $\sigma(x, z, t)$  takes the form

$$\sigma(x, z, t) = \frac{e^{\frac{1}{2}t} + z e^{-t}}{1 + x e^{2t}} \exp [1 - z e^{-3/2t}] \quad (2.2.6)$$

The Fig. 7a, 7b and 7c (on page 37 ) have been obtained for  $t = -3$ ,  $t = -2$  and  $t = -1$  respectively. The Fig 7a contains a very sparse, low-level, nearly horizontally uniform concentrations in the vicinity of x-axis along which there lie successively but slowly decreasing maximum values with increasing x. It appears that convergence displaces these concentrations to new heights in one unit of time, as shown in Fig. 7b. By this time, the maximum concentrations on the z-axis have increased by over 60 per cent. The strength of the convergence effects are however not apparent until we take a look at the distribution for  $t = -1$  (Fig 7c), when tilted contour lines of constant concentration begin to appear with larger gradients in the vicinity of the vertical axis, indicating greater vertical displacement of that area than elsewhere. The concentration in the corner has increased by  $2\frac{1}{2}$  times the corresponding value in the Fig. 7a.

These effects become more pronounced with time particularly after  $t = 0$  which gains more than  $4\frac{1}{2}$  times the maximum concentrations at

$t = -3$ . As concentrations progress towards convergence zone and move away from it, its contours become steeper and get closer and closer and a very rapid horizontal piling up effect takes place. When five units of time have elapsed, that is at  $t = 2$  (see Fig 10), the contours are very nearly vertical, and maxima, slowly decreasing with height, occur on the  $z$ -axis, whereas those existing on the  $x$ -axis are decreasing very swiftly. It is, in fact, true to say that  $\frac{\partial \sigma}{\partial z}$  varies much more slowly in all distributions drawn for positive time than  $\frac{\partial \sigma}{\partial x}$  for negative times and  $\frac{\partial \sigma}{\partial x}$  varies slowly for negative time than for positive time. The maximum concentration values obtained for  $t = 3$  (Fig 11) are twenty times that for  $t = -3$ .

#### Case II

The falling speed of the particles here is  $\nu = \frac{1}{2}w$  (i.e.  $n = 1$ ), and the equation (2.2.5) takes the form

$$\sigma(x, z) = \frac{z + e^t}{1 + x e^{2t}} \exp [1 - z e^{-t}] \quad \dots \quad (2.2.7)$$

Again commencing from the distribution at  $t = -3$  (Fig 12a) where the concentration is sparse but almost uniformly distributed, we are reminded to realise how prominent a role the particle falling speed plays in forming those cumuliform swarm-type vertical columns of distribution in the vicinity of  $z$ -axis. The concentration ascends higher and higher with time. The contour lines assume rather similar position to those discussed in the Case I, and this time the maximum concentration produced become more pronounced when  $t = 2$  (Fig 15) and  $t = 3$  (Fig 16), when 150 times and over 400 times the maximum concentration produced for  $t = -3$  are achieved respectively.

The Figures 12a, 12b, 12c, 13, 14, 15 and 16 show the contours for the times interval  $t = -3$  to  $t = 3$ .

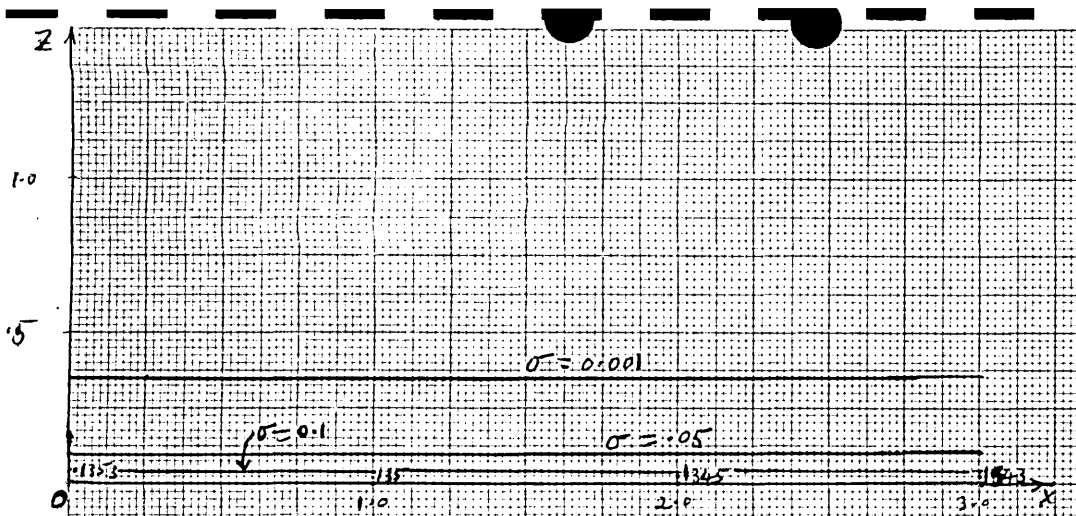


Fig. 12a All of the following distributions, up to Fig. 16, have been obtained for the falling speed  $v = W/2$ . This distribution like Fig. 7a forms our convenient starting point at  $t = -3$ .

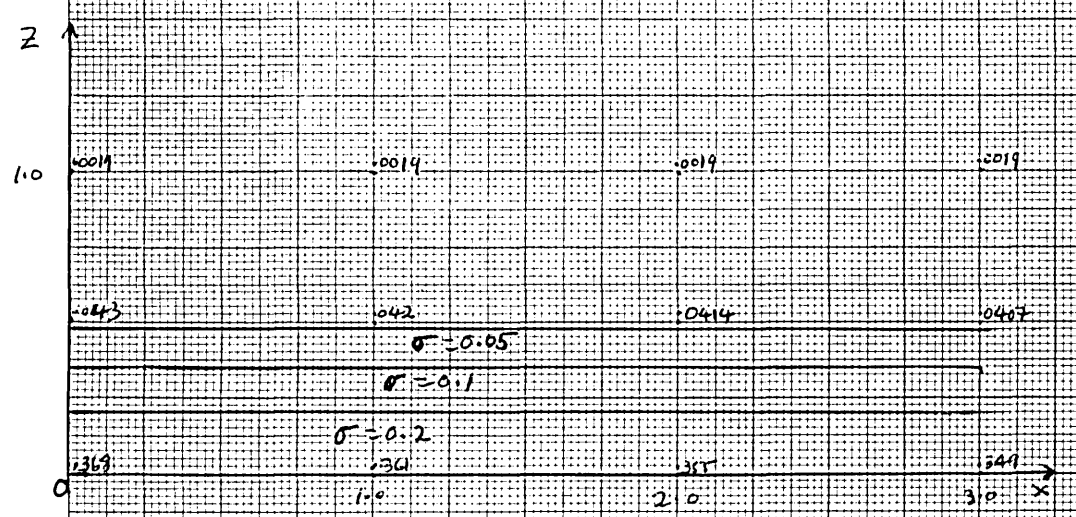


Fig. 12b Slow upwards displacement of particles is observed with a small uniform increase in concentration, when  $t = -2$ .

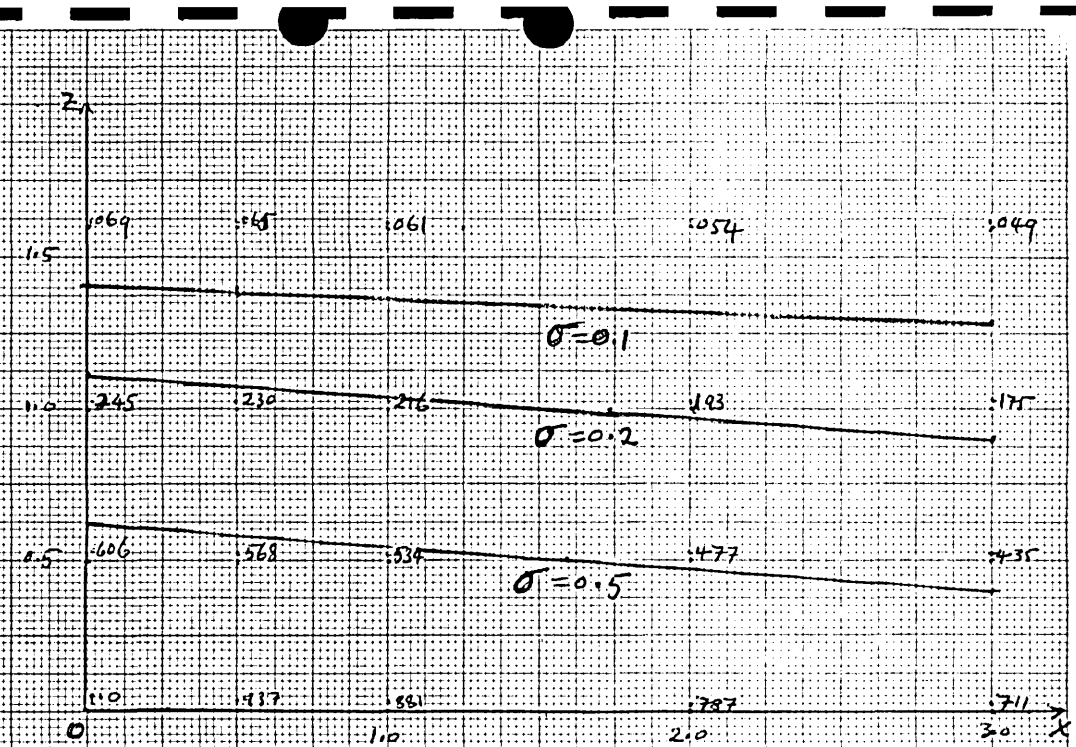


Fig. 12c The effects of convergence are to displace upward the particles faster, and, hence, the sloping contour lines. The growth in concentration amounts to about 8 times over that in Fig. 12a.

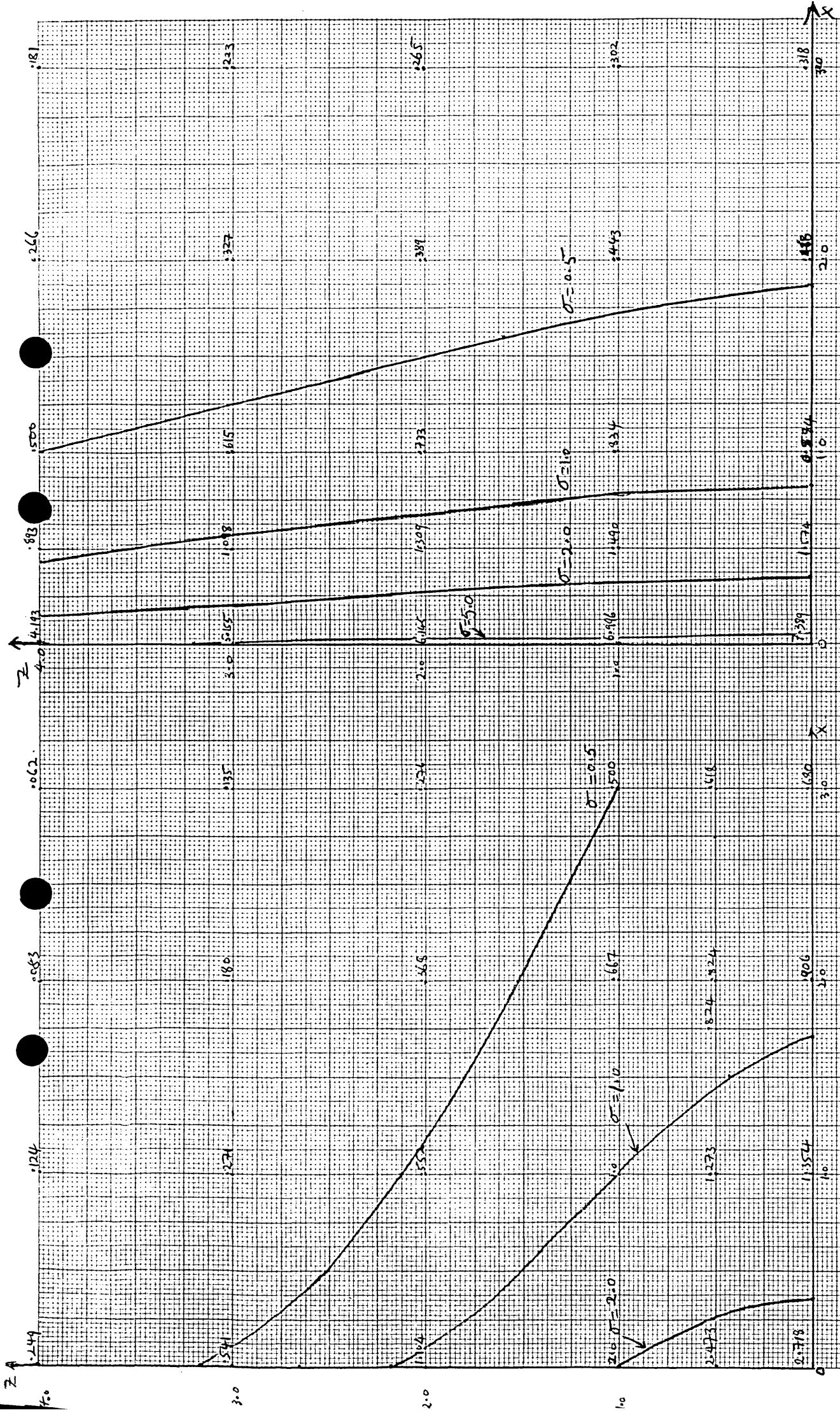


Fig. 13 The equation (2.2.3a) ( $t=0$ ) gives this distribution which is the same as that in Fig. 8.

Fig. 14 Like contours in Fig. 9, the above ones enable us to observe some transportive properties of the flow; values of concentration in the corner rise to over 50 times those in Fig. 12a.

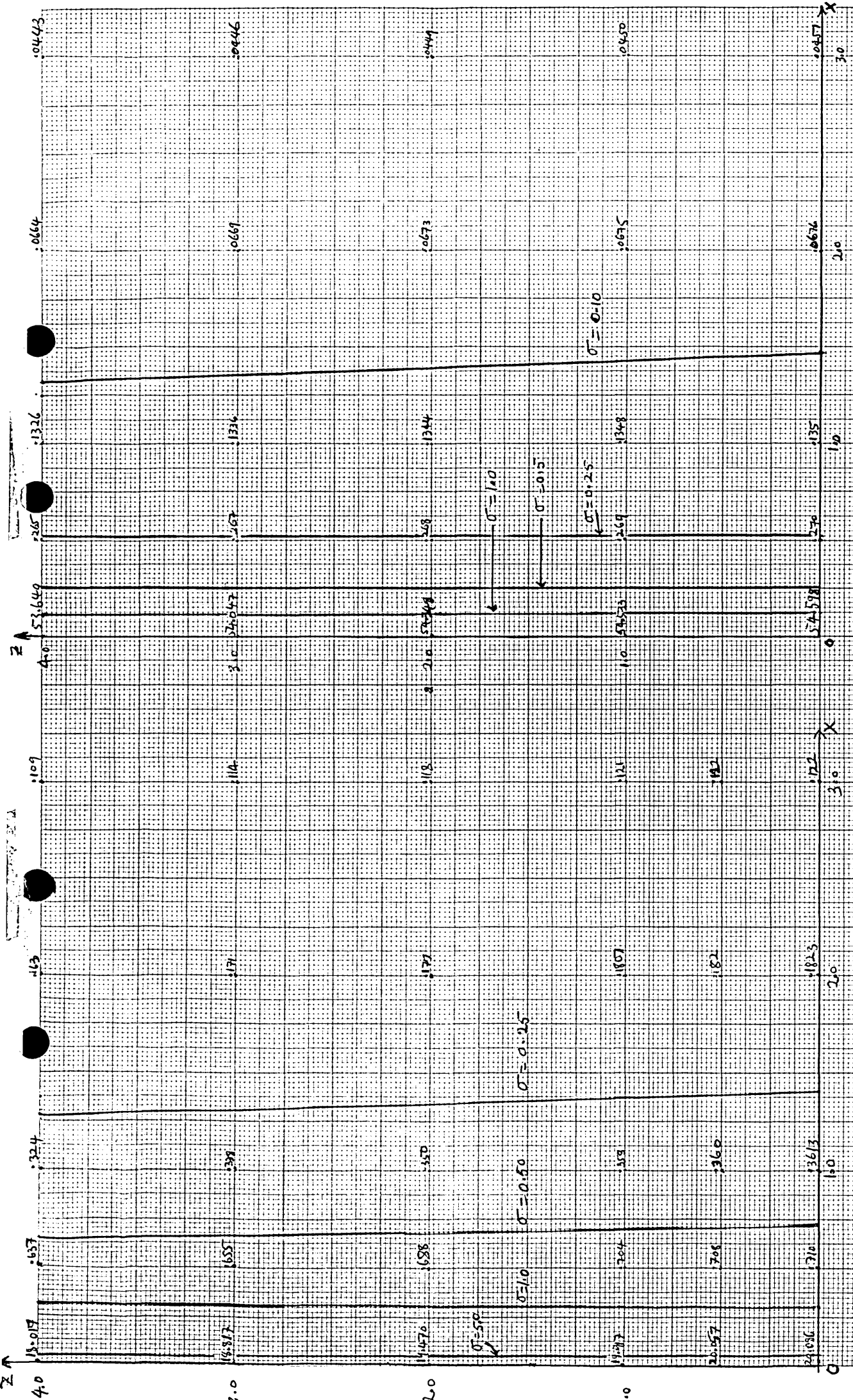


Fig. 15 Vertical columns of growing concentration in the vicinity of z-axis are apparent here when  $t = 2$ .  
 Fig. 16 Again we have a situation where, when  $t = 3$ , large concentrations of the order of hundreds of times those found in 12a appear on the z-axis and in its vicinity.



Section III Steady Concentration in a Convergence-Divergence zone.

From the last two sections we have seen that although concentrations produced downstream are higher, the fact of the matter is that the flow pattern we have used carries the concentrations away to infinity. Moreover, it is not even a crude representation of an atmospheric flow pattern; the converging motions, as mentioned in Chapter I, invariably are accompanied by diverging motions above. We, therefore, devote this section to working out downstream concentrations moving (with constraint similar to those used before) in a flow containing convergence and divergence.

Employment of the well-known Schwarz-Christoffel transformation enables us to evaluate the stream function of the fluid motion shown in the sketch below.

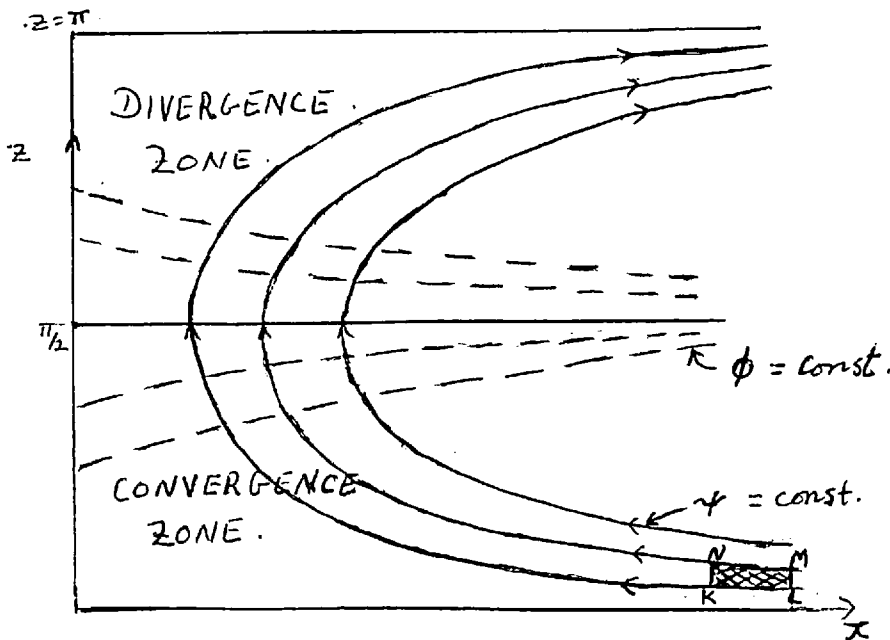


Diagram 4 Sketch of stream lines  $\psi = \text{const}$  and equipotential lines  $\phi$  with divergence occurring above  $z = \pi/2$  in the  $z$ -plane flow

The transformation is given by

$$W(Z) = \cosh(\pi Z/a)$$

or simply

$$W(Z) = \cosh(Z)$$

when the 'strip' in which the entire motion occurs has a width  $a = \pi$ .

The potential function

$$\phi(x, z) = U \cosh x \cos z \dots \quad (2.3.1a)$$

and the stream function

$$\psi(x, z) = U \sinh x \sin z \dots \quad (2.3.1b)$$

obtained from the transformation above form the basis of the flow.

As  $\underline{U} = -\text{grad } \phi$ ,

the flow velocity is

$$\underline{U} = (-U \sinh x \cos z, 0, U \cosh x \sin z)$$

where  $U$  is a constant velocity in the  $w$ -plane. A quick glimpse

at this velocity vector informs that the behaviour of this motion is more complicated than that of the motion in the last two sections.

Each point in the fluid along a line, say,  $KL$  of rectangular parcel  $KLMN$  (see the diagram 4) possesses a velocity which is function

of both  $x$  and  $z$ . The flow in the lower half

of the region commences at infinity, decelerates to zero velocity at

$x = 0$  and rises to the upper half to diverge and to

return to infinity with infinite velocity.

Supposing that the particle falling speed is

$$v = nw = nU \cosh x \sin z,$$

then the particle velocity is

$$\underline{U} = (-U \sinh x \cos z, 0, (1-n) U \cosh x \sin z)$$

and the resulting equation of continuity for steady concentration is

$$-\tanh x \frac{\partial \sigma}{\partial x} + (1-n) \tan z \frac{\partial \sigma}{\partial z} = n\sigma \dots \quad (2.3.2)$$

which is equivalent to stating (by characteristics)

$$\frac{d\sigma}{n\sigma} = \frac{dz}{(1-n)\tan z} = \frac{dx}{-\tanh x}$$

This yields by integration

$$\sigma(x, z) = A_1 / \sinh^n x$$

and

$$\sinh x (\sin z)^{\frac{1}{1-n}} = B_1,$$

from which, writing  $A_1$  as a function of  $B_1$ , the general solution

$$\sigma(x, z) = \frac{1}{\sinh^n x} g(\sinh x (\sin z)^{\frac{1}{1-n}}) \dots \quad (2.3.3)$$

is obtained, where  $A_1$  and  $B_1$  are constants of integration.

Let the initial distribution specified at a distance  $\pi$  away from the  $z$ -axis be defined by a function

$$\sigma(\pi, z) = \frac{\sin z}{\sin h^n \pi} \exp \left[ \frac{-\sin z}{\cos^4 z} \right] \dots \dots \quad (2.3.4)$$

Using this and the general solution (2.3.3),  $g(x, z)$  is worked out to get the solution

$$\sigma(x, z) = \frac{\sin z (\sinh x / \sinh \pi)^{1-n}}{\sin h^n x} \exp \left\{ \frac{-\sin z (\sinh x / \sinh \pi)^{1-n}}{[1 - \sin^2 z (\sinh^2 x / \sinh^2 \pi)]^{1-n}} \right\} \dots \dots \quad (2.3.5)$$

for all  $x$  and  $z$ .

An original and interesting feature of this solution is what may be called a 'zero-line', a curve along which there is no concentration and whose position solely depends on the values of  $n$  in the denominator

$$[1 - (\sinh^2 x / \sinh^2 \pi)^{1-n} \sin^2 z]^2$$

of the exponential power.

This means that it is all right to suppose that no flux is forming a zero-line, and that for the purpose of our analysis, consideration of motion in the region bounded by the axes and a zero-line should alone be adequate to meet our requirement effectively for the aggregation of particles as they move downstream. The zero-line accompanies concentration contours for the three cases discussed below.

Case I The range in which this case occurs is  $0 \leq n < \frac{1}{2}$ . For all  $n$

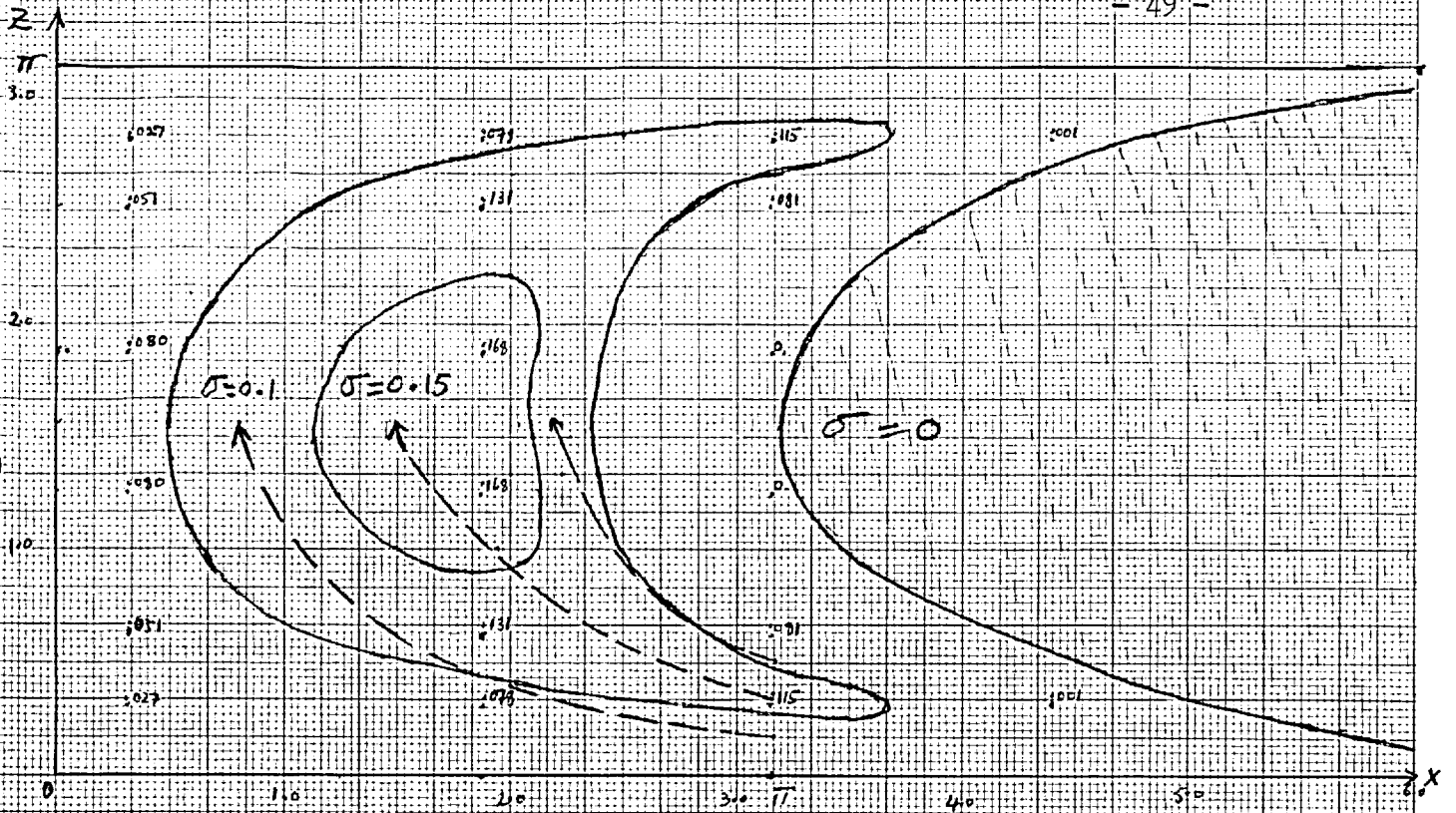


Fig. 17 Illustrating case I when  $n = 1/4$  these contours show that in spite of growth in concentration along particle paths there is no accumulation in the corner in the convergence zone. The max. values located near  $x = 2$ , however, move towards  $z$ -axis as  $n$  increases.

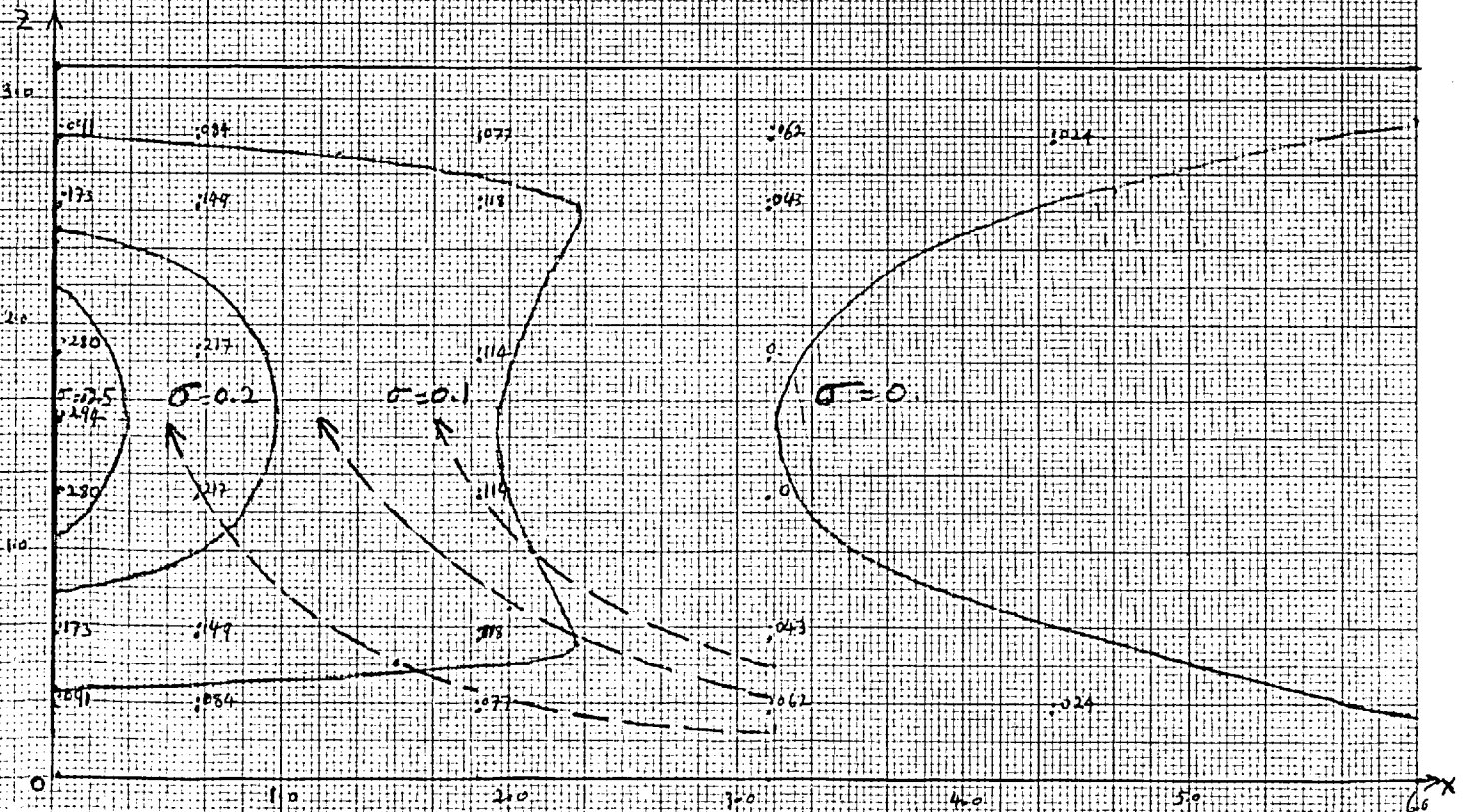


Fig. 18 This critical case (case II) shows that max. concentration formed on the  $z$ -axis is 5 times the upstream max. at  $x = 0$ .

in this range, the concentration forming on the z-axis is zero and the position of maximum concentration which varies with the values of n moves closer to z-axis as n increases. For example, when n = 0, maximum concentration is located at x = π. But when n = 1/4 (which we have chosen to show what a typical distribution looks like in this case), it has moved to the line x = π/2 and when n = 1/2 (see the next case) it actually is displaced to reach the z-axis.

For n = 1/4

$$\sigma(x, z) = \frac{\sin z \sin h^{\frac{1}{2}}x}{\sin h^{\frac{3}{4}}\pi} \exp\left\{ \frac{-\sin z (\sinh x/\sin h \pi)^{3/4}}{[1 - \sin^2 z (\sinh x/\sin h \pi)^{3/2}]^2} \right\} \dots (2.3.6)$$

the distribution of which is shown in the Fig. 17 (page 49). The highest downstream values of concentration at this juncture exceed the original values by 0.05 or there is about 1 1/2 times increase over the original values.

Case II This is a critical case where

$$\sigma(x, z) = \frac{\sin z}{\sin h^{\frac{1}{2}}\pi} \exp\left\{ \frac{-\sin z (\sin h x/\sinh \pi)^{\frac{1}{2}}}{(1 - \sin^2 z (\sin h x/\sinh \pi))^2} \right\} \dots (2.3.7)$$

The Fig. 18 (page 49) indicates the appearance on the z-axis of concentration, the maximum value of which is six times the upstream original maximum.

Case III The range of consideration is 1/2 < n < 1. Taking a typical value n = 3/4, the distribution (see Fig 19) given by

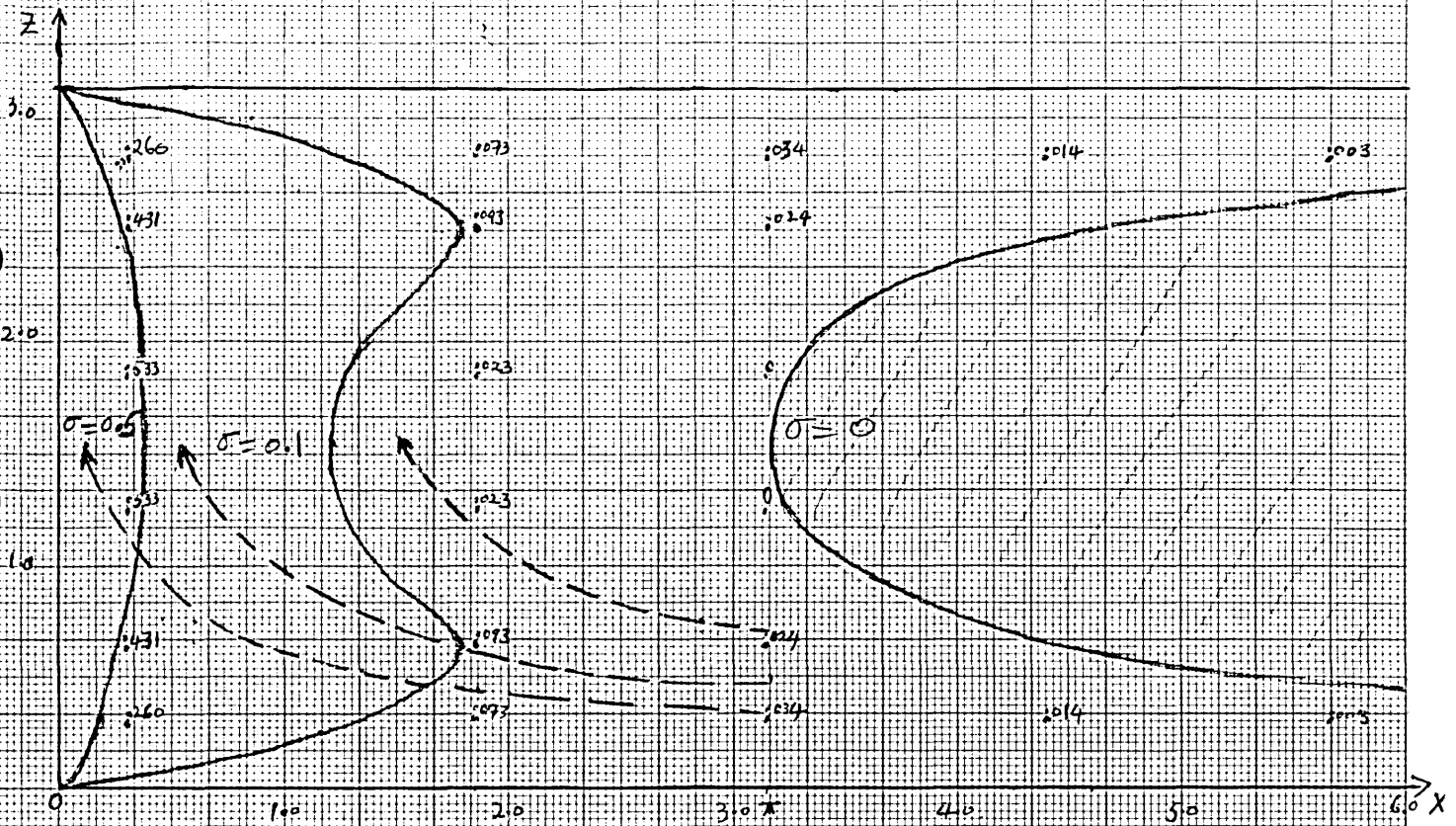


Fig. 19 When  $n > \frac{1}{2}$  a gradual downstream increase leading to infinite concentration on the z-axis is found. We have taken the above distribution for  $n = \frac{3}{4}$  to demonstrate this.

$$\sigma(x, z) = \frac{\sin z}{\sinh \frac{1}{2}x \sinh^{1/4}\pi} \exp\left\{ \frac{-\sin z (\sinh x / \sinh \pi)^{1/4}}{[1 - \sin^2 z (\sinh x / \sinh \pi)^{1/2}]^2} \right\} \dots (2.3.8)$$

is illustrated. This case explicitly demonstrates the consequences of increasing  $n$  above the critical value; for infinite concentration results on the  $z$ -axis; This is mainly due to the behaviour of the equation (2.3.5) and could have been avoided, and it is not necessarily due to the falling speed.

All distributions on pages 49 and 51 are accompanied by the paths of particles, indicated by dotted lines.



Chapter III

Consideration of Non-potential Flows

Preamble: We have learnt that there is a major disadvantage, insofar as our purpose is concerned, in the inherent properties of the flows employed in the last chapter. The velocity becomes infinitely large at infinity where concentrations are carried. This calls for a modification in the velocity field structure so as to have a realistic flow with finite velocity at infinity.

Therefore, one principal assumption that has been made in this chapter in order to create a compressible flow of a fluid having a coefficient of expansion due to heating is that there is a heating field, the effects of which is to expand the fluid, setting up temperature (and density) gradients and lowering the pressure in the region towards which the air masses from the surrounding displace themselves. Depending upon the extent of the region being heated, three kinds of motions in reality could ensue.

First, heating on a small scale could set up convection currents. Second, on a very large scale, baroclinic waves can develop with horizontal pressure gradients, a good example of which is a mid-latitude cyclone where there is a continuous heating over long periods. On an intermediate scale a situation similar to a sea breeze develops. The motion, therefore, is produced by temperature differences between the air masses in the heated region and their surrounding, by the operation of gravity on them, and by release of potential energy and its conversion to motion.

To commence from a density distribution to work out the velocity field of the flow by integration of equations of motion would usually be much too cumbersome and difficult, if not impossible. Even if the integration were possible, there is no guarantee that the resulting

velocity field would give a desirable pattern of motion. On account of this, the problem has been dealt with by a method of guesswork to form an *realistic* velocity field rendering a converging motion accompanied by divergence above. This is more than guesswork, in a sense, for careful consideration has also been given to retain fair distributions of vorticity and its rate of change to match them with the atmospheric situations in reality.

In addition to that, the density distributions obtained from our specified velocity fields actually agree with some of the situations related to the occurrence of convergence in which density distributions of air masses involved could greatly vary. For instance, convergence, in the vicinity of zone of which there may be rainfall, may constitute totally different densities of air masses from that in which there is a cold downdraught or rain cooling the air virtually at any level. The latter situation may be typical of an ephemeral thunderstorm in which locations of relatively higher densities could occur due to cooling, and is capable of supporting the density distribution obtained for the flow used in the second section of this chapter.

Another basis from which to start may have been to define the pressure fields. However, as Professor Scorer points out, consideration of 'motion producing pressure gradients and new pressure gradients producing more new motion' is unprofitable because 'the pressure fields and the velocity fields develop simultaneously'. But one is not the cause of the other, and vorticity distribution alone provides a strong indication of how the motion will evolve.

Section I A Flow with max. horizontal velocity on the x-axis

Let us define non-dimensional cartesian co-ordinates  $x = l_0 x'$  and  $z = l_0 z'$  and a non-dimensional velocity vector  $\underline{U} = U_0 U'$ . Throughout this work  $U_0$  will be taken to be  $1 \text{ m sec}^{-1}$  and  $l_0$  to be  $10^3 \text{ m}$ . Henceforth we will drop the primes and write  $x, z$  and  $\underline{U}$  for the non-dimensional quantities.

We shall use the same axes of reference as before. Assuming the velocity vector as  $\underline{U} = (u, 0, w)$ , the vorticity vector  $\underline{\omega}$  is defined by  $\underline{\omega} = (0, \eta, 0)$  and, hence, its rate of change by

$$\frac{D\eta}{Dt} = u\eta_x + w\eta_z,$$

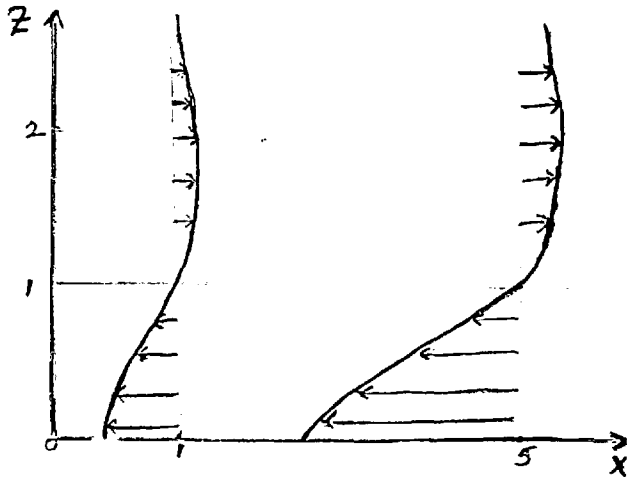
where  $\eta = \nabla^2 \psi$  ( $\nabla^2$  being a Laplacian operator and  $\psi$  being a stream function),  $\eta_x$  and  $\eta_z$  are partial derivatives with respect to  $x$  and  $z$  respectively, and  $D/Dt$  denotes the rate of change following a parcel of fluid.

We embark upon this exercise by specifying the velocity field  $\underline{U}$  of the flow given by

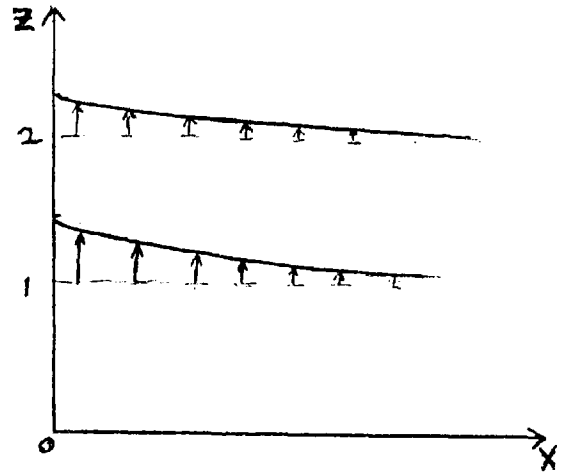
$$\underline{U} = (-k_0 (1-z) e^{-z} \sinh(1-e^{-x}), 0, k_0 z e^{-(x+z)} \cosh(1-e^{-x})) \dots (3.1.1)$$

which satisfies the equation of continuity and where  $k_0$  is taken to be 3 in our examples.

The following are the profiles of horizontal and vertical components of  $\underline{U}$ ; the length of arrows may be supposed to make reference to the magnitudes.



Diag 5a The horizontal vel. profiles of the flow at  $x=1$  and at  $x=5$ .



Diag 5b profiles of the vertical velocity of the flow.

It is observable from (3.1.1) that a desirable feature of the horizontal velocity is that it retains finite values at large distances away from the convergence zone. Its maximum occurs at  $x = \infty$  at the lowest level of the incoming flow and would have a value of 3.53. But as the magnitude of the horizontal velocity at  $x = 5$  would have a value of 3.49, which differs very slightly from the value at  $x = \infty$ , we shall resort to the consideration of downstream motion from  $x = 5$ .

This kind of velocity structure with its greatest value to be found at the lowest level of the flow implies the absence of friction, and, consequently, of the possibility of any boundary layers. Its vertical variation is such that its values decrease to zero at  $z = 1$  and then increase (with the reversed flow) up to a height  $z = 2.0$  where it is about  $1/7$  of the maximum values, before diminishing away rapidly with height to zero at infinity.

As far as the vertical velocity is concerned, it increases from zero on the  $x$ -axis with height up to  $z = 1$ , then slowly dies away. On the line  $z = 1$ , it obtains successively decreasing maxima for all non-negative  $x$  varying from 1.141 at  $x = 0$  to 0.0114 at  $x = 5$  and tending to zero as  $x \rightarrow \infty$ .

In physical units this amounts to a flow progressing towards the convergence zone with the maximum horizontal velocity at  $x=5$  of  $3.49 \text{ m Sec}^{-1}$  on the  $x$ -axis and entering into the divergence zone with maximum vertical velocity of  $1.141 \text{ m Sec}^{-1}$  at the point  $(x=0, z=1)$ , reading 1 unit in  $x$ - and  $z$ -direction as 1km. One could envisage situations in reality where horizontal and vertical velocities three or four times the values used in this exercise are found.

The differential equation

$$\frac{dz}{w} = \frac{dx}{u} \quad \dots \quad (3.1.2a)$$

renders the stream function

$$\psi(x, z) = 3 ze^{-z} \sinh(1-e^{-x}) \dots \quad (3.1.2)$$

which is as shown in the Fig 20(a).

The corresponding vorticity distribution is given by the function

$$\eta = 3ze^{-(x+z)} (\cosh(1-e^{-x}) - e^{-x} \sinh(1-e^{-x})) + 3(2-z)e^{-z} \sinh(1-e^{-x})$$

The variation of vorticity enables us to look at the mechanism of the flow.

The rate of change of vorticity

$$\begin{aligned} \frac{D\eta}{Dt} = & -4.5(2-z+z^2) e^{-(x+2z)} \sinh 2(1-e^{-x}) \\ & + 9(z-z^2) e^{-2(x+z)} (2 - \cosh 2(1-e^{-x})), \end{aligned}$$

which, in agreement with what we want, decreases to zero at both horizontal and vertical infinite distances. In the corner, there is a positive rate of change which accounts for the overturning of the air as it rises.

Linking the rate of change of vorticity with the density  $\rho$  of air is the equation

$$\frac{D\eta}{Dt} = g \wedge \text{grad} (\log \rho) \dots \quad (3.1.3)$$

which when integrated with respect to  $x$  yields the equation

$$\rho(x, z) = \exp \left[ \frac{1}{g} \int \frac{D\eta}{Dt} dx + c \right]$$

where  $c$  is a constant of integration.

Hence,

$$\rho(x, z) = \exp \left\{ c - \frac{g}{2g} e^{-2z} [\cosh 2(1-e^{-x}) + z(1-z)e^{-x} (2e^{-x} + \sinh 2(1-e^{-x}))] \right\}$$

If the flow at infinity has a value  $\rho = 1.0$ , then from the equation above  $c$  is calculated to be

$$c = \frac{g}{2g} e^{-2z} \cosh (2) \dots$$

Therefore

$$\rho(x, z) = \text{Exp} \left\{ -\frac{g}{2g} [\cosh 2(1-e^{-x}) - \cosh (2) + z(1-z)e^{-x}(2e^{-x} + \sinh 2(1-e^{-x}))] \right\} \dots (3.1.4)$$

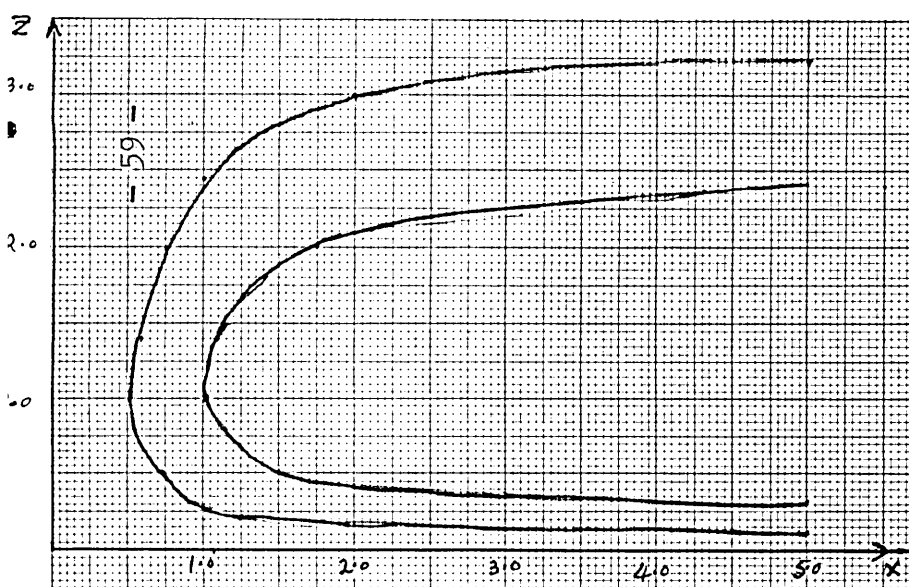


Fig. 20a Streamlines of flow in Section I given by (3.1.2).

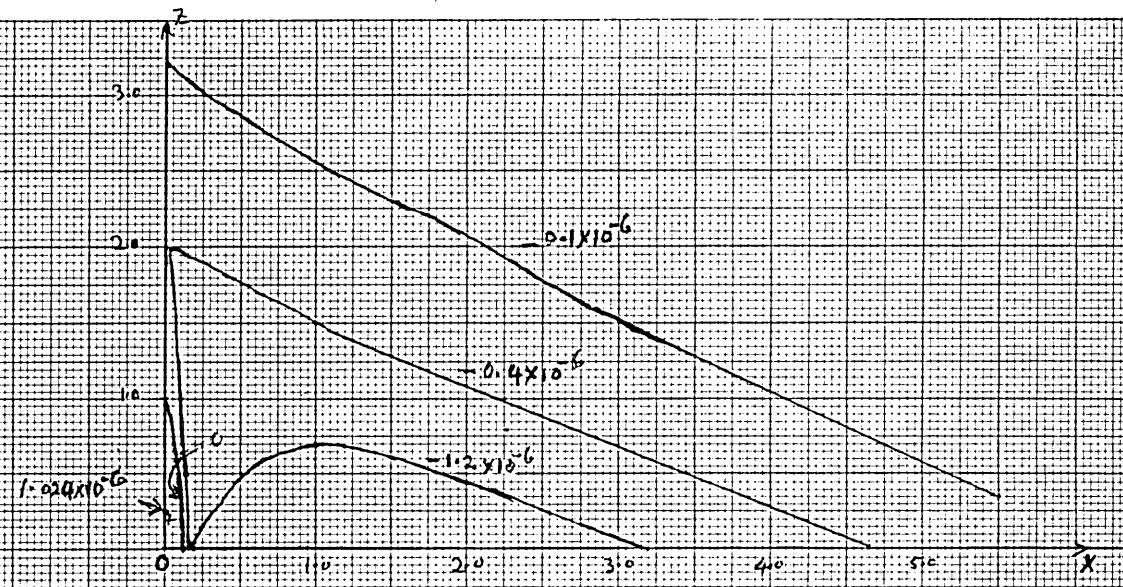


Fig. 20c Rate of change of vorticity shows values in the corner accounting for overturning of air.

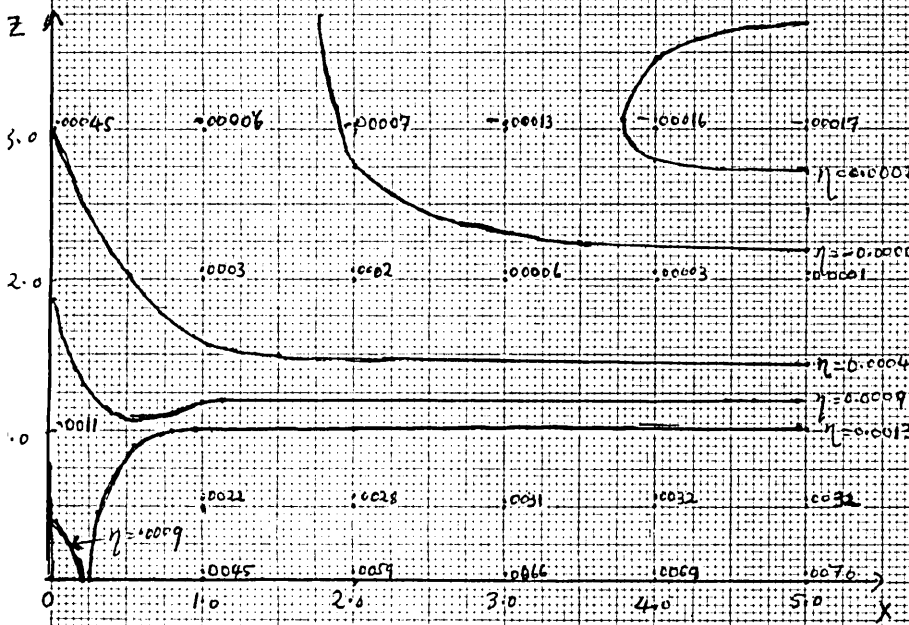


Fig. 20b Associated vorticity distribution, given by on p. 58.

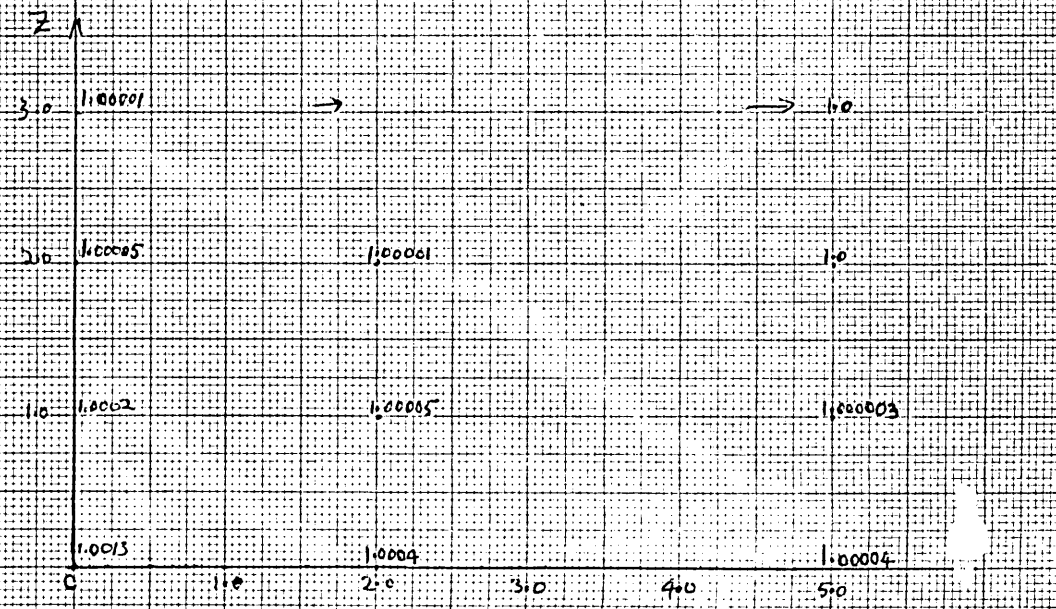


Fig. 20d This density distribution obtained from (3.1.4) is reminiscent of a situation where cooling takes place at a lower level.

Putting vorticity, its rate of change and associated density in physical units, their distributions have been worked out as shown by Figs 20(b), 20(c), 20(d) on page 59.

The density distribution is undoubtedly reminiscent of a situation where a certain amount of cooling takes place within the convergence zone.

Calculation I(i) Steady concentration

Let the falling speed, relative to the flow, of the particles introduced at the line  $x = 5$  be defined by

$$v = \frac{zw}{z + c_0} \quad \dots \quad (3.1.5)$$

where  $c_0$  is a constant. It may be noted that this specification marks the departure from our usual definition of the falling speed of particles whose motion in all other flows employed in this thesis has been examined. This function behaves in such a way that the greater the height to which the particles ascend the larger the falling speed and, eventually, when  $z \rightarrow \infty$ ,  $v \rightarrow w$ . This combination of height (as (3.1.5) can be written as  $v = w/(1+c_0/z)$ ) and the flow velocity may represent an improved specification because the locusts may respond to height as well as to the flow velocity tending to carry them up.

The particle velocity becomes

$$\frac{U}{P} = (-3(1-z)e^{-z} \sinh(1-e^{-x}), 0, \frac{3c_0}{z+c_0} z e^{-(x+z)} \cosh(1-e^{-x})) \dots \quad (3.1.6)$$

The resulting vertical velocity of particles increases with  $c_0$  and it is zero when  $c_0 = 0$ . We shall therefore decrease  $c_0$  to increase



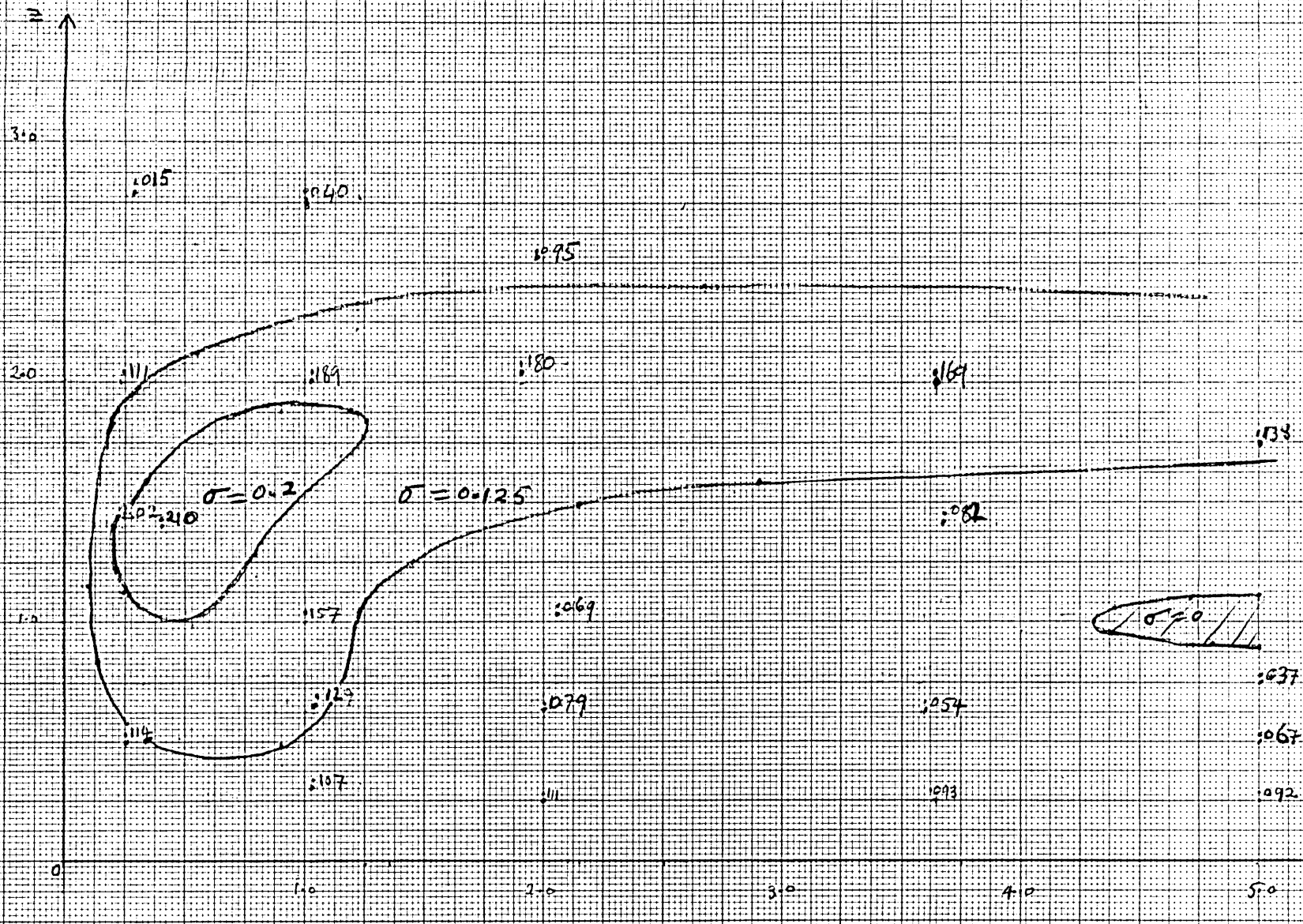


Fig. 21 By putting  $c_0 = 1$  in the eqn. (3.1.7), which is solved with (3.1.8) we get max. downstream values, lying just above convergence zone, amounting to twice the max. upstream initial values.

the falling speed.

Substituting (3.1.6) into (1.4.1), we have the partial differential equation

$$-(1-z)e^{-z} \sinh(1-e^{-x}) \frac{\partial \sigma}{\partial x} + \frac{c_0 z e^{-(x+z)}}{(z+c_0)} \cosh(1-e^{-x}) \frac{\partial \sigma}{\partial z}$$

$$\sigma \left\{ \frac{2c_0 - z^2 + z(1-c_0)}{(z+c_0)^2} \right\} z e^{-(x+z)} \cosh(1-e^{-x}), \dots \dots \dots \quad (3.1.7)$$

By computer methods this equation has been solved, with the initial condition

$$\sigma(x, z) = z e^{-4z} \dots \dots \dots \quad (3.1.8)$$

on the line  $x=5$  and

$$\sigma(x, z) = 0$$

for all

$$z e^{-z} \sinh(1-e^{-x}) \geq 0.425$$

From this formulation three cases have been worked out for decreasing values of  $c_0$ . The Figs. 21, 22 and 23 illustrate downstream increases in the steady concentration  $\sigma$ , starting values being the same in all cases on the line  $x=5$ . It is apparent that most of the higher values of concentration at divergence level are found to exist in an area bounded by the contour line  $\sigma = 0.125$ , which marks the region of maximum divergence velocity. As  $c_0$  decreases, the

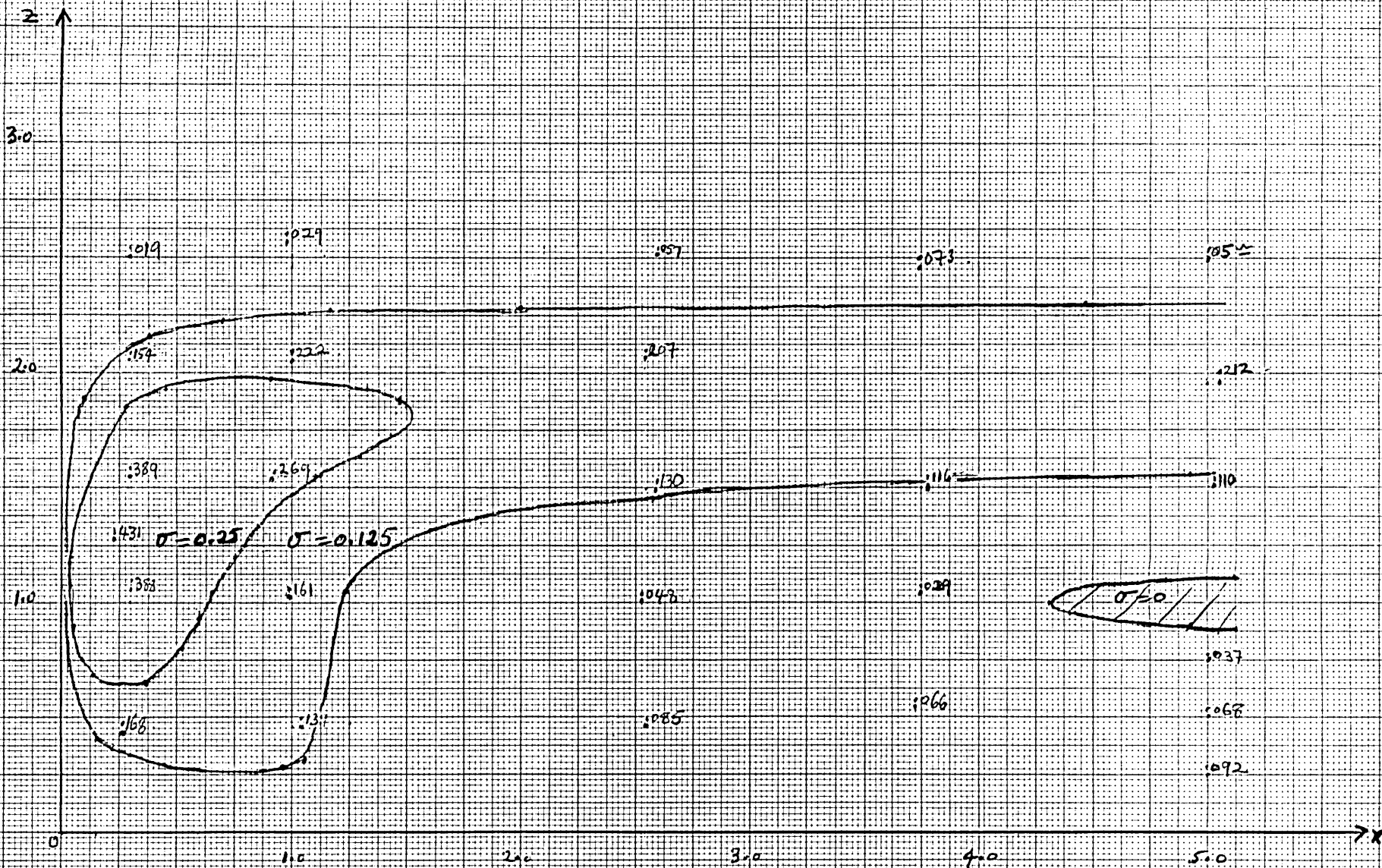


Fig. 22 Substitution of  $c_0 = \frac{1}{2}$  in (3.1.7) renders the above distribution where 5 times the initial values are found. This increased concentration sinks and moves closer to z-axis.

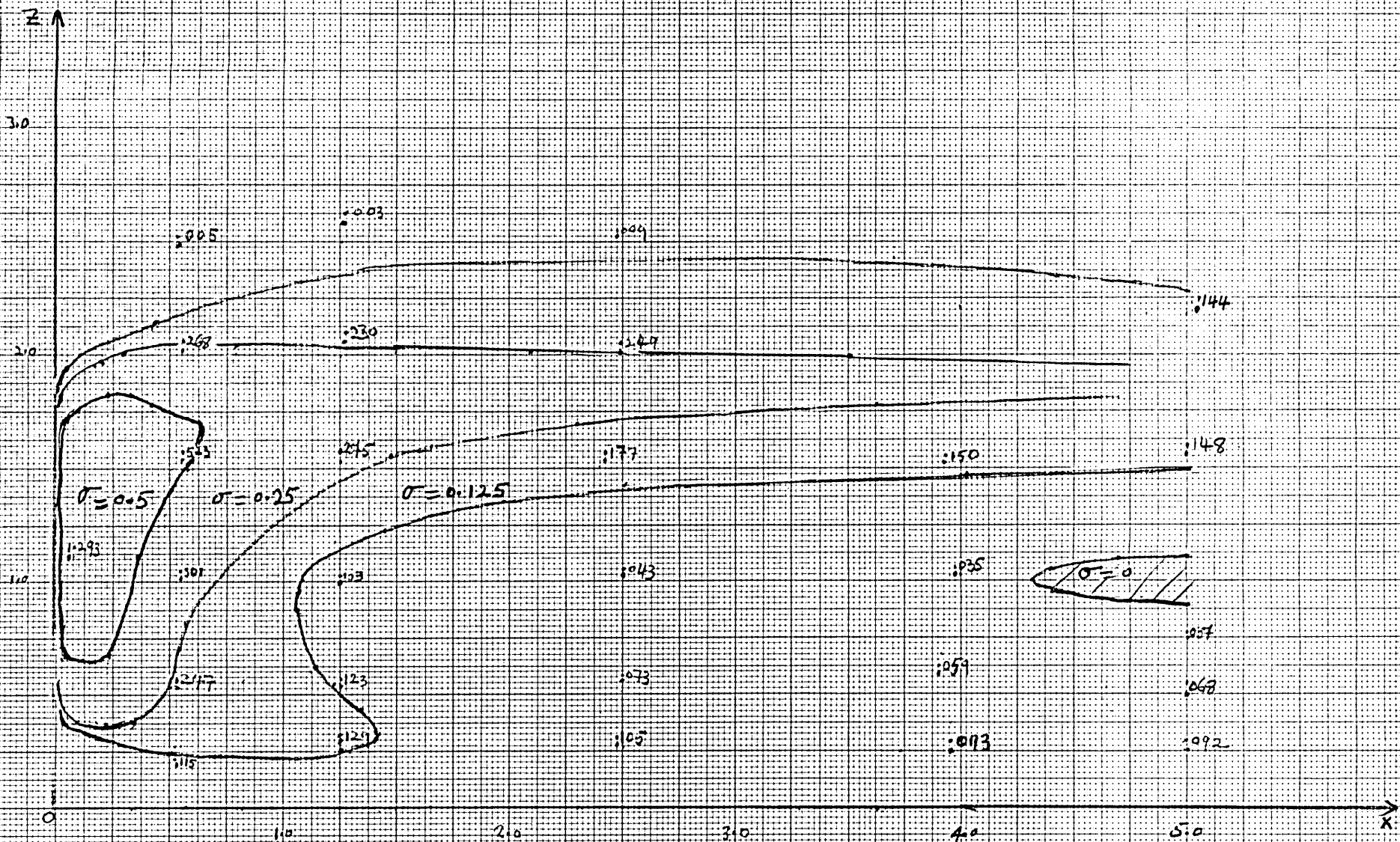


Fig. 23 For  $\sigma_0 = 1/4$  in (3.1.7), max. values formed in the convergence zone are 14 times those at  $x = 5$ . Further sinking of contours is noticeable.

contour  $\sigma = 0.125$  'sinks' in the convergence zone but remains almost fixed in position in the divergence zone, with higher concentration resulting in the convergence and in its vicinity. The zero-line curve (i.e. where  $\sigma=0$ ) has been obtained by using the second part of the initial condition.

When  $c=1$ , the maximum concentration,  $\sigma = 0.210$ , forms near the point  $(x=0.4, z=1.4)$  which is about twice the upstream original maximum (see Fig 21, P 61 ). The next case (Fig 22, p 63 ) confirms that the downstream increase, which, in fact, moves down towards convergence zone and closer to  $z$ -axis, amounts to approximately five times the upstream maximum value on the line  $x=5$ . It is in the last case (Fig 23, p 64 ) when  $n = 1/4$  that we witness a significant growth in concentration in the convergence zone, The maximum concentration  $\sigma = 1.293$  is 14 times greater than upstream maximum value on the line  $x=5$ .

In all the cases we have discussed, the particles do get very close to the  $z$ -axis without touching it. Should we want any deposition on the  $z$ -axis we would have to put  $c_0=0$ , i.e. when the particles are moving horizontally. Indeed, when  $c_0$  is given a negative value, all particles would be constrained to a downward motion. Consequently, maximum concentration would develop on the  $z$ -axis and possibly on the  $x$ -axis as well.

It is not unreasonable to affirm that there may be a 'large' mathematical gap between  $c_0 = 1/4$  and  $c_0 = 0$ , insofar as the difference in the degree of their effects upon downstream growth in particle concentration is concerned.

Calculation I(ii) Unsteady concentration

We now proceed to solve for an unsteady case and ascertain what the effects of this kind of flow are. In this calculation and in Calculation I(ii) of the next section, we shall commence with the same initial distribution which will enable us to compare the downstream effects of the two flows.

The differential equation which we shall solve is

$$\frac{1}{3} \frac{\partial \sigma}{\partial t} - (1-z)e^{-z} \sinh(1-e^{-x}) \frac{\partial \sigma}{\partial x} + (1-n)e^{-(x+z)} \cosh(1-e^{-x}) z \frac{\partial \sigma}{\partial z} = n\sigma (1-z) e^{-(x+z)} \cosh(1-e^{-x}), \dots \quad (3.1.9)$$

taking the particle falling speed as being proportional to the vertical component  $w$  of the flow,

$$\text{i.e. } \nu = 3nze^{-(x+z)} \cosh(1-e^{-x}), \dots \quad (3.1.10)$$

The function expressing our initial distribution at  $t=0$  is

$$\sigma(x, z) = ze^{-6z}/(1+x) \dots \quad (3.1.11)$$

defined in the area bounded by the ellipse

$$\left[ \frac{x-4}{0.75} \right]^2 + \left[ \frac{z-0.25}{0.5} \right]^2 = 1 \dots \quad (3.1.12)$$

and the line  $z = 0.05$ ,

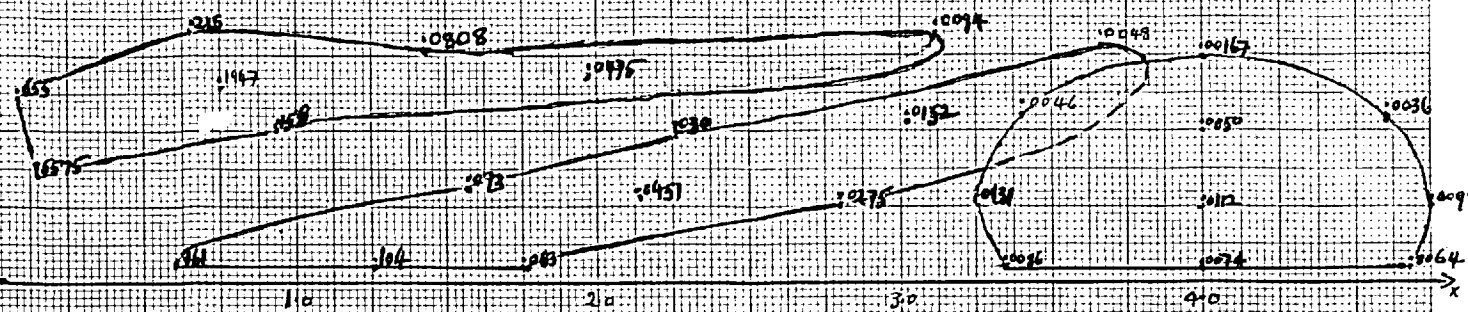


Fig. 24 Given above and below are three distributions indicated how the movement and concentration of a 'swarm' may be affected by a wind field pattern. When  $V = W/4$ , the above obtained at  $t = 1000$  and  $t = 2500$ , 12 and nearly 50 times the max. initial values respectively.

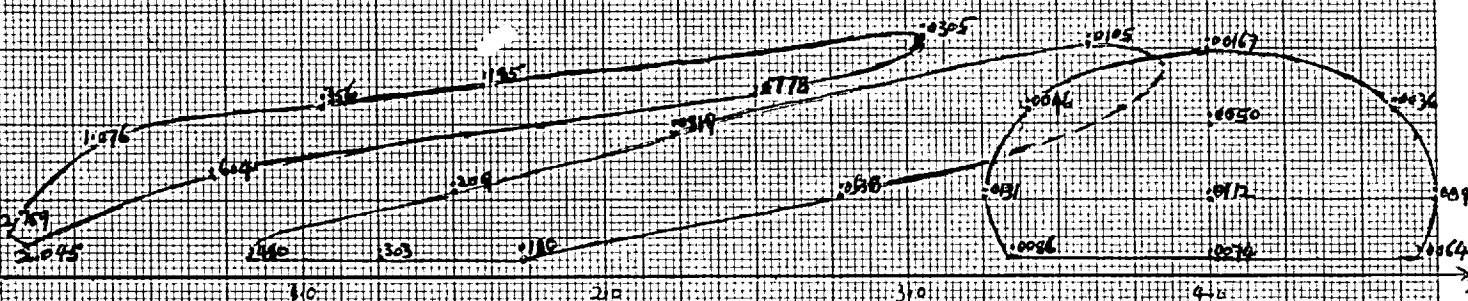


Fig. 25 When  $V$  is increased to  $3W/4$ , amount of time elapsed before the 'swarm' reaches the divergence zone gets longer and when  $t = 2500$ , values of 200 times the initial max. are found.

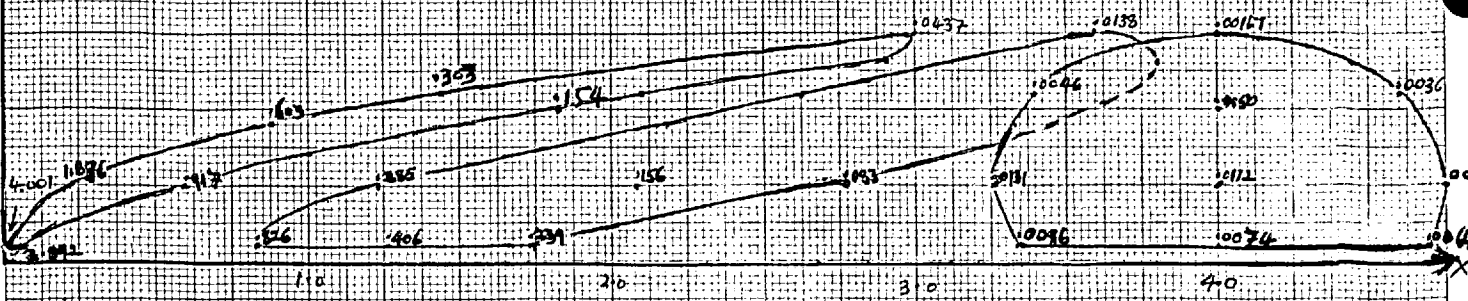


Fig. 26 Under horizontal motion, the rate of growth of downstream concentration is much higher; when  $t = 2500$ , a value of nearly 500 times the initial max. is observed.

elsewhere the concentration being defined as zero.

By computing, we obtain three cases having downstream distributions (p 67) for subsequent times: the one above (Fig 24) is for a case where  $\nu = w/4$ ; the middle one (Fig 25) is for  $\nu = 3w/4$ ; and the below (Fig 26) is for  $\nu = w$ , i.e. when the vertical velocity of particles is zero. We find that the nature of the flow pattern plays a cardinal role in relation to the downstream displacement behaviour of the swarm as a whole; since the horizontal velocity increases as  $z$  decreases, in all these cases, the swarm is distorted in such a way that its base contracts, but the swarm as a whole is elongated.

In the first case, by the time 1000 units of time have elapsed, the maximum concentration produced in the lowest parts of the swarm is increased by about 20 times along the particle paths, and is about 13 times the maximum upstream concentration at  $t=0$ . In a further 1500 units of time when the swarm has ascended a little the concentration increases 75 times along the particle path in question, and is 50 times the maximum concentration at  $t=0$ .

The next distribution (Fig 25) enables us to conclude that there is a more rapid rise in downstream concentration at the leading edge in the lowest parts, as the falling speed increases to  $\nu = 3w/4$ . The maximum increases found in 2500 units of time along a particle path, whose starting point at  $t=0$  is where  $\sigma = 0.0086$ , are over 300 times the original, and in a further 1000 units of time at the point  $(x = 0.004, z = 0.252)$ , it will have become 500 times over the original.

When the particles are constrained to travel horizontally, the



downstream distribution is very similar to the previous two cases, apart from the fact that the elongated shape becomes still narrower. The concentration rise of nearly 500 times greater than upstream value ( $\sigma = 0.0086$ ) occurs in 2500 units of time, which is achieved for  $\nu = 3w/4$  (Fig 26 ) in  $t = 3500$  units.

Downstream motion of the swarm reveals that  $\partial \sigma / \partial x$  decreases with increasing  $x$  and  $\partial \sigma / \partial z$  decreases with increasing  $z$ .

Section II A flow with max. horizontal velocity away from x-axis

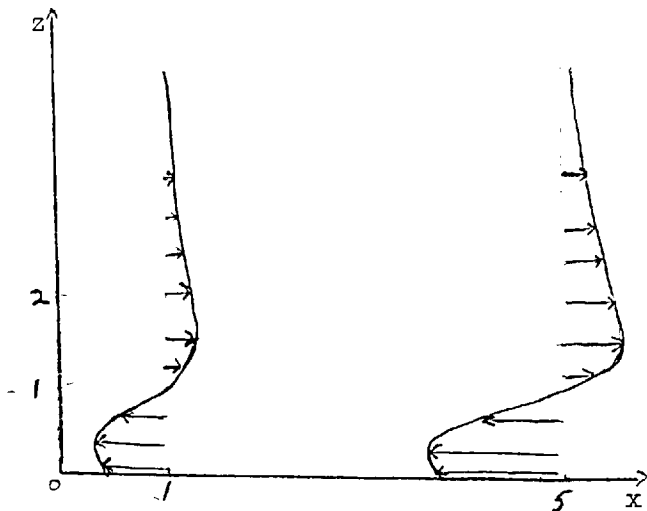
In this section also two calculations have been attempted: the first has dealt with a steady case and the second has assessed a time-dependent particle concentration distribution in a steady flow. Again we employ all the same non-dimensional variables as in the Section I.

Let the flow velocity field  $\underline{U}$  be defined by

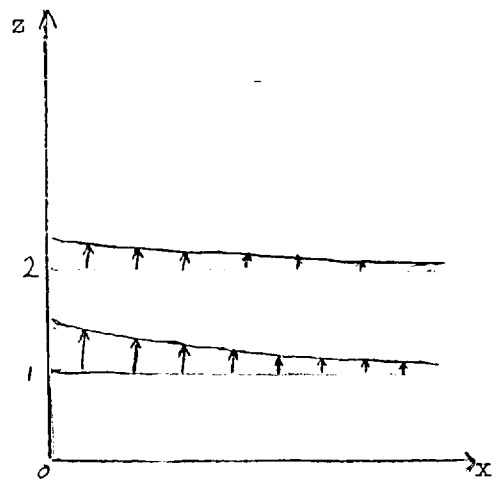
$$\underline{U} = \left( \frac{-k_0 x}{2(x^2+4)^{3/2}} (1+2z(0.5-z)) e^{-(0.5-z)^2}, 0, \frac{2k_0 z}{(x^2+4)^{3/2}} e^{-(0.5-z)^2} \right) \dots (3.2.1)$$

which satisfies the equation of continuity and where  $k_0$  is fixed at 5.294.

Given below are the profiles of horizontal and vertical components of  $\underline{U}$ , which lucidly illustrate an important improvement over the structure of the velocity field defining the flow used in the last section and is undoubtedly a more realistic representation of velocity fields occurring in the atmospheric flows.



Diag 6a The horizontal velocity profile of flow at  $x=1$  and  $x=5$



Diag 6b Profiles of vertical velocity of flow.

The structure of the incoming flow is such that its horizontal velocity increases from non-zero values on the  $x$ -axis to maximum values at  $z = 0.35$ . Then it decreases with height to zero on the line  $z = 1$ , above which divergence takes place. Its successively increasing maxima are found on the line  $z = 0.35$ , varying from zero at the  $z$ -axis to 2.79 at  $x = 5$  and tending to 2.90 as  $x \rightarrow \infty$ . In fact, the incoming flow is such that it can be thought of as having a boundary layer due to friction up to a height of first 0.35km (taking 1 unit in the  $x$ - and  $z$ - direction as 1 km).

The vertical velocity increases from zero on the  $x$ -axis to a maximum value on the line  $z = 1$ , then swiftly diminishes in the divergence zone with height. Its successively decreasing maxima (on the line  $x = 1$ ) vary from the value 1.031 at  $x = 0$  to .052 at  $x = 5$ . On account of the finite values occurring at  $x = \infty$ , we again resort to consideration of downstream motion from  $x = 5$ .

The stream function (See Fig 27(a) p 72 ) calculated using (3.1.2a) and (3.2.1) is

$$\psi(x, z) = k_0 \frac{xz}{2(x^2+4)^{\frac{1}{2}}} e^{-(0.5-z)^2}$$

Differentiating this equation partially with respect to  $x$  and  $z$ , the corresponding vorticity distribution

$$\eta = \frac{-k_0}{(x^2+4)^{\frac{1}{2}}} \left\{ \frac{6xz}{(x^2+4)^2} - x[1-3z+2z(0.5-z)^2] \right\} e^{-(0.5-z)^2}$$

is evaluated and differentiation of  $\eta$  renders its rate of change

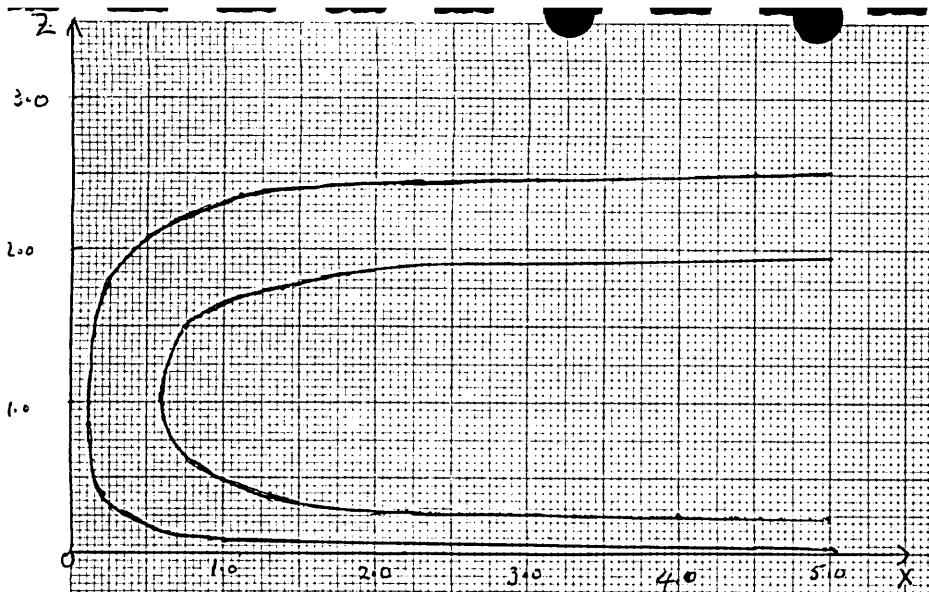


Fig. 27a Streamlines of flow given by  $\psi(x, z)$  on p. 71

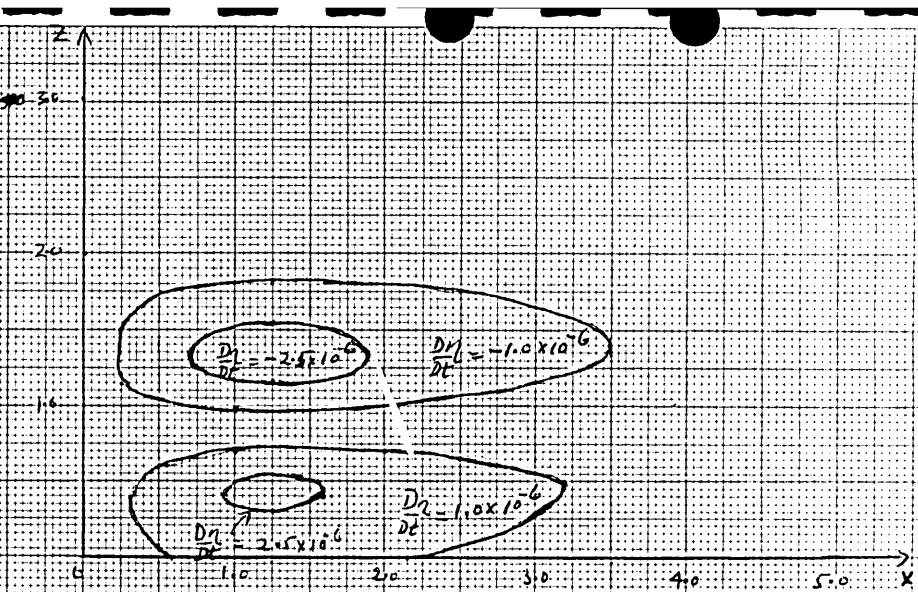


Fig. 27c A corresponding rate of change of vorticity,  $D\eta/Dt$ , gives a picture of a situation similar to that produced by cooling due to rain.

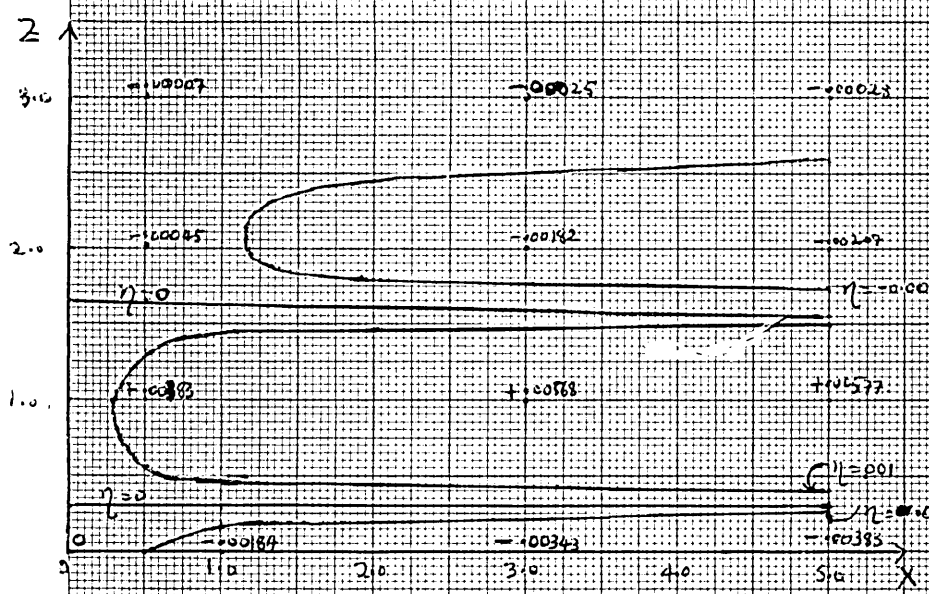


Fig. 27b An expression for  $\eta$  on p. 71 obtains the associated vorticity distribution.

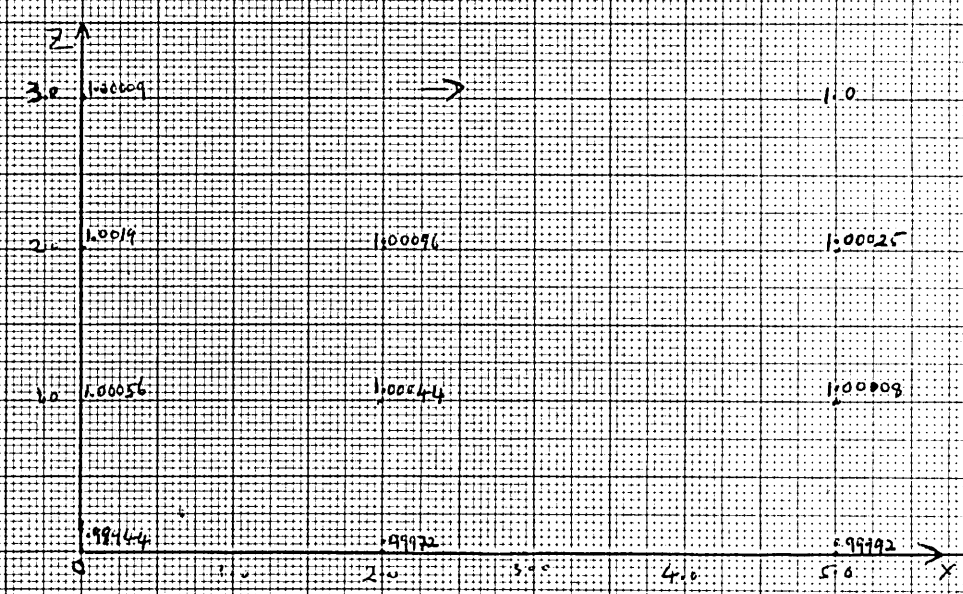


Fig. 27d This is the density distribution evaluated from  $\rho(x, z)$  on p. 73

$$\frac{D\eta}{Dt} = \frac{k_0^2}{(x^2+4)^2} \left\{ \frac{12x^3z}{(x^2+4)^2} [1+2z(0.5-z)] + 2x[1+4z^2(0.5-z)] \right\} e^{-2(0.5-z)^2}$$

And using the equation (3.1.3) for the density  $\rho$ , the following is obtained:

$$\rho(x, z) = \text{Exp} \left\{ \frac{2k_0^2}{g} [z[1+2z(0.5-z)]] \left[ \frac{4}{(x^2+4)^3} - \frac{1.5}{(x^2+4)^2} \right] - \frac{1}{2(x^2+4)} [1+4z^2(0.5-z)] \right\} e^{-2(0.5-z)^2}$$

Putting vorticity  $\eta$ , its rate of change  $\frac{D\eta}{Dt}$  and the associated density  $\rho$  of the flow in physical units, their distributions represented respectively by the Figs 27(b), 27(c) and 27(d) have been worked out.

The vorticity distribution constituting three divisions made by the lines  $z = 0.3$  and  $z = 1.675$  is such that the middle division contains positive vorticity whereas the other two contain negative values. Expected vorticity on the x-axis implying the presence of friction responsible for boundary layers exist. The situation which the rate of change of vorticity depicts may be produced by cooling due to rain in a thunderstorm. Hence, values comparable to those in the convergence zone also exist in the divergence zone wherein relatively larger values of density are found.

Writing the particle falling speed relative to the flow as

$$v = nw,$$

the actual particle velocity is designated by

$$\underline{U}_p = \left( \frac{-k_0 x}{2(x^2+4)^{3/2}} [1+2z(0.5-z)] e^{-(0.5-z)^2}, 0, \frac{2k_0(1-n)z}{(x^2+4)^{3/2}} e^{-(0.5-z)^2} \right) \dots \quad (3.2.2)$$

where  $n$  is the constant of proportionality.

Calculation II(i) Steady concentration

Using this particle velocity vector, we work out distributions for steady concentrations. By equation of continuity, we have

$$\begin{aligned}
 -k_0 \frac{x}{2(x^2+4)^{\frac{1}{2}}} [1+2z(\frac{1}{2}-z)] e^{-(\frac{1}{2}-z)^2} \frac{\partial \sigma}{\partial x} + \frac{2k_0(1-n)z}{(x^2+4)^{3/2}} e^{-(\frac{1}{2}-z)^2} \frac{\partial \sigma}{\partial z} \\
 = 2nk_0 \sigma \frac{1}{(x^2+4)^{3/2}} [1+2z(\frac{1}{2}-z)] e^{-(\frac{1}{2}-z)^2} \dots \quad (3.2.3)
 \end{aligned}$$

which can be written as

$$- \frac{dx}{\frac{x}{2(x^2+4)^{\frac{1}{2}}} [1+2z(\frac{1}{2}-z)]} = \frac{dz}{\frac{2z(1-n)}{(x^2+4)^{3/2}}} = \frac{d\sigma}{\frac{2n\sigma}{(x^2+4)^{3/2}} [1+2z(\frac{1}{2}-z)]}$$

by the method of characteristics.

Integration ensures the relationship between  $\sigma$ ,  $x$  and  $z$ .

Thus:

$$z e^{-(\frac{1}{2}-z)^2} \left( \frac{x^2}{x^2+4} \right)^{\frac{1-n}{2}} = R \quad \dots \quad (3.2.4)$$

and

$$\sigma(x, z) = A_0 \left( \frac{x^2}{x^2+4} \right)^{\frac{-n}{2}} \quad \dots \quad (3.2.5)$$

where  $A_0$  and  $R$  are arbitrary constants of integration. Hence elimination of  $R$  and  $A_0$ , simply by writing  $A_0$  as a function of  $R$ ,

$$\text{i.e. } A_0 = g(R) = g(z e^{-\frac{1}{2}z})^2 \left( \frac{x^2}{x^2+4} \right)^{\frac{1-n}{2}},$$

renders the general solution

$$\sigma(x, z) = \left( \frac{x^2}{x^2+4} \right)^{\frac{-n}{2}} g(z e^{-\frac{1}{2}z})^2 \left( \frac{x^2}{x^2+4} \right)^{\frac{1-n}{2}}, \dots \quad (3.2.6a)$$

Selecting the function

$$g(R) = \frac{R(1+R)}{1+R^2} \exp \left[ \frac{1-n}{2} \frac{-(1.25)R}{(1-2R)^2} \right]$$

where  $R(x, z)$  is as defined in (3.2.4), we arrive at the solution

$$\sigma(x, z) = \left( \frac{x^2}{x^2+4} \right)^{\frac{-n}{2}} \frac{R(1+R)}{1+R^2} \exp \left[ \frac{1-n}{2} \frac{-(1.25)R}{(1-2R)^2} \right] \dots \quad (3.2.6)$$

where  $R$  is as given by (3.2.4).

This expression has been obtained with a view to studying three possible cases. It was specified thus in order to have finite concentrations far upstream and to avoid infinite concentration on the  $z$ -axis, when  $x = 0$  is put into the equation (3.2.5).

Beginning with  $n=0$ , we find a steady growth in downstream concentration as  $n$  increases. When  $n = 0$ , the distribution (Fig 28, p77 )



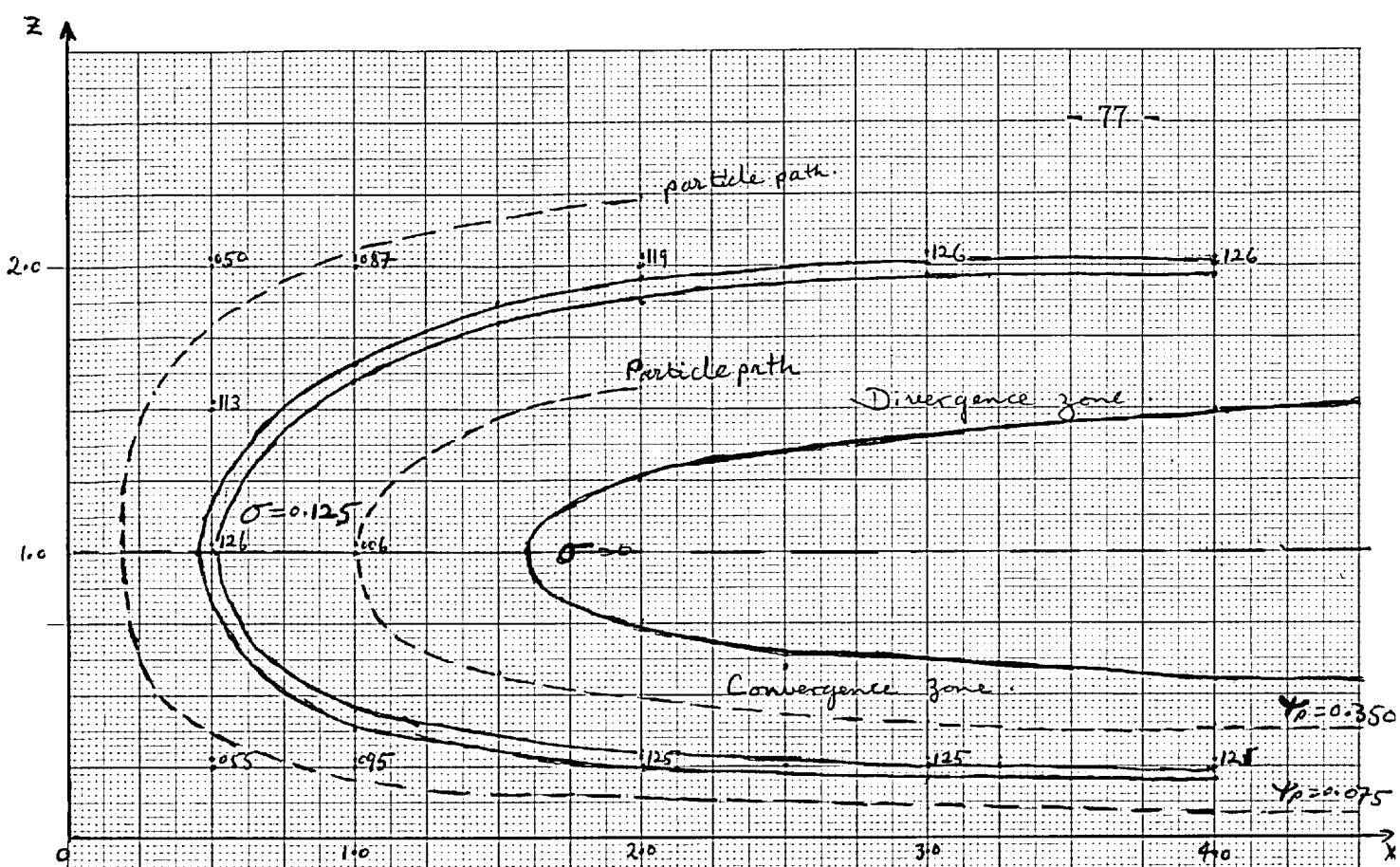


Fig. 28 Substitution of  $n = 0$  in (3.2.6) obtains concentration contours showing that no downstream increase can be effected.

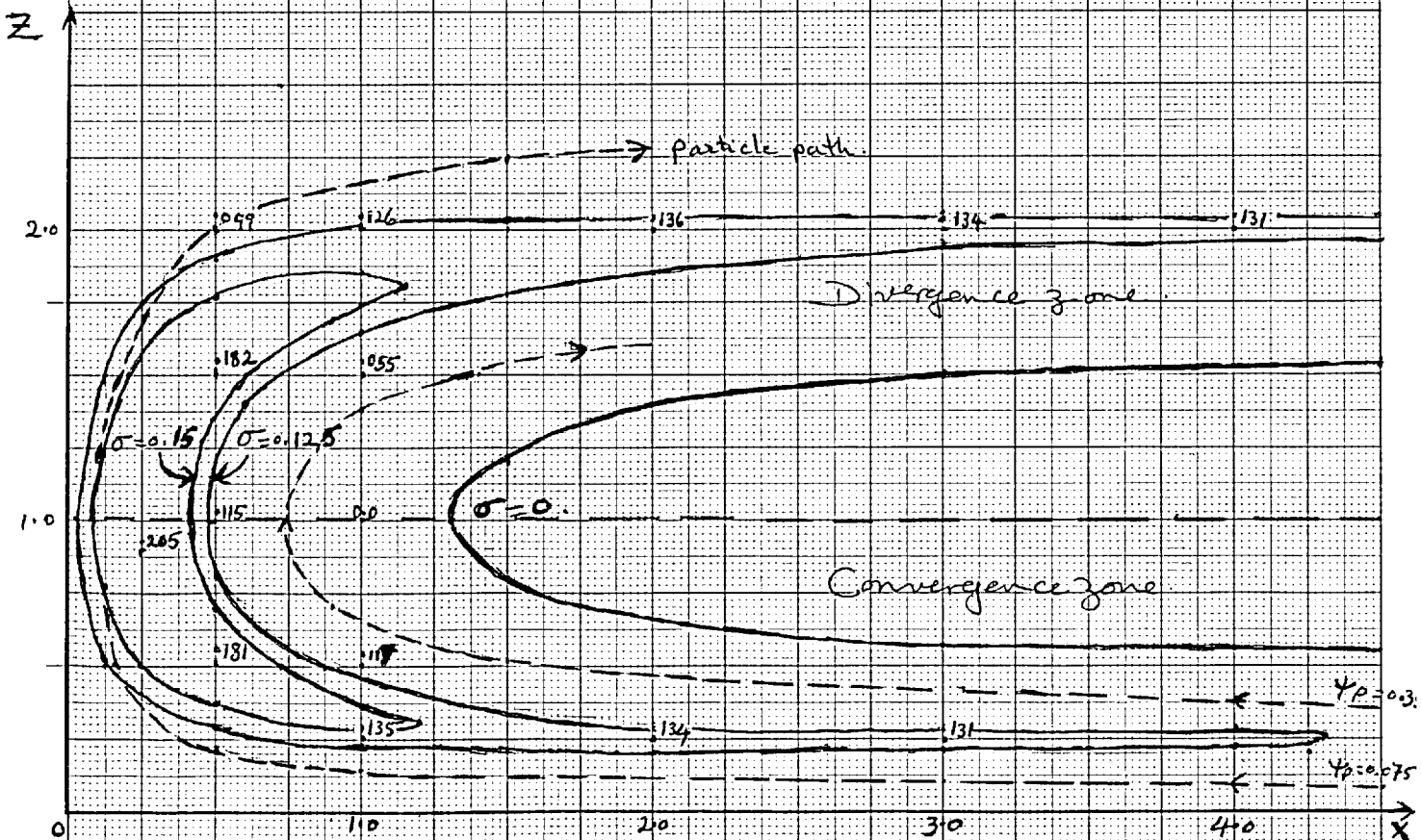


Fig. 29 When  $n > 0$ , increase in concentration is apparent downstream in this example, where  $n = 1/4$  values of  $1\frac{1}{2}$  times the initial max. are achieved in the convergence zone.

obtained is indicative of a situation in which downstream development of higher concentration is non-existent and all the material is carried up and away from the convergence zone.

Two other cases occur in the range  $0 \leq n \leq \frac{1}{2}$ .

First we put  $n = 1/4$  in (3.2.6) which becomes

$$\sigma(x, z) = \left( \frac{x^2}{x^2+4} \right)^{-1/8} \frac{R(1+R)}{1+R^2} \exp \left[ \frac{-(1.25)^{3/8} R}{(1-2R)^2} \right]$$

where

$$R = Z e^{-\left(\frac{1}{2}-z\right)^2} \left( \frac{x^2}{x^2+4} \right)^{3/8}$$

... (3.2.7)

From the distribution (Fig 29, p 77 ) for this case we find a small downstream increase in the convergence zone and it is one and two third times the original upstream maximum. Second, when  $n = \frac{1}{2}$  in (3.2.6) we have the critical case with

$$\sigma(x, z) = \left( \frac{x^2}{x^2+4} \right)^{1/4} \frac{R(1+R)}{1+R^2} \exp \left[ \frac{-(1.25)^{1/4} R}{(1-2R)^2} \right]$$

where

$$R = \left( \frac{x^2}{x^2+4} \right)^{1/4} z e^{-\left(\frac{1}{2}-z\right)^2}$$

... (3.2.8)

Contours given on the page 79 (Fig 30) show that the downstream increases become relatively large, with maximum values forming on the z-axis which are six times the original maximum at  $x=5$ .



Any value of  $n$  greater than  $\frac{1}{2}$  produces infinite concentration on the  $z$ -axis which from the point of view of locust densities is undesirable. A typical value of  $n = \frac{3}{4}$  has been chosen to show a distribution (Fig 31) of this case.

It is possible that this 'earlier occurrence' of infinite concentration on the  $z$ -axis may be mainly due to the initial distribution and not due to the particle falling speed alone.

Calculation II(ii) Unsteady concentration

Here again we conduct a calculation similar to Calculation (ii) in the previous section to assess the development of downstream concentration in a 'typical' swarm moving with a flow designated by the velocity field (3.2.1).

By equation of continuity (for unsteady particle concentration), we have

$$\frac{\partial \sigma}{\partial t} - k_0 \frac{x}{2(x^2+4)^{3/2}} [1+2z(0.5-z)] e^{-(0.5-z)^2} \frac{\partial \sigma}{\partial x} + \frac{2k_0(1-n)z}{(x^2+4)^{3/2}} e^{-(0.5-z)^2} \frac{\partial \sigma}{\partial z} = \frac{2n\sigma k_0}{(x^2+4)^{3/2}} [1+2z(0.5-z)] e^{-(0.5-z)^2} \dots \quad (3.2.9)$$

which is solved in conjunction with the initial condition defined by (3.1.11) and (3.1.12).

The computed results are shown in the Figs 32, 33, and 34 on the page 82 . Fig 32 has been drawn for  $n=1/4$  ( $w_p = 3w/4$ ), Fig 33 for  $n = 3/4$  ( $w_p = w/4$ ) and Fig 34 for  $n=1$  ( $w_p = 0$ ). Generally speaking, in all the cases presented here the downstream shape of the 'swarm' becomes much protruded in the middle at the leading edge; this is attributable to the nature of the flow whose horizontal velocity is such that its maximum values lie on the line  $z = 0.35$ . Following any particle path enables us to understand in respect of the first two cases the effects of convergence and divergence. It is observed

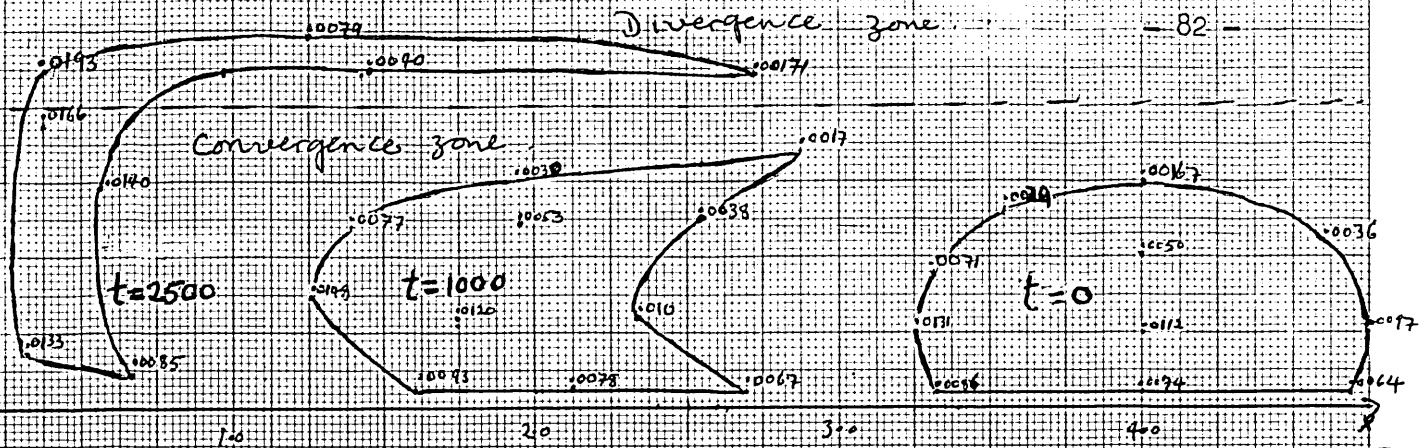


Fig. 32 Given by (3.1.11) and (3.1.12) when  $n = 1/4$ , this distribution (with those given below on this page) indicate that there is an influence by wind fields upon shape and concentration of a swarm. When  $t = 2500$ , less than twice the initial max. is obtainable in the convergence zone.

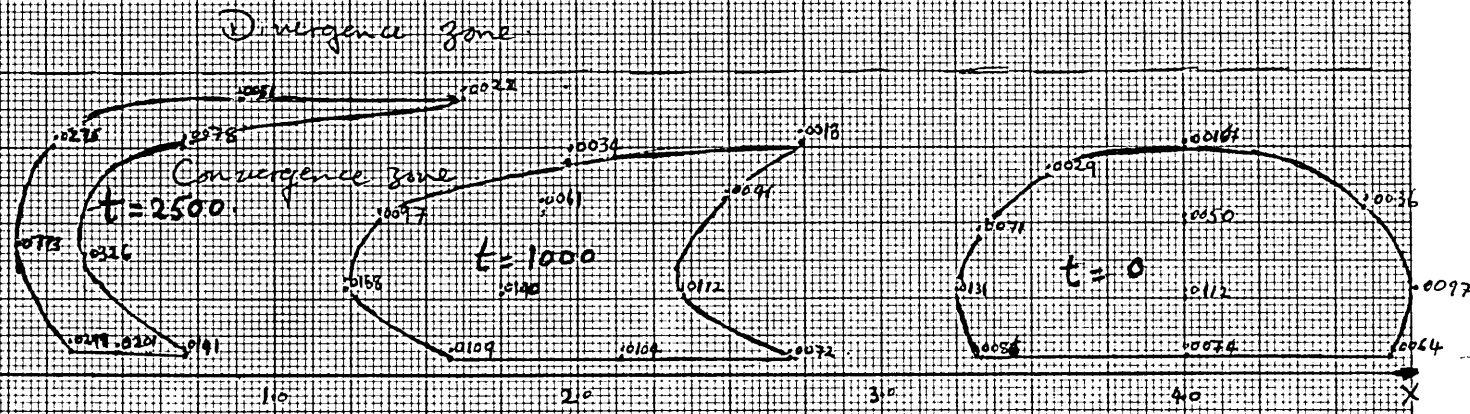


Fig. 33 Comparing this with Fig. 32, it is evident that the higher the falling speed  $v$ , the longer the 'swarm' takes to reach divergence zone, and the higher the concentration.

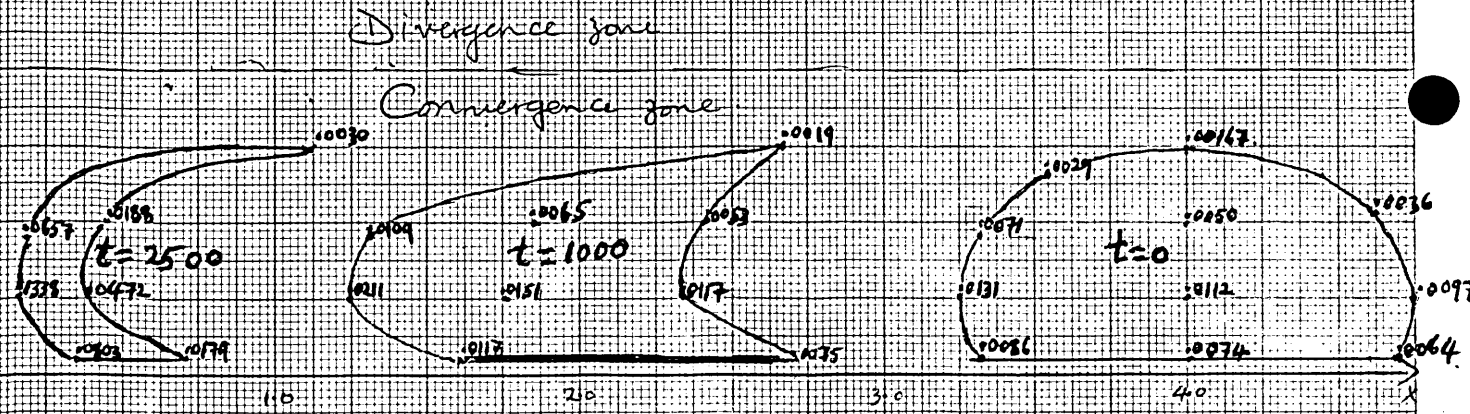


Fig. 34 Under horizontal motion, growth of downstream concentration becomes much pronounced; 10 times the upstream max. occurs at the leading edge when  $t = 2500$ .

that the concentration keeps on growing along a particle path until it reaches the divergence zone (above the line  $z = 1$ ), where it slowly begins to diminish. This truly is demonstrative of convergence as a concentrator and divergence as a disperser.

In Fig 32 the estimated downstream distributions for 1000 and 2500 units of time indicate only a small rise in the downstream concentration. Indeed, the strip of concentration, bounded by the lines  $z = 0.05$  and  $z = 0.1$  of the initial distribution at  $t = 0$ , remains longer in the convergence zone (partly owing to the structure of velocity distribution) than the rest of the 'swarm' and in doing so produces in 3500 units of time twice the maximum concentration found at the leading edge when  $t = 0$ .

The effects of the falling speed, however, are found to become much more pronounced in the next case (Fig 33) for  $n = 3/4$ . Here, approximately the lower half of the initial distribution (in the elliptic region) remains in the convergence zone for a much longer period, and if the particle path, starting from the point where concentration is  $\sigma = 0.0131$  at the leading edge at  $t = 0$ , is followed, about six times that original value is produced 2500 units of time, and if this path is followed for a further 1000 units of time a staggering increase amounting to 16 times over that original value occurs at the point (0.043, 0.592). Possibly even higher values occur during the same amount of time along a particle path whose starting point is still at a lower level.

Next distribution (Fig 34) gives an indication of the difference in the degree of effects of falling speeds  $\nu = 3w/4$  and  $\nu = w$ , but apparently these effects become observably more pronounced when the 'swarm' enters

the region bounded by the axes and the lines  $z = 1$  and  $x = 1$ . A distribution drawn in this region for  $t = 2500$  units shows an increase in values 10 times over the maximum found at  $t = 0$ . As it further advances towards  $z$ -axis, concentration rises with immense rapidity.



Chapter IV More Potential Flows

Section I Particle Concentration in a Flow with a tilted Interface

Differential heating along coastlines is one example where a front may be produced with a well-defined boundary between the air flowing from the sea and the air already existing over land. The boundary becomes tilted when the cold air on the one side descends and the warm air on the other ascends, the angle of tilt being dependent upon the strength of convergence etc.

In this section, therefore, we have considered a flow pattern similar to a motion on one of the sides of a front with a tilted boundary. Owing to the fact that an analytical description of a flow incorporating an interface (as well as providing a desirable distribution of vorticity etc.) is very difficult, we have undertaken to work with a potential flow, where the line of interface has been taken to be at  $60^\circ$  to horizontal in order to simplify mathematics.

The velocity potential

$$\phi(x, z) = U_0 x(x^2 - 3z^2)$$

obtains the velocity field

$$\underline{U} = (-3U_0(x^2 - z^2), 0, 6U_0xz) \dots \quad (4.1.1)$$

as  $\underline{U} = -\underline{\text{grad}} \phi$ . For convenience we have taken  $U_0 = 1/3$ .

It is observed from the diagram below that the flow commences asymptotically at infinity with infinite value and is parallel to x-axis. On entering the convergence zone it rises to diverge above the line  $z = x$  (i.e. the line on which the horizontal component of

velocity has a zero value) and returns to infinity so that it is asymptotic to the line  $z = \sqrt{3} x$ , which is represented in the diagram by an axis  $z'$ .

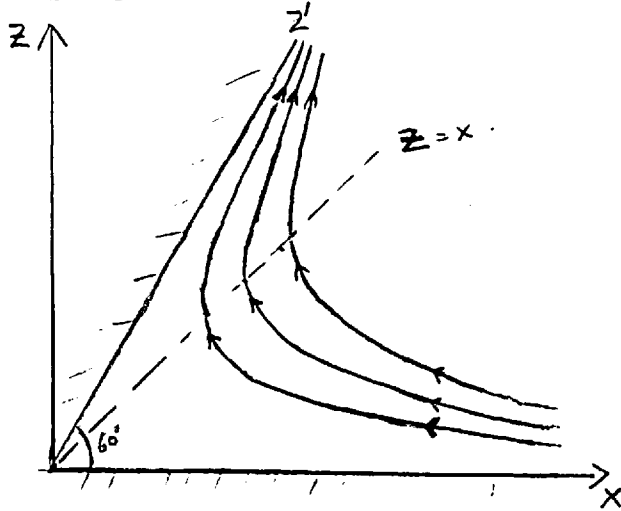


Fig. 7: Sketch of streamlines  $\psi = \text{Const.}$   
Assuming the particle falling speed to be

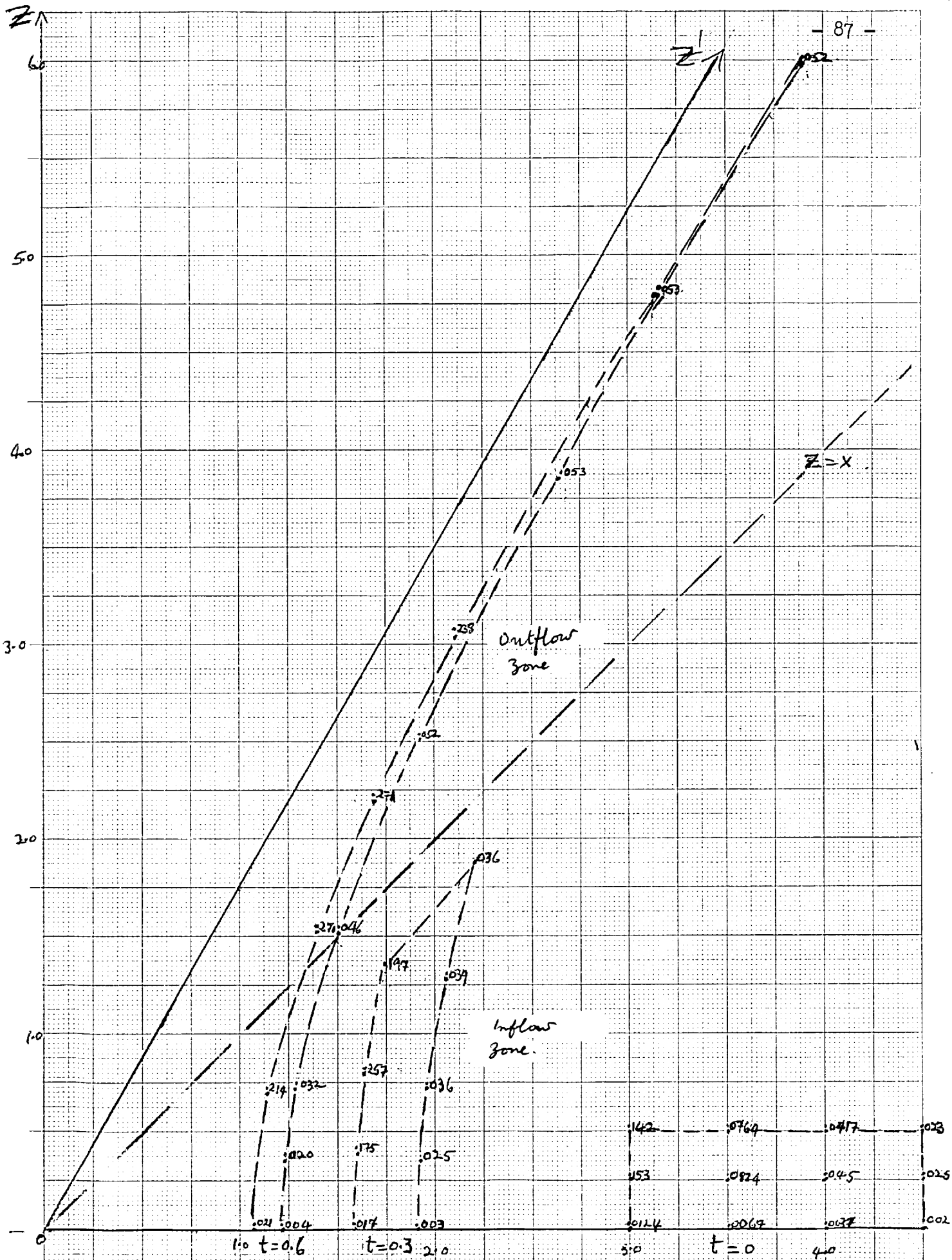
$$v = nw \tag{4.1.2}$$

the particle velocity  $\underline{U}_p$  is

$$\underline{U}_p = (-(x^2 - z^2)0, 0, 2(1-n)xz) \tag{4.1.3}$$

Of the seven calculations we have so far attempted, three have been devoted to working out time-developing distributions, which have enabled us to understand better the particle behaviour in the convergence zone, especially. Consequently we have decided not to carry out any calculation in this chapter for steady concentration, but to focus our attention straight away to the consideration of time-developing distributions.

Hence, substituting (4.1.3) into equation of continuity for unsteady particle concentration, we have



$$\frac{\partial \sigma}{\partial t} - (x^2 - z^2) \frac{\partial \sigma}{\partial x} + 2(1-n)xz \frac{\partial \sigma}{\partial z} = 2n\sigma x \quad (4.1.4)$$

which we have solved (using computer methods) for two values of  $n$ , with the initial condition at  $t = 0$  given by

$$\sigma(x, z) = \frac{1+100z}{1+x} \exp[-(x+3z)] \quad (4.1.5)$$

defined in the area bounded by the inequalities  $3 \leq x \leq 4.5$  and  $0 \leq z \leq 0.5$ , elsewhere the concentration being taken as zero.

#### Case I

For this case we have chosen to consider the falling speed  $v = w/4$ , when (4.1.4) becomes

$$\frac{\partial \sigma}{\partial t} - (x^2 - z^2) \frac{\partial \sigma}{\partial x} + 1.5 xz \frac{\partial \sigma}{\partial z} = 0.5x\sigma \quad (4.1.6)$$

The solution for which has been graphically plotted in the Fig 35 (p 87 ) for regular time intervals. The initial condition at  $t=0$  is such that its maximum  $\sigma = 0.155$  is found at  $z = 0.30$  on the line  $x = 3$  which forms the front edge of a 'swarm', as it were, moving towards corner of convergence zone. In 0.3 units of time, the swarm as a whole has been displaced just over one unit towards the corner and horizontal contraction and vertical stretching have altered the shape in such a way that its location is just below the line  $z = x$  above which outflow occurs. The maximum concentration occurs at the leading edge at the height  $z = 0.8$ . When the swarm has been displaced for a further time  $t = 0.3$ , a very elongated stretch has been produced because some

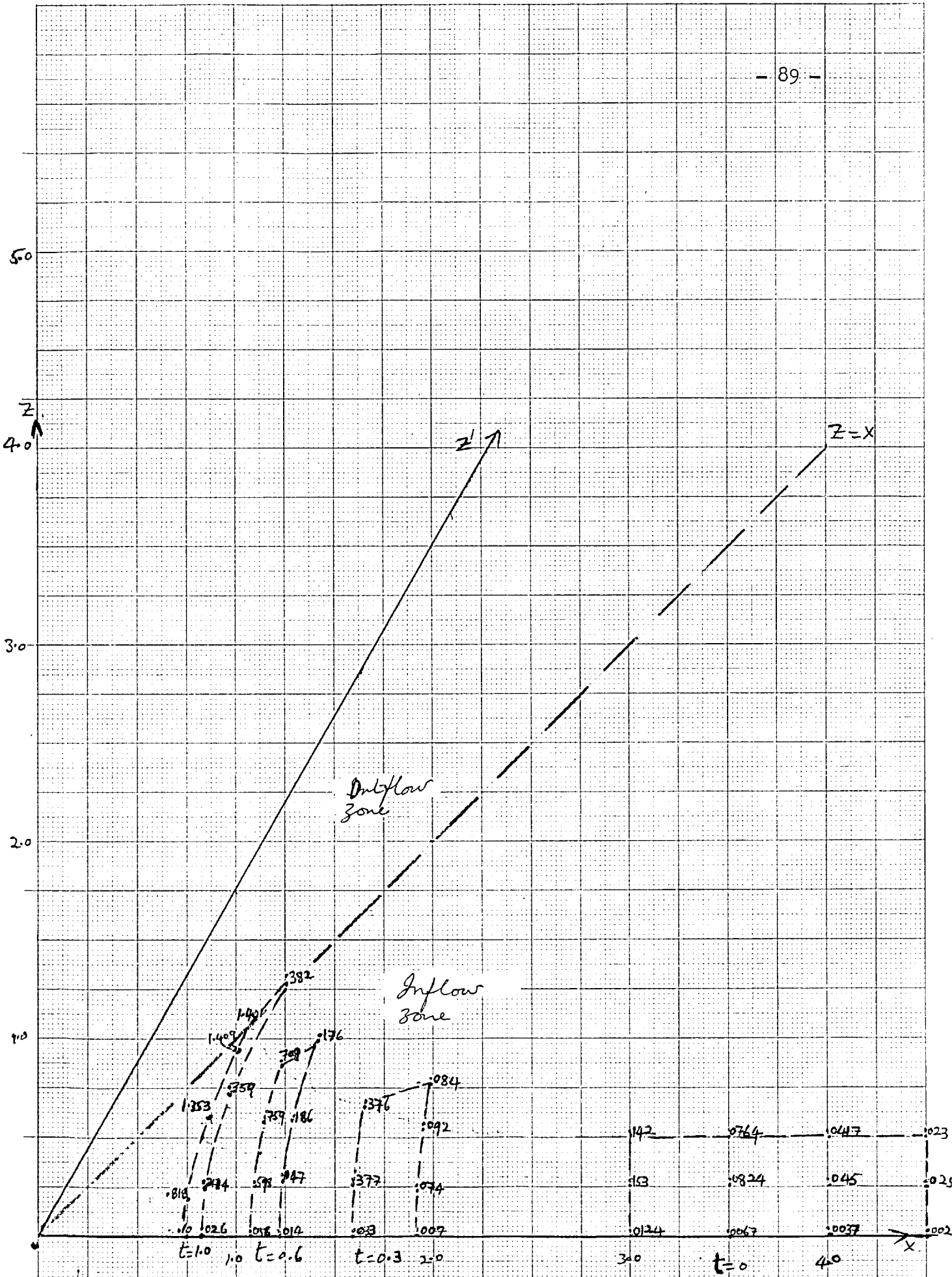


Fig. 36 Increasing falling speed to  $v = 3w/4$ , enables us to include the distribution at  $t = 1$ , when 9-times the initial max. (at  $t=0$ ) is produced.

of the upper part of the swarm enters the outflow zone where the vertical component of velocity becomes large.

As a result, the downstream maximum values have been found to increase noticeably gradually; when  $t = 0.6$ , the maximum is even less than twice the upstream maximum at  $t = 0$ . Any further downstream motion would transport much of the concentration away from the inflow region in which only lowest parts of the swarm may remain for longer periods of time to produce higher concentration.

### Case II

This case has been studied for  $n = 3/4$  in (4.1.2) when (4.1.4) reduces to

$$\frac{\partial \sigma}{\partial t} - (x^2 - z^2) \frac{\partial \sigma}{\partial x} + 0.5 xz \frac{\partial \sigma}{\partial z} = 1.5 x \sigma \quad . \quad (4.1.7)$$

The initial distribution on Fig. 36 at  $t = 0$  is the same as that in the Case I. Generally speaking, the effects of raising the particle falling speed are decidedly stronger: it takes longer for the distribution to reach the outflow region; and resulting concentration is higher. We have constructed successive downstream distributions for  $t = 0.3$ ,  $t = 0.6$  and  $t = 1.0$ , all of which are located still in the inflow region, with the exception of the topmost part of the distribution at  $t = 1.0$ .

Following a particle path starting at the point  $(3.0, 0.25)$  where  $\sigma = 0.153$ , an increase of  $2\frac{1}{2}$  times can be noted at the leading edge when  $t = 0.3$ . By this time, too, the hind-edge values have increased by 3 to  $3\frac{1}{2}$  times those at the hind-edge of the initial distribution.

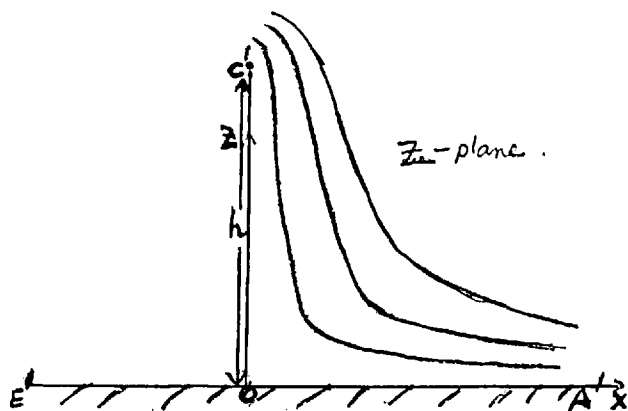
Following the same particle path a further 0.3 units of time, it is found that the concentration is 5 times greater than that of the maximum value at  $t = 0$ .

When the 'swarm' has progressed further downstream the diminution of area of distribution, and therefore a very rapid growth in concentration, are observed. Indeed, when  $t = 1, 9$  to  $9\frac{1}{2}$  times original maximum values can be noted. However at the hind edge, 13 to 15 times their original counterparts have been achieved.

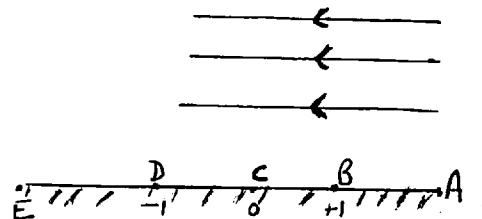
Although we have succeeded in calculating these interesting distribution, one inevitable problem cannot escape our attention: due to the nature of the flow, the whole swarm would be distributed over a large area as soon as it enters the outflow region and would get carried up to infinity.

Section II : A Calculation using a flow past an obstacle.

We have by now considered several suitable flows ( simulating certain patterns of atmospheric convergence ) to ascertain the effects of falling speed of particles on their concentration as they move towards, into and out of the convergence zone. There is, however, one kind of flow pattern that still remains to be employed: a flow past a vertical obstacle of finite height (which for our calculation will be taken to be 3) as shown in the diagram below. This flow is obtained by mapping the points B, C and D of the W-plane on to the points of the z-plane such that B and D map on to O and C on to C', thereby creating an obstacle C'O of height h.



Diag 8a Streamlines of a flow past an obstacle of height h.



Diag 8b W-plane flat flow

The relationship between the flow in the two planes is found by solving the differential equation

$$\frac{dz}{dw} = \frac{KW}{(w^2-1)^{\frac{1}{2}}}$$

which in fact is due to Schwarz-Christoffel transformation. Using the



initial condition that  $Z = 0$  when  $W = 0$  and  $Z = ih$  when  $W = 0$ , we arrive at the equation

$$W(Z) = (Z^2 + h^2)^{\frac{1}{2}} / h$$

where  $Z = x + iz$  is a complex number.

Assuming that the complex potential is denoted by

$$\bar{\phi} = U_0 W = \phi(x, z) + i\psi(x, z)$$

we calculate the velocity field potential

$$\phi(x, z) = \frac{U_0}{h} [(x^2 + h^2 - z^2)^2 + 4x^2 z^2]^{1/4} \cos \left\{ \frac{1}{2} \tan^{-1} \left( \frac{2xz}{x^2 + h^2 - z^2} \right) \right\}$$

which on differentiating obtains the velocity

$$\underline{U} = (u, 0, w)$$

$$= \left( -\frac{1}{P} [A \cos Q + B \sin Q], 0, \frac{1}{P} [B \cos Q + A \sin Q] \right) \dots \quad (4.2.1)$$

where

$$P = [(x^2 + 9 - z^2)^2 + 4x^2 z^2]^{3/4},$$

$$Q = \frac{1}{2} \tan^{-1} \left( \frac{2xz}{x^2 + 9 - z^2} \right),$$

$$A = x(x^2 + z^2 + 9)$$

and

$$B = z(9 - x^2 - z^2),$$

} \dots \quad (4.2.2)

taking  $U_0 = h = 3$

This velocity field is such that its values are finite everywhere on the plane, with the exception of the value at C' where it is infinity. It is because of this value at C' that the computer methods break down and it is not possible to study the motion of the particles outside right-hand quadrant.

Taking the falling speed  $\nu$  to be proportional to the vertical component of flow velocity, the particle velocity  $U_p$  is given by

$$\begin{aligned}
 U_p &= (U_p, 0, w_p) \\
 &= \left( -\frac{1}{P} [A \cos(Q) + B \sin(Q)], 0, (1-n) [B \cos(Q) + A \sin(Q)] \frac{1}{P} \right)
 \end{aligned}
 \tag{4.2.3}$$

where  $n$  is the constant of proportionality.

For unsteady particle concentration, the equation of continuity

$$\frac{\partial \sigma}{\partial t} + \text{div} (U_p \sigma(x, z, t)) = 0$$

becomes

$$\frac{\partial \sigma}{\partial t} + u_p \frac{\partial \sigma}{\partial x} + w_p \frac{\partial \sigma}{\partial z} = - \frac{\partial \nu}{\partial z} \sigma \tag{4.2.4}$$

where  $u_p$  and  $w_p$  are given in (4.2.3).

The right-hand side expression is such that

$$\frac{\partial \nu}{\partial z} = \frac{1}{P} \left\{ \frac{1}{P^{4/3}} [B w_p - AB \sin(Q) + A^2 \cos(Q)] + C \sin(Q) - D \cos(Q) \right\}$$

where  $P$  and  $Q$ ,  $A$  and  $B$  are as defined in (4.2.2), and

$$c = 2xz$$

and  $D = 9 - x^2 - 3z^2$ .

The equation (4.2.4) is solved by computer methods in conjunction with the initial condition

$$\sigma(x,z) = z e^{-6z} / (1+x) \quad \dots \quad (4.2.5)$$

at time  $t = 0$ , defined in an area bounded by an ellipse

$$\left(\frac{x-4}{3/4}\right)^2 + \left(\frac{z-1/4}{1/2}\right)^2 = 1 \quad , \quad \dots \quad (4.2.6)$$

elsewhere the concentration being zero.

The function (4.2.5) has been chosen to give its distribution a kind of swarm-like appearance, in which higher values of concentrations are found at the leading edge.

Here, we examine two cases for  $n = 1/3$  and  $n = 2/3$  to find out the downstream behaviour of particles.

Case I

The distribution on the page 96 (Fig 37) is a case where  $n = 1/3$  i.e.  $w_p = 2w/3$ . Successive downstream distributions are constructed at regular time interval  $t = 2.5$ . As the 'swarm' progresses towards the convergence zone, the area of confinement slowly becomes narrower and taller, and there is a small but observable rise in concentration. When  $t = 7.5$  the upper half of the swarm becomes 'tilted' towards z-axis by the effects of the flow pattern, and nearly twice the original upstream maximum is obtained. It would have been interesting to ascertain

← Obstacle

Fig. 37 These successive downstream distributions show, when  $n = 1/3$  in (4.2.3), how fast the particles get carried up. Downstream increases amount to about twice the initial maximum.

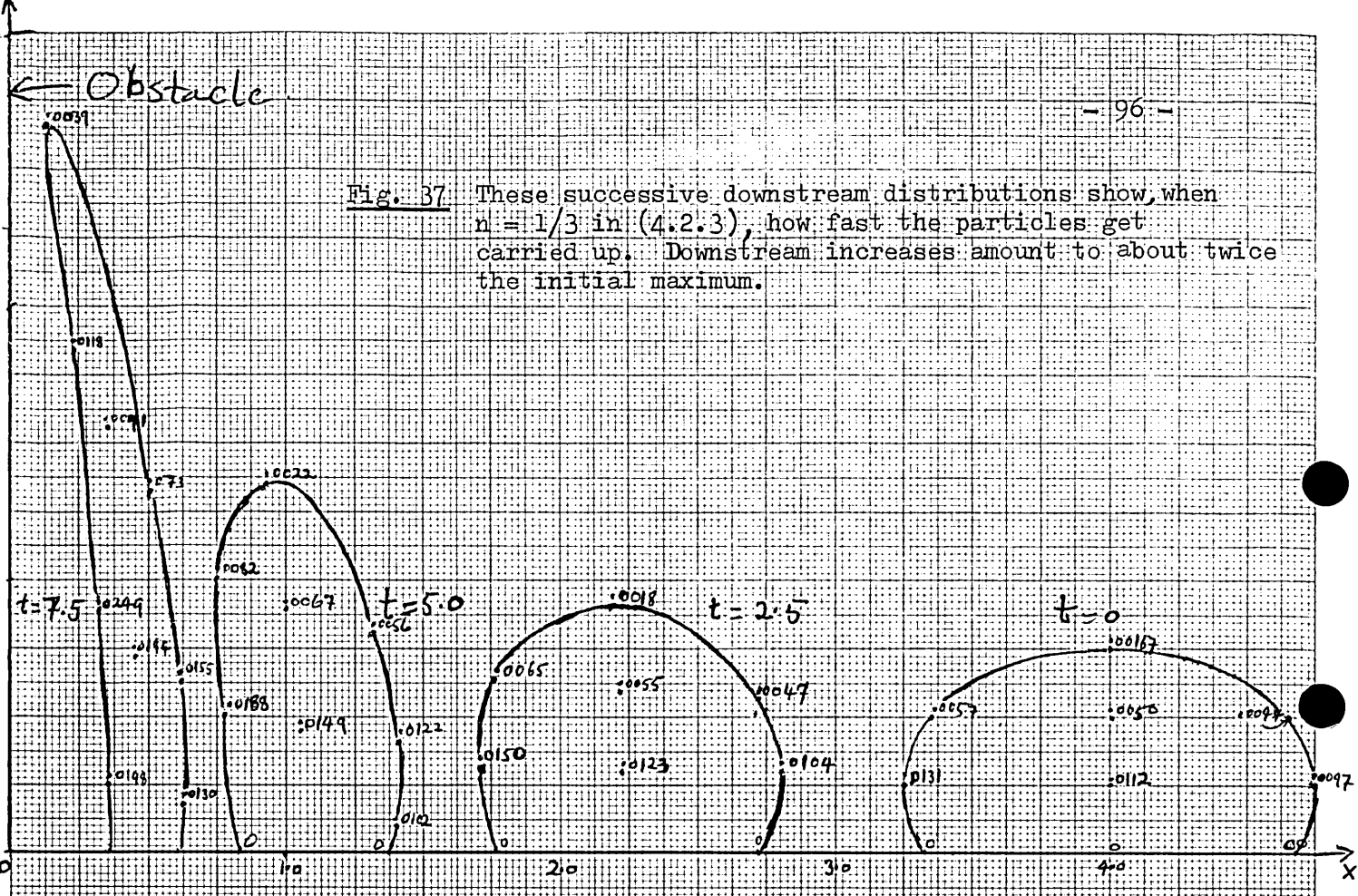
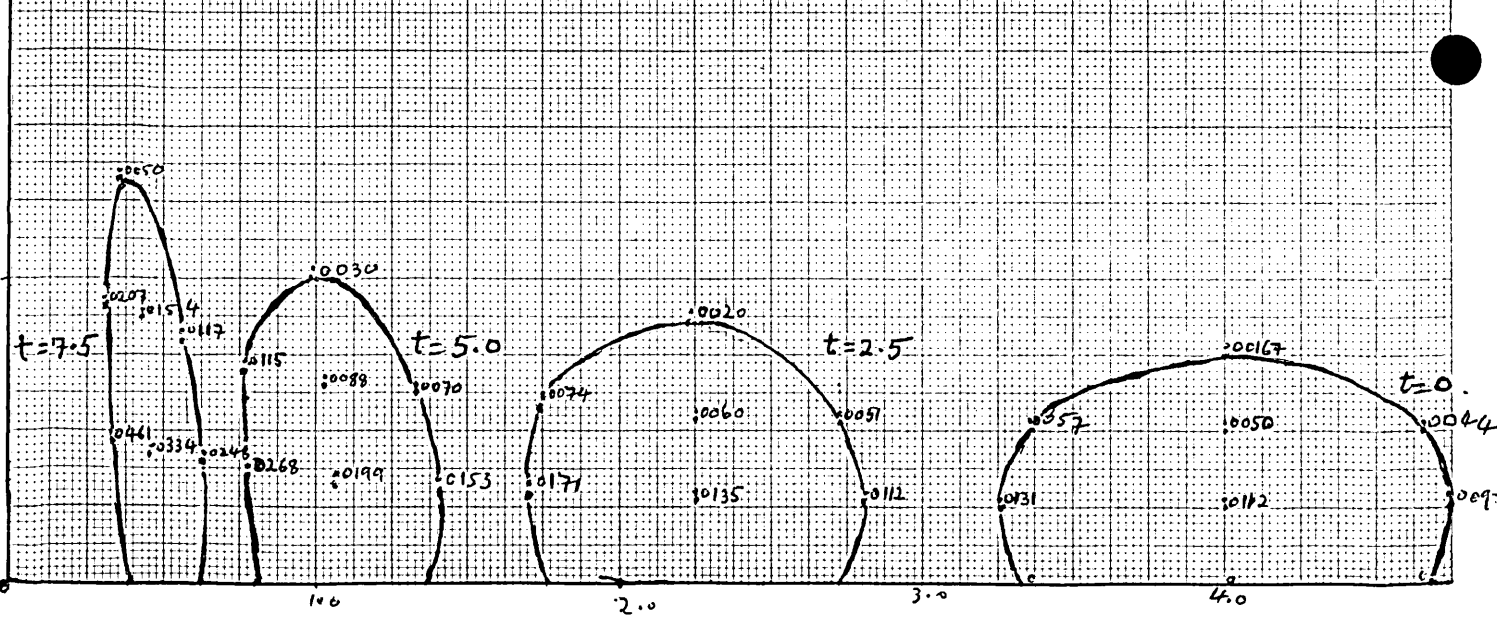


Fig. 38 This shows that before even the topmost particles rise to a full height of the obstacle, much higher downstream concentration would be produced.

← Obstacle



what kind of further contribution is made with time. However, owing to the fact that at the top of the vertical axis (at  $z = 3.0$ ) the velocity is infinite and therefore the computing methods break down.

### Case II

Starting with the same swarm at  $t = 0$ , we find that when  $n = 2/3$  (or  $w_p = w/3$ ), twice and three and a half times the maximum upstream values are obtained when  $t = 5.0$  and  $t = 7.5$  respectively. This time the downstream motion of particles is such that there is a perceptible horizontal contraction (see Fig. 3.8p 96 ).

When  $n = 1$  the particles are moving horizontally and concentrative effects expectedly become very strong. There is perhaps a large mathematical gap between  $n = 2/3$  and  $n = 1$  insofar as the degree of effects are concerned.

## Chapter V

### Summary and Conclusion

Taking the falling speed  $\nu$  to be constant at the end of Chapter I has been a significant step in the construction of our model in that it has served to demonstrate the need for some other specification in order to achieve downstream accumulation. Keeping  $\nu$  equals constant would also cause a cloud of particles to divide into two parts; the lower part being such that the particles in it would be constrained to move downwards, furnishing us with a situation where the particle behaviour may in reality contribute to the growth of downstream concentration in the lower levels of convergence. In Chapter II, wherein the potential flows have been employed, the falling speed  $\nu$  has been proportional to the vertical velocity of the flow which in Section I and II has worked out to be proportional to height. Section I has seen construction of steady distributions, but the effect of this falling speed has become more apparent when a time-dependent analysis is conducted in Section II, where the distributions in the vicinity of x-axis at  $t = -3$  have been our starting point.

Achievement of vertical columns, similar to those occurring in the cumuliform swarm, of exceedingly high concentration in the vicinity of the z-axis in six units of time has been a feature of the flow in a corner illustrative of its potentially transportive properties. A convergence - divergence flow has been used in Section III, where steady distributions for various values of falling speed have been evaluated.

The third chapter has involved development and use of our own flows -

which are almost potential flows (see their properties on the p 59 and 72 ) with reasonably realistic velocity distributions. The contours constructed for steady concentration in both parts of this chapter have provided reasonably good indications as to the downstream effects of raising particle falling speed, however, the time-developing distributions of particles in each flow has given better insight into how concentration would grow in any part of a 'swarm' in the convergence zone. The time taken for a swarm to reach divergence zone has been found to be entirely dependent upon the value of falling speed. A fleeting glimpse at the downstream distributions reveals alteration of shape of the swarm as it progresses downstream; this is mainly attributable to the nature of the flow. It has been found that the concentration increases with the falling speed, and that it continues to increase along particle paths until the divergence zone is reached when the rate of growth begins to diminish.

Two situations hitherto not considered have been dealt with in Chapter IV, which contains two sections: the first entails the construction of time-developing distributions of particles moving under a constraint of falling speed relative to the flow incorporating a line of interface inclined at  $60^{\circ}$  to horizontal. Though this angle is too large, there are inflow and out flow regions which have been useful in demonstrating that falling speed produces aggregation. The distributions have indicated also a very swift upward transport of the swarm as soon as it enters the outflow region; this is only counteracted by increasing the falling speed.

Owing to the nature of this potential flow, only the flow in the corner would be considered most relevant for our purposes, as other regions would be accompanied by large values of velocity. Therefore, assessment of

of concentration in the inflow region has alone been considered to be adequate and of some value.

Only one side of the flow in Section II, which is representative of a flow over a finite vertical wall, has been considered and again time-dependent distribution have been constructed to assess quantitatively the relationship between downstream concentration and falling speed. We can now hereby conclude from the results of the second, third and fourth chapters that particles moving under constraint of falling speed (not equal to constant) will generally give rise to higher downstream concentration, and that the whereabouts of the production of higher concentration within a swarm may partly depend upon a velocity field structure of flow, as we saw in Chapter III. Also, particles moving closest to the x-axis would be most likely to rise to concentration in the vicinity of the interface or vertical axis. The constructed time-dependent concentration distributions related to Chapter III affirm how influential wind fields can be in the determination of downstream shape of swarms. In the light of this work, it is also possible to appreciate Cochmé's treatment in respect of his use of the equation of continuity for particles airborne at a constant level. It should be pointed out, however, that Cochmé considered the horizontal aspect of atmospheric motion (on a large scale) and, in that sense, he concerned himself mainly with horizontal motion of particles and its effects. We have gone a little further and assessed the implication of vertical motion. Superimposition of our work onto his may enable us to produce a three-dimensional picture of the behaviour of locusts and, in that sense, our work complements Cochmé's work.



Recommendation

The falling speed is one of the observable features of the Desert Locust flight behaviour in the convergence zone responsible for high concentration: because the locusts begin to hover and glide down when temperature reductions of air masses above a certain height render their flight muscles inefficient to continue further flight. And it is true that a cloud of particles may assume a behaviour similar to our particles when under similar constraints. It should however be pointed out that there may be several intervening (possibly interdependent) factors which come into play when a locust swarm is airborne. We must, in the light of this fact, recognise the limit of interpretation of our results insofar as the production of downstream aggregation of locusts is concerned. Nevertheless we can emphasise the existence of a relationship between the falling speed and resulting downstream concentration.

In addition to this, the approach we have adopted to carry out this work may represent one of the significant starting points that may form a basis for further mathematical ideas and models eventually leading to a practical model applicable to locust problem. It is evident, therefore, that a vast amount of work, mathematical and otherwise, needs to be done. For further successful modelling, we need to understand better how factors such as the weight of an insect, its body temperature contribution to its surroundings, the temperature of air masses, the edge-effect and the biological interactions (between neighbouring insects) operate upon and affect the movement of individual locusts and of a swarm as a whole.

Also, these factors must be quantifiable if they are to take part in a mathematical model. In fact, at least three of the above-mentioned factors can be treated as mathematical variables (which may be dependent upon some other fundamental variables such as height, range of spacings

between insects etc.), The weight of an insect (which is responsible for its sinking) can be easily included; the edge-effect, according to Dr. Rainey, may be treated as 'surface tension' effect on the edges and therefore a modified mathematical expression could be found to designate it; and the temperature of air masses may be readily available from the formulation of a velocity field. The temperature contribution of the body of insect to its surrounding which adds to its bouyancy and biological factors can also be included to complete the picture of the locust flight behaviour.

In our model, we applied the falling speed throughout the regions considered and this needs rectification, for the locusts maintain their upward flight steadily until they find their flight muscles operating with inefficiency. Moreover,  $V = \text{constant}$  may be applicable to locust behaviour in the light of factors discussed such as its *own* weight which produces a downdraught effect when concentration / unit volume gets very high.

As far as the improvement in the specification of the flow fields is concerned, inclusion of coriolis forces and some other factors (turbulence etc.) may be taken into account when solving the equation of motion. Further extension can be made by evaluating time-developing two-and three-dimensional flows, both of which are extremely complicated.

Then, a number of models can be formulated to describe a variety of situations in which locust swarms are confronted during insecticide spraying operations.

Then it will be possible to suggest amelioration in spraying techniques, requirement of, the possible reduction in, the size of droplets, and concentration strength of pesticides for better control and anti-locust strategy.

Appendix I

To prove that  $\text{div } \underline{U} = \frac{gW}{c^2}$

In adiabatic motion

$$\frac{Dp}{Dt} = \frac{D\rho}{Dt} c^2 \quad (1)$$

The equation of continuity is

$$\frac{D\rho}{Dt} = -\rho \text{ div } \underline{U} \quad (2)$$

and the equation of inviscid motion in the atmosphere is

$$\frac{D\underline{U}}{Dt} = -\frac{1}{\rho} \underline{\text{grad}} p + g + \underline{U} \times \underline{f} \quad (3)$$

so that taking the scalar product with  $\underline{U}$  we have

$$\begin{aligned} \frac{D\rho}{Dt} &= \frac{\partial \rho}{\partial t} + (\underline{U} \cdot \underline{\text{grad}}) \rho \\ &= \frac{\partial \rho}{\partial t} - \rho \underline{U} \cdot \frac{D\underline{U}}{Dt} + \rho \underline{U} \cdot g \\ &= \frac{\partial \rho}{\partial t} - \rho \left[ \frac{D}{Dt} \left( \frac{q^2}{2} \right) + gw \right] \end{aligned} \quad (4)$$

Combining this with (1) and (2) we obtain

$$\text{div } \underline{U} = - \frac{1}{\rho c^2} \frac{\partial p}{\partial t} + \frac{1}{c^2} \left[ \frac{D}{Dt} (q^2/2) + gw \right] \quad (5)$$

The terms on the r.h.s. of this equation represent the divergence due to change in pressure and therefore contain the velocity of sound, for this is one of the quantities by which we can represent the elastic properties of air.

The kinetic energy of the parcel is due to the bouyancy of the parcel and therefore

$\frac{D}{Dt} (\frac{1}{2} q^2) \sim gw \frac{\delta T}{T}$  is much smaller than  $gw$ , where  $\frac{g\delta T}{T}$  is the rate of change of potential energy of the parcel moving upwards. Therefore in steady state,

$$\nabla \cdot \underline{U} = \frac{gw}{c^2}$$

Appendix II

Let us consider a differential equation

$$A \frac{\partial z}{\partial x} + B \frac{\partial z}{\partial y} = C$$

where A, B and C are function of x, y and z.

Comparing this equation with

$$\frac{\partial z}{\partial x} dx + \frac{\partial z}{\partial y} dy = dz$$

we obtain simultaneous equations

$$\frac{dx}{A} = \frac{dy}{B} = \frac{dz}{C}$$

which entail that the tangent to a certain curve at the point (x,y,z) has direction-cosines proportional to (A,B,C), and that  $\phi(u,v) = 0$  represents a surface through such curves, given that  $u = \text{const.}$  and  $v = \text{constant}$  are particular integrals of simultaneous equations.

If A,B and C are constants, we thus get a straight line, or rather a doubly infinite set of straight lines as one such line goes through any point of space. If A,B and C are functions of x,y and z, we get a system of curves, anyone of which may be considered as generated by moving a point which continuously alters the direction of motion. The lines of electrostatic force is such a system.

Bibliography

1. J. Cocheme Assessment of Divergence in relation to the Desert Locust.  
(UN report Technical Notes 69, p 23).
2. P.T. Haskel The Hungry Locust.  
(Science Journal, Jan. 1970)
3. R.S. Scorer Toward More Efficient Application of Pesticides.  
(Chemistry and Industry, 1974 2nd March p 181).
4. R.S. Scorer Natural Aerodynamics (1958 Pergamon).
5. R.C. Rainey Some Observation of flying Locusts and Atmospheric Turbulence in eastern Africa.  
(Quart. J.R. met. sco. 84, 334-354).
6. R.C. Rainey Weather and the Movement of Locust Swarms.  
A new hypothesis (Nature vol. 168 Dec. 22, 1951).
7. H.J. Sayer Desert Locust and Tropical Convergence.  
(Nature vol 194, p 330-336).
8. UN Report Technical Note no. 54. Meteorology and Migration of Desert Locust p 7-11, 18, 28-30).
9. UN Report Technical Note no. 69 Meteorology and Migration of Desert Locust p 29, 269, 274.
10. Z. Waloff Orientation of flying locusts in Migrating swarms.

73, Headstone Rd,  
Harrow,  
Middx.

10th January, '76

Prof. Scorer,  
Maths Dept.,  
Imperial College,  
Queens Gate,  
London S.W.7.

Dear Professor Scorer,

It was a great pleasure seeing again, however briefly it may have been.

I am writing to you to say that the copy of your correction sheet seems to have disappeared, or even possibly been thrown away. Therefore, I am sending you the copy that I recently made from your correction sheets and Professor Pearce's marks made on the original copy. The point is that Professor Pearce's pencil marks have been deliberately rubbed out because I thought that if I did not, then nobody would. Most of the corrections have been made by hand, and they should be easily located.

At any rate, the copy I am sending you will suffice. If any anomaly arises  
P.T.O.

for which I need to be communicated,  
Tina has my 'phone number; the ~~best~~ best  
time would be in evening after six.

Yours sincerely,  
A Patel.



contents: "Cocheme": - spelling

P. 9. correction of English grammar: a comma erased after 'Although'

P. 10. End of 2nd paragraph 'causes the whole area to blossom'

P. 12. One reason why the atmosphere . . . 'why the' inserted  
line 3 more inserted before ephemeral

\* line 4 the last word 'they' replaced <sup>by</sup> 'insects'.

P. 14. Correction of <sup>spelling of</sup> Cocheme's name at 3 places.

P. 15. Last paragraph retyped out, with the replacement of the <sup>definite</sup> article 'the' between 'of' and 'mathematical' and 'of' and primitive. Also the phrase 'stream of convergence' has been replaced by a better phrase 'converging airstream'.  
(a) has been corrected.

P. 16. three 'the's have been replaced

P. ~~16~~ 17. The first paragraph used to read: The locusts normally can fly with . . . . This has been corrected by switching around the positions of 'normally' and 'can'.

P. 18. of eqn. (1.4.2) corrected

P. 19. Following eqn (1.4.4) the mistake corrected is the replacement of 'a constant' by 'the acceleration'

P. 23. 3 lines from the bottom: spelling 'higher' corrected.

P. 24. sixth line from the top. 'irrational' changed to 'irrotational'.

P. 26. the last word 'correlation' changed to 'relationship'

P. 27. After eqn (2.1.5). Let a hypathetical . . . : spelling mistake put right

P. 30. 'yet another' dealt with by erasing 'yet'

P. 35. Half way down, 'Elimination of  $A_0$ ,  $B_0$  and  $C_0$ , ...' rewritten.

P. 41. line 7 (from top).  $\frac{\partial \sigma}{\partial z}$  varies much more slowly. ~~more~~ included.

P. 45. the caption corrected.

P. 46. 2nd line from bottom 'decelerate' spelling corrected.

In the ~~4th~~ and 3rd line from the bottom 'different from that of any other point on the line' is replaced by 'a function of both  $x$  and  $z$ '.

P. 47. The sentence continuing from P. 47 is 'completed' by also writing what  $A_i$  and  $B_i$  are.

P. 53. line 4 (from top) ; 'to' erased.

P. 54. In lines 13 & 14 & 15, spelling corrected

Also, ~~is~~ the line 3 (from top) is made to read 'to form a realistic velocity field' . . . which prof Pearce thought would read better.

And the last sentence used to read 'But one is not necessarily the cause of the other, - - -'. From this I have removed 'necessarily'

P. 55. spelling mistake 5th line from bottom corrected.

P. 60. 2nd line spelling corrected.

P. 83. 7. 3rd line truly  $\rightarrow$  truly.

P. 104. rewritten. ~~see~~ see theses.

P. 106. Bibliography - redone.